Nitric Oxide in Biological Denitrification: Fe/Cu Metalloenzyme and Metal Complex NO x Redox Chemistry

5 AUTHORS, INCLUDING:

Simon de Vries
Delft University of Technology
147 PUBLICATIONS **6,642** CITATIONS

SEE PROFILE

Pierre Moënne-Loccoz
Oregon Health and Science University
109 PUBLICATIONS **3,172** CITATIONS

SEE PROFILE

Imke Schroeder
University of California, Los Angeles
57 PUBLICATIONS **2,744** CITATIONS

SEE PROFILE

Nitric Oxide in Biological Denitrification: Fe/Cu Metalloenzyme and Metal Complex NO$_x$ Redox Chemistry

Ian M. Wasser,[†] Simon de Vries,[‡] Pierre Moënne-Loccoz,[§] Imke Schröder,[||] and Kenneth D. Karlin*,[†]

Department of Chemistry, The Johns Hopkins University, Charles and 34th Streets, Baltimore, Maryland 21218, Kluyver Laboratory for Biotechnology, Delft University of Technology, 2628 BC Delft, The Netherlands, Department of Biochemistry and Molecular Biology, OGI School of Science and Engineering at OHSU, Beaverton, Oregon 97006, and Department of Microbiology and Molecular Genetics, University of California, Los Angeles, California 90095

Contents

I. Introduction

As an alternative to photosynthesis or aerobic respiration, many microbial species can respire anaer-

* To whom correspondence should be addressed. . Phone: 410-516-8027. Fax: 410-516-8420. E-mail: karlin@jhu.edu.
[†] The Johns Hopkins University.
[‡] Delft University of Technology.
[§] OGI School of Science and Engineering at OHSU.
[||] University of California, Los Angeles.

Ian M. Wasser was born in 1973 in the suburbs of Detroit, Michigan and graduated from Detroit Country Day School. He received a B. S. Chemistry degree in chemistry from the University of Michigan in 1995, where he conducted undergraduate research under the direction of Professor James E. Penner-Hahn. This was then followed in 1998 by an M. S. degree in chemistry from the University of California at Berkeley, where he studied organometallic chemistry and X-ray crystallography with Professor Peter Vollhardt. He is currently a doctoral candidate, working toward his Ph.D. in bioinorganic chemistry under the direction of Professor Kenneth D. Karlin at Johns Hopkins University, where his research focuses on the interactions of synthetic iron and copper complexes with nitric oxide.

obically to gain energy for cell growth.[1–4] A variety of bacteria employ a process referred to as denitrification. Denitrification is the four-step, five-electron reduction of nitrate (NO$_3^-$) to dinitrogen (N$_2$) (Figure 1) to support oxidative phosphorylation (ATP synthesis) in the absence of dioxygen.[2,3,5–7] A similar process is also found in certain archaea.[8–12] A different form of denitrification yielding nitrous oxide (N$_2$O) as the end product from nitrate (NO$_3^-$) or nitrite (NO$_2^-$) is catalyzed in the mitochondria of several fungi and yeasts.[2,13–17] In bacteria and archaea, each of the four reduction steps is catalyzed by one (or more) distinct metalloenzyme complexes, employing various transition metals (Mo, Fe, Cu) that are found in varying ligand environments (i.e. heme, histidine ligation, sulfide ligation, etc.).

In recent years, bioinorganic researchers, including biophysicists, biochemists, and synthetic inorganic chemists, have joined forces to elucidate the fundamental coordination chemistry of the metal ions and their interactions with NO$_x$ species. This information adds insight into aspects of the active site structure or reaction mechanism for each of these metallo-

Simon de Vries received his M. S. in Biochemistry and his Ph.D. (E. C. Slater) at the University of Amsterdam in the field of Bioenergetics. The latter was awarded with the prize of the Dutch Society for Biochemistry. After his postdoctoral research at the University of Pennsylvania (Les Dutton) he returned to the University of Amsterdam as a post doc and was granted with a Senior Research fellowship of the Royal Dutch Academy of Sciences. At that time, his research was in the field of yeast molecular biology and mitochondrial physiology, but when he joined the Delft University of Technology in 1992 as an Assistant Professor he switched (back) to the field of metallo-protein/enzyme research. He is currently the Antoni van Leeuwenhoek Professor at Delft. His particular interest is in the study of the molecular mechanism of action of metalloenzymes by means of pre-steady state kinetics and the development of microsecond freeze-quench equipment. He is particularly interested in structure–function relationships of the metalloenzymes involved in denitrification in both mesophilic and (hyper) thermophilic microorganisms.

Imke Schröder was born in Jever, Germany, in 1958. She obtained her Ph.D. in Microbiology in 1987 under the direction of Achim Kröger with a thesis on elemental sulfur catabolism in a strict anaerobic bacterium at the University of Marburg, Germany. She was awarded with the German Microbiology Society best thesis award. After a brief postdoctoral period in Achim Kröger's group, then in Frankfurt, Germany, she joined the group of Robert Gunsalus at the University of California, Los Angeles, in 1988. Here she investigated the structure and function of fumarate reductase and its regulation on the transcriptional level by nitrate. In 1993, she went to the Veterans Administration Medical Center in San Francisco where she studied the structure and function of succinate dehydrogenase. Since 1994, she has been a faculty member at the University of California, Los Angeles, where she focuses on the investigation of nitrate and iron respiration of microorganisms that thrive at extremely high temperatures.

Pierre Moënne-Loccoz (born in 1964) received is Ph.D in 1989 from Université Pierre et Marie Curie (Paris, France) for his work on higher plants photosystem I and II under the supervision of Marc Lutz and Bruno Robert (CE Saclay, France). He continued to study photoactive proteins first with Warner Peticolas at the University of Oregon and then with Mike Evans and Peter Heathcote at University College London. He then joined Thomas Loehr and Joann Sanders Loehr at the Oregon Graduate Institute, with whom he participated in many collaborative efforts in the field of metalloproteins and oxygen activation. He is now an Assistant Professor at the OGI School of Engineering at OHSU where he continues to work for a better understanding of enzyme catalysis through structural characterization of reaction intermediates.

Kenneth D. Karlin was born in Pasadena, California, in 1948. He received his B. S. in Chemistry from Stanford University (1970) and his Ph.D. in 1975 at Columbia University while working with Prof. S. J. Lippard. After organometallic chemistry postdoctoral work with Professor Lord Jack Lewis and (now) Professor Brian F. G. Johnson at Cambridge, England, he joined the faculty at the State University of New York (SUNY) at Albany in 1977 as Assistant Professor. In 1990, he moved to Johns Hopkins University as Professor, where he now holds the Ira Remsen Chair in Chemistry. He is a recipient of the 1991 Buck-Whitney Award for Research (ACS Eastern New York Section) and was elected as a Fellow of the American Association for the Advancement of Science. His research interests are in bioinorganic chemistry and synthetic modeling, emphasizing elucidation of fundamental aspects of structure, spectroscopy, and reaction mechanisms relevant to copper and heme enzyme active sites that process molecular oxygen or nitrogen oxide species. More recent activities include environmental inorganic chemistry and metal-complex interactions with DNA and proteins/peptides.

enzymes. Over the past years, it has become evident that nitric oxide (NO) is a compulsory intermediate in bacterial denitrification.[2,3] The study of bacterial NO-binding (and -releasing) enzymes and relevant model complexes might provide valuable structural, spectroscopic, and mechanistic information also relevant to other important NO-binding enzymes. For example, heme proteins that interact with NO include soluble guanylate cyclase, which utilizes NO to regulate signal transduction in mammals,[18,19] and

the nitrophorins of the blood-feeding insect *Rhodnius prolixus,* which reversibly transports NO.[20–22] Therefore, it is of great interest to study both the metalloenzymes that produce NO from nitrite, nitrite reductase (NIR),[23–25] and also the metalloenzymes that reduce NO to nitrous oxide, nitric oxide reductase (NOR).[2–4,26–28] Nitrous oxide reductase (N_2OR),

$$NO_3^- \xrightarrow[\text{I}]{\text{NAR}} NO_2^- \xrightarrow[\text{II}]{\text{NIR}} NO$$

$$\xrightarrow[\text{III}]{\text{NOR}} N_2O \xrightarrow[\text{IV}]{\text{N}_2\text{OR}} N_2$$
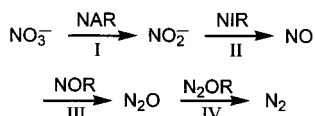
Figure 1. Four consecutive reduction steps of bacterial denitrification, converting nitrate to dinitrogen. (I) NAR: nitrate reductase; (II) NIR: nitrite reductase; (III) NOR: nitric oxide reductase; (IV) N_2OR: nitrous oxide reductase.
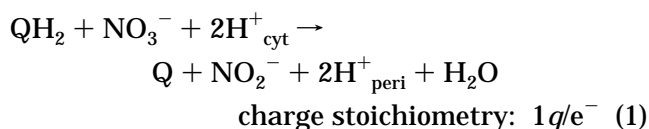
which will not be discussed here, is nonetheless of great interest; recent X-ray structural insights reveal a novel active site containing a $Cu_4(S)(His)_7$ catalytic core, the first example of a copper-sulfide cluster in biology.[29-31] This review has a two-part focus, following an initial introductory section on relevant bioenergetics: (1) an examination of metalloenzyme reactivity with NO, specifically, metalloenzymes that both produce NO from nitrite (nitrite reductases) and those that reduce NO to nitrous oxide (nitric oxide reductases); and (2) a review of the inorganic coordination complex reactivity with NO, including $Cu-NO_x$ and $Fe-NO_x$ redox chemistries, since these metals are cofactors for the NO-producing (NIR) and NO-consuming (NOR) enzymes.

A. Bioenergetic Aspects of Respiration and Denitrification

All microorganisms have evolved to adapt to varying environmental conditions. Depending on the microbial species, microbes are capable of expressing a vast array of photosynthetic, anaerobic, and aerobic respiratory chains to meet their bioenergetic demands. The diversity of life on this planet is embedded in these chains of electron-transferring enzymes that enable the microbes to either utilize sun light as an energy source or make use of the redox free energy difference between complex organic compounds (carbohydrates, proteins, lipids, etc.) or inorganic electron donors and terminal electron acceptors (N-oxyanions, dioxygen, sulfate, sulfite, CO_2, etc.). If complex organic compounds are used as the energy source, they are transported into the cell via the microbe-specific transport systems. Within the cell, the organic compound is oxidized to an end product, which is consequently released to the environment. The resulting reducing equivalents ("H"-atoms, i.e., electron plus proton pairs) enter the respiratory chains and are transferred to the terminal electron acceptor either via diffusable soluble carriers (NAD, *c*-type cytochromes, or blue copper proteins) or by membrane-bound carriers (ubiquinone, menaquinone, plastoquinone, or membrane-bound *c*-cytochromes).
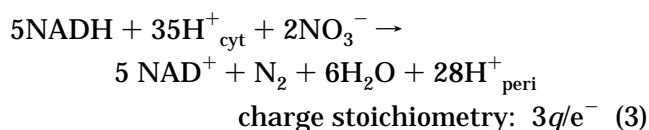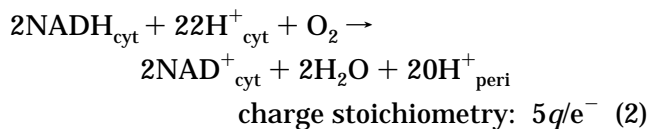
The anaerobic denitrification pathway and the aerobic respiration pathway share two respiratory enzyme complexes that are linked to energy conservation: the NADH dehydrogenase and the cytochrome bc_1 complex (Figure 2). Thus, in a physiological sense, denitrification is an anaerobic analogue to dioxygen-based respiration. The key enzymes in aerobic respiration are cytochrome *c* or quinol oxidases acting as terminal oxidases. The nitrate, nitrite, NO, and N_2O reductases fulfill this same "terminal oxidase" function collectively or individually in the denitrification pathway.

There are two general mechanisms[32-36] by which membrane-bound redox enzymes conserve the redox free energy in the form of a proton motive force, $\Delta\mu H^+$. The proton motive force itself is the sum of a concentration term (ΔpH) and the electrical potential gradient Δp ($\Delta\mu H^+ = \Delta p + \Delta$pH). According to one mechanism, the enzymes catalyze transmembrane electron transfer ($\Delta\mu H^+ = \Delta p$). Proton binding and release on one (bacterial photochemical reaction center) or both (NAR, Q-cycle of the bc_1 complex) sides of the membrane may follow the initial electron transfer, but this does not change the thermodynamics, i.e., $\mu\Delta H^+$ remains the same, and part of Δp is transformed into ΔpH. Enzymes acting according to this mechanism do not actually translocate protons; only proton binding (generally by quinones or hydroxide) and release of protons (from the substrate) occurs. Nevertheless, the overall reaction can be written as "net" proton translocation from cytoplasm to periplasm (see Figure 2),[33,34] e.g., for NAR:

$$QH_2 + NO_3^- + 2H^+_{cyt} \rightarrow$$
$$Q + NO_2^- + 2H^+_{peri} + H_2O$$
$$\text{charge stoichiometry: } 1q/e^- \quad (1)$$

This particular mechanism leads to a stoichiometry of $1H^+$ (or one charge, q) translocated per electron transferred. In the other mechanism, the enzyme catalyzes a true proton translocation from the cytoplasm to the periplasm involving "proton channels". Examples of such redox-linked proton pumps are the cytochrome oxidases and the Complex I NADH dehydrogenase.[32,35,37-44] This mechanism can yield H^+/e^- stoichiometries of 2 (see Figure 2).

In denitrification, the NIR and N_2O reductases are, in general, water-soluble enzymes, and the free energy of the reaction catalyzed by these enzymes is lost as heat. NOR, though membrane bound, does not translocate protons, because the protons and electrons enter NOR from the same (periplasmic) side of the membrane. As a consequence, in NO reduction, the redox free energy is wasted.[1,45] Only nitrate reduction catalyzed by the membrane bound NAR is associated with transmembrane electron transfer and the net translocation of protons.[1,6,7] As a summary, the overall reactions for bacterial aerobic respiration and denitrification with NADH as the electron donor and the H^+/e^- stoichiometries shown in Figure 2 can be written as:

$$2NADH_{cyt} + 22H^+_{cyt} + O_2 \rightarrow$$
$$2NAD^+_{cyt} + 2H_2O + 20H^+_{peri}$$
$$\text{charge stoichiometry: } 5q/e^- \quad (2)$$

$$5NADH + 35H^+_{cyt} + 2NO_3^- \rightarrow$$
$$5\ NAD^+ + N_2 + 6H_2O + 28H^+_{peri}$$
$$\text{charge stoichiometry: } 3q/e^- \quad (3)$$

The efficiency expressed as charges (q) translocated per electron transferred equals 5 for oxygen respiration (4 when using a quinol oxidase as the terminal reductase versus a cytochrome *c* oxidase) and 3 for
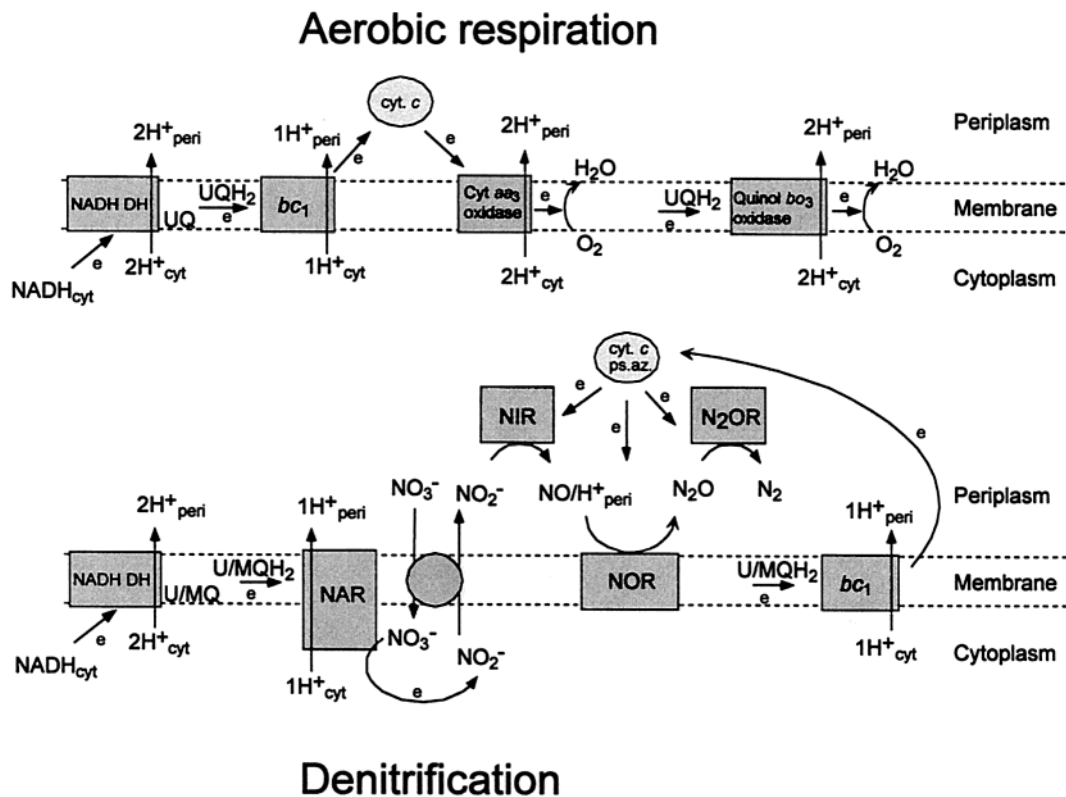
Aerobic respiration

Denitrification

Figure 2. Comparison between the bioenergetics of bacterial aerobic respiration and denitrification. The overall proton translocation stoichiometries per electron transferred of the various membrane-bound enzyme complexes are indicated by vertical arrows crossing the membrane. Electron transport is indicated by the other arrows and the symbol "e". Note that in the case of the membrane-bound NOR, protons and electrons (from cyt *c* and/or pseudoazurin) come from the same (periplasmic) side, making the overall reaction nonelectrogenic. The precise identity of the carrier(s) involved in transport of nitrate and nitrite is currently unknown. NADH DH, NADH dehydrogenase (complex I); UQ(H_2), ubi(hydro)quinone; MQ(H_2), mena(hydro)quinone; ps.az, pseudoazurin; cyt *c*, cytochrome *c* (NB: membrane-bound cytochrome *c* has been omitted from the figure). Protons liberated upon oxidation of UQ(H_2) or MQ(H_2) by the bc_1 complex, NAR, or the bo_3 quinol oxidase are ejected into the periplasmic space. Peri, periplasm; cyt, cytoplasm.

denitrification. In other words, aerobic metabolism is more efficient. Facultative (an)aerobic microorganisms have evolved "sensors" for NO_3^-, NO_2^-, NO, and O_2 to switch between aerobic and anaerobic metabolism, opting to express those enzymes active in the more efficient aerobic metabolism when dioxygen is present.[3,6,46−49]

Comparing the efficiencies between denitrification and aerobic respiration more directly, i.e., from the level of quinone, the stoichiometries are $1H^+/e^-$ for denitrification and $3H^+/e^-$ for oxygen respiration ($2H^+/e^-$ for respiration with quinol oxidase), a substantial difference. Given the toxicity of nitrite and nitric oxide, the biological driving force to evolve enzymes to convert these metabolites might have been both in the context of detoxification and in cellular bioenergetics.

II. Metalloenzymes

A. Nitrite Reductase

General Considerations. In bacterial denitrification, two genetically unrelated enzymes carry out the one-electron reduction of nitrite to nitric oxide:

$$NO_2^- + 1e^- + 2H^+ \rightarrow NO + H_2O \qquad (4)$$
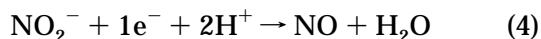
These are either copper- or heme-containing nitrite reductases produced from the structural genes *nirK* or *nirS*, respectively. Current studies indicate that all denitrifying bacteria opt for one out of these two biological apparatus, but the taxonomic distribution appears to be random. The reason behind this redundancy and the rules of selection are not known.[3]

1. Cytochrome cd₁ Nitrite Reductase:

Heme-containing nitrite reductases are soluble enzymes located in the periplasmic space of the bacteria. NIR-cd_1 has been purified to homogeneity from a wide variety of denitrifying bacteria, including *Pseudomonas aeruginosa*, *Paracoccus denitrificans*, *Paracoccus pantotropha*, and *Pseudomonas stutzeri*.[331] The enzyme is a homodimer of ~120 kD that contains one heme *c* and one heme d_1 per subunit. The *c* heme acts as the electron entry of the enzyme and accepts electrons from soluble cytochrome c_{551} and azurin. The d_1 heme is the site of nitrite reduction and is a unique prosthetic group, a dioxoisobacteriochlorin.[50,51] The saturation of two pyrrole bonds and the addition of two keto groups and one acrylate peripheral group conjugated to the π-macrocycle severely alter the physical properties of this heme (Figure 3). This unique cofactor requires a specific biosynthetic pathway.[3] Partly saturated porphyrins are prone to nonplanar deformations, and polar peripheral groups
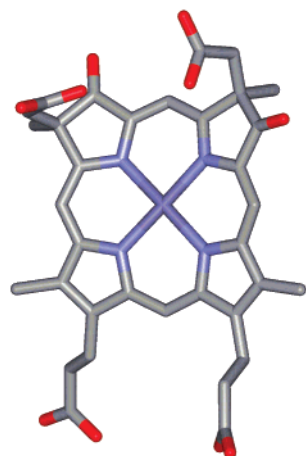
Figure 3. Structure of the heme d_1 of heme cd_1 NIR.

offer an additional source of noncovalent anchorage to the protein moiety. The Fe^{III}/Fe^{II} reduction potential of d_1 heme models are ~200 mV less negative than iron porphyrins.[51]

The reaction mechanism (outlined in Figure 4) of NIR-cd_1 is proposed to involve NO_2^- coordination through its nitrogen to the ferrous d_1 heme and dehydration leading to the formation of a [$Fe^{II}-NO^+$ ↔ $Fe^{III}-NO^{\bullet}$] (reactive $NO^{\bullet}$ species will herein be referred to as simply NO) nitrosyl d heme intermediate,[52] an {FeNO}⁶ species in Enemark and Feltham formalism (discussed further in section III.A).[53] Release of NO and heme c to heme d_1 intramolecular electron transfer complete the catalytic cycle. X-ray crystal structures of the dithionite ($S_2O_4^{2-}$)-reduced enzyme where a reaction byproduct SO_2 is S-bound to the d_1 heme support the N-coordination geometry of nitrite.[54] Stopped flow absorption and rapid-freeze quench EPR experiments on *P. aeruginosa* NIR indicate the formation of an EPR silent species within the ms dead time of the mixing apparatus that was assigned to such an {FeNO}⁶ d_1 heme nitrosyl intermediate.[55] An {FeNO}⁶ species was also detected by its $\nu(N-O)$ at ~1910 cm⁻¹ in FTIR difference spectra obtained during the back-reaction of NO with the fully oxidized enzyme of *P. stutzeri*,[56] and the same spectroscopic signature was detected in time-resolved FTIR measurement with cd_1 NIR from *P. pantotropha*.[57]

The study of the NIR-cd_1 mechanism is severely hindered by the buildup of a ferrous d_1 heme nitrosyl {FeNO}⁷ complex during in vitro assays. Stable {FeNO}⁷ (i.e., $Fe^{II}-NO$) d_1 heme species can form as dead-end products if electron transfer occurs before NO release from {FeNO}⁶, or via product inhibition if released NO rebinds to the reduced enzyme. The mechanisms by which the enzyme regulates internal electron transfer and promotes NO release have wide relevance to NO chemistry in hemoproteins. The first detailed three-dimensional structure of NIR-cd_1 was obtained from *P. pantotropha*.[54,58] The two subunits of the functional homodimer are related by a 2-fold symmetry (Figure 5). As previously shown from limited proteolysis,[59] each heme is located in a distinct domain, an N-terminal α-helical domain containing the c heme and a C-terminal eight-blade β-propeller domain containing the d_1 heme. Iron-to-
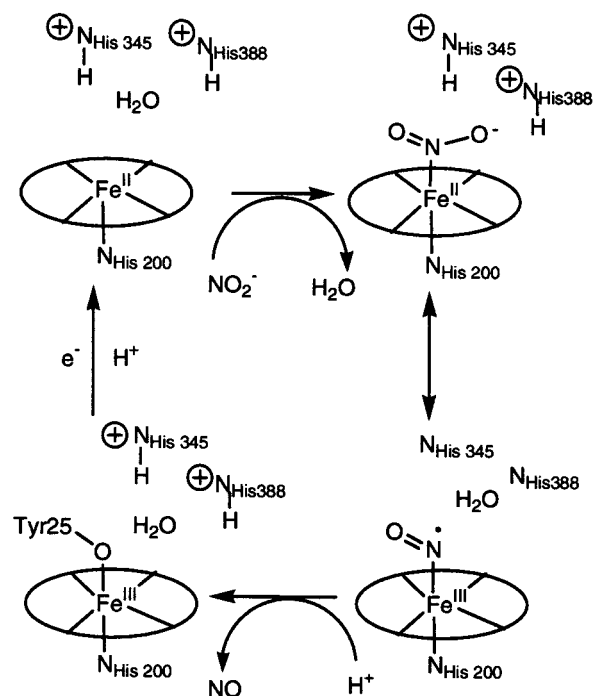

Figure 4. Proposed mechanism for the reduction of nitrite at the heme d_1 active site, showing the involvement of Tyr-25 in promoting the release of NO.
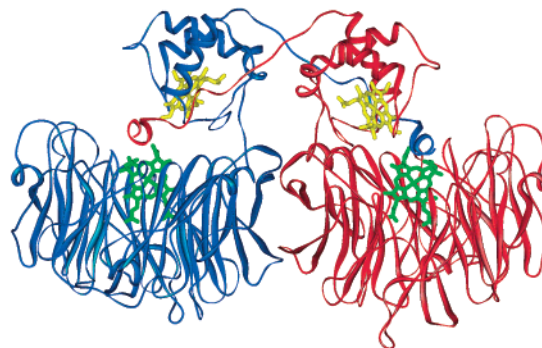

Figure 5. Heme cd_1 structure and ribbon representation of oxidized nitrite reductase from *Pseudomonas aeruginosa*. The two identical subunits are composed of an N-terminal domain containing the c heme (yellow) and a C-terminal domain that forms a β-propeller domain that carries the d_1 heme (green). The first ~20 residues of each subunit form an α-helix engaged in interdomain and intersubunit interactions.

iron and edge-to-edge distances between c and d_1 hemes within a monomer are ~20 and ~10 Å, respectively, whereas they are greater than 40 Å when hemes from different subunits are considered. The heme−heme edge distance within one monomer correlates well with the submillisecond electron-transfer rate measured in pulse radiolysis and CO photodissociation studies.[60−62]

The crystal structure clearly identified His-345 and His-388 as important residues in the distal pocket of the d_1 heme. These two histidines are likely to favor ligation of anions to the ferrous d_1 heme and act as proton donors in the nitrite dehydration step of the catalytic cycle.[58] They are also believed to cause the unusual high affinity of the reduced enzyme for cyanide.[63] However, the unprecedented feature of the crystal structures of NIR-cd_1 from *P. pantotropha* is

the variation in iron ligands with oxidation state. The ferric c heme iron is coordinated to two histidines, His-69 and His-17, rather than the common His-Met ligation of c-type cytochromes. It confirms early spectroscopic data showing variable coordination of the heme c depending on the source of the enzyme.[64,65] Within the α-helical domain and contiguous to Cys-65 and Cys-68 that covalently bind the c heme, His-69 is an expected c heme ligand. On the other hand, His-17 is part of a short loop that includes Tyr-25, one of the axial ligands of the hexacoordinated ferric d_1 heme (Figure 4). The first 30 residues and both of these unusual ligands become disordered in the crystal upon reduction of the enzyme leaving the ferrous d_1 heme pentacoordinated to His-200 and the c heme with a classic c-type ligation set that includes Met-106 and His-69. Understandably, these ligand exchanges were initially proposed to play a role in the coupling of electron transfer and substrate binding during catalysis.[54] However, the lack of a homologous N-terminal loop in other sources of cd_1-NIR[66−69] led to the proposal that the X-ray structure of the oxidized enzyme represented a resting state of the enzyme.[70] Recent monitoring of the reduction of hydroxylamine by *P. pantotropha* NIR-cd_1 and electron transfer from pseudoazurin confirmed that the ferric bis-His coordination of the c heme corresponds to an "as isolated" resting configuration.[71] NIR-cd_1 catalysis can be summarized as shown in Figure 4.

Shortly after the first X-ray crystallography study,[54] NIR-cd_1 from *P. aeruginosa* was also characterized.[72,73] The overall architecture of NIR in *P. aeruginosa* was shown to be the same as that in *P. pantotropha*, *except* for the N-terminal tails. In *P. aeruginosa*-NIR, the first 29 residues form an arm that wraps around the interface between the two domains of the opposite subunit. No ligand switch is observed at the c heme of *P. aeruginosa*-NIR, a His-Met coordination being present in both oxidation states. As expected, the ferric d_1 heme is hexacoordinated in the NIR-*P. aeruginosa* crystal structure, but the sixth ligand is a hydroxyl group. Interestingly, Tyr-10 from the opposite subunit engages a hydrogen bond with the coordinating hydroxyl,[72,73] but mutation of this tyrosine to a phenylalanine was reported to have no significant effect on the enzyme catalysis.[74]

After relegating unusual Fe[III] ligands to a resting state rather than an active form of the enzyme NIR-cd_1, catalysis by *P. aeruginosa* NIR is very similar to that already discussed. Two distal (protonated) histidines enhance the nitrite binding affinity of the ferrous d_1 heme, donate protons for the nitrite dehydration reaction, and form a hydrogen bond network that includes a mobile tyrosine to favor the competitive coordination of a hydoxyl group to the ferric d_1 heme and promote release of NO. Since at neutral pH both hemes have similar reduction potentials,[75−77] minor changes of solvent exposure, local charges, or nonplanar distortions of the d_1 heme could be sufficient to regulate the internal electron-transfer rate[78−83] and the equilibrium (away from unwanted states, Fe[II]−NO). Resonance Raman studies of both NO- and CO-bound d_1 heme have sug-

gested a novel heme-substrate environment in cd_1-NIR, significantly different from previously studied heme proteins.[84] Recently, mutants of the active site histidines have been described in NIR-cd_1 from *P. aeruginosa*.[85] In both mutants, the nitrite reductase activity is impaired with rapid formation of the $\{FeNO\}^7$ dead-end product. The loss in hydrogen bonds is proposed to impair the hydroxyl-mediated removal of NO from the ferric d_1 heme. Mutation of the histidine sitting directly above the d_1 heme iron is also shown to result in a large decrease in substrate affinity.[85]

Stabilizing an $\{FeNO\}^6$ d_1 heme nitrosyl and promoting the release of NO are challenges also met by nitrophorins, the reversible NO-binding ferric heme proteins from the saliva of blood-sucking insects.[20−22,86] How nitrophorins prevent the autoreduction of the Fe[III]−NO complex is still unclear. The release of NO is pH dependent, faster at the neutral pH in the host blood than in the acidic insect saliva. It is also facilitated by the competitive binding of histamine produced by the host immune response.[21,87,88] Some evidence in favor of a reversible binding of NO to the ferrous cytochrome c' of *P. denitrificans* has led to the proposal that this periplasmic hemoprotein might shuttle NO from NIR-cd_1 to NOR.[89] However, recent experiments with *Rhodobacter capsulatus* have shown unchanged denitrifying growth whether the strain produces cytochrome c' or is cytochrome c' deficient.[90] Cytochrome c' is not required for the denitrification process and may instead play a protective role against elevated NO levels.[91−93]

Apart from its physiological reaction, cd_1-NIR can also catalyze the four-electron reduction of O_2 to water. Recent freeze-quench EPR experiments indicated the formation of a d_1 heme Fe[IV]-oxo species along with a protein radical proposed to be a tyrosine residue.[94] Such a species is reminiscent of the P-intermediate in the reaction cycle of cytochrome c oxidase.[95] However, the unspecific character of this O_2 reductase activity in NIR-cd_1 is underlined by its lack of sensitivity to mutations of either active site histidine to alanine.[85]

2. Copper Nitrite Reductases

Copper-containing nitrite reductases catalyze the one-electron reduction of nitrite (NO_2^-) to nitric oxide. While the iron-containing NIRs are more abundant in nature, copper NIRs are found in a greater variety of ecological systems and therefore demonstrate more physiological diversity.[2,96] Copper-containing NIRs comprise roughly one-third of the total denitrifiers found in terrestrial soil.[2] To date, no biological system has been shown to contain both Fe− and Cu−NIRs. This section will briefly recount some findings regarding Cu−NIR, while the more interested reader is directed to several recent reviews[2,4,97,332] and a recent account[98] on this subject.

The first X-ray structure of a Cu−NIR was solved at 1.9 Å resolution by Adman and co-workers.[24,99] This green NIR isolated from *Achromobacter cycloclastes* is composed of three identical subunits of 37 kD that bind a total of six coppers. A comparable

structure was subsequently obtained from the green Cu−NIR of *Alcaligenes faecalis*.[25,100,101] More recently, a blue Cu−NIR isolated from *Alcaligenes xylosoxidans* was also characterized by X-ray crystallography.[102−104] In agreement with extensive homologies in primary sequences,[97,98] both blue and green Cu−NIRs exhibit very similar structural features. The overall structure exhibits a 3-fold axis with a 5−6 Å central channel. Each monomer folds into two domains and bind one type 1 and one type 2 copper per subunit. Coppers from the same subunit are separated by ∼13 Å, while Cu−Cu distances are 30 Å or more when considering metals from different subunits. Type 1 coppers are buried ∼4−6 Å away from the protein surface in one of the two β-barrel domains. The type 2 copper centers are bound in the second domain at the interface between two subunits. The latter site is accessible to the surrounding milieu through a 12 Å channel.

The green and blue colors of Cu−NIRs relate to their type 1 copper. The absorption spectrum of a type 1 copper site is usually dominated by an intense sulfur-to-copper LMCT band near 600 nm ($\epsilon > 3000$ M^{-1} cm^{-1}) that leads to a blue color. Green Cu−NIR arises from an additional λ_{max} at ∼460 nm also identified as a sulfur-to-copper LMCT band by resonance Raman spectroscopy.[105] The green and blue type 1 Cu^{II} also exhibit different EPR signals with more rhombic or axial parameters, respectively. Despite these spectral differences, the structure of these type 1 Cu centers is nearly identical in the blue and green NIR; both are four-coordinate, ligated by a methionine thioether, a cysteine thiolate, and two histidine imidazoles. The geometry of the green type 1 copper is described as a flattened tetrahedron with a short $Cu-S_{met}$ bond length of 2.55 Å (for comparison, plastocyanin has a $Cu-S_{met}$ length of 2.82 Å). It is suggested that the color difference is influenced by a variation in the His−Cu−Met angle. The blue Cu NIRs have His−Cu−Met angles near 115°, while the green Cu NIRs have His−Cu−Met angles near 132°.[106]

In oxidized NIR, the type 2 copper centers are tetrahedral with three histidine imidazole ligands. The fourth ligand position is occupied by a water molecule. It is interesting to note that two of the histidine imidazole ligands are from one subunit, while the third histidine imidazole is from an adjacent subunit. This bonding arrangement positions the type 2 copper centers directly between monomer units. Within the same subunit, the type 1 and type 2 copper centers are linked by adjacent amino acid residues in the same polypeptide chain. The cysteine ligand of the type 1 center is sequentially adjacent to one of the histidine ligands of the type 2 center (Cys-136 and His-135 in *A. cycloclastes*). This covalent link between metal centers may facilitate electron transfer. The type 1 copper centers are likely to be the electron entry of NIR, accepting electrons from pseudoazurin. Electron transfer from the type 1 to type 2 sites has been studied using pulse radiolysis.[107−110]

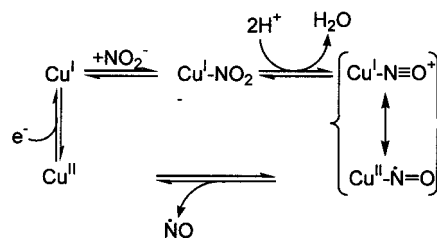The active site for nitrite reduction clearly involves the type 2 copper center. Type 2 Cu-depleted enzyme lacks enzymatic activity.[111] NIR activity is efficiently inhibited by cyanide and carbon monoxide.[3] Site-directed mutagenesis studies of direct copper ligands further support the involvement of the type 2 copper ion as the active site.[25,100] ENDOR, EXAFS, and X-ray crystallography have shown that nitrite bound to the oxidized enzyme in an asymmetric η^2-O,O bound nitrito ligand to the type 2 copper center in place of the coordinated solvent.[99,101,112,113]

Two distinct mechanisms for Cu-mediated nitrite reduction have been proposed. The first mechanism, proposed by Hulse and Averill,[2,114] is similar to the mechanism of nitrite reduction in cytochrome cd_1 NIR. This mechanism, outlined in Figure 6, involves the binding of nitrite to a reduced Cu(I) center (although NO_2^- may bind to Cu(II), which could then be reduced to Cu(I)). Protonation of nitrite to yield water and a Cu(I)-bound NO^+ (NO^+ is of an oxidation state equivalent to NO_2^-) species would be followed by the formation of an unstable $\{CuNO\}^{10}$ (equivalent to $Cu^{II}-NO^•$) system (again, see section III.A for more discussion of Enemark−Feltham notation), which would readily release NO and continue the catalytic cycle.

Although not depicted in the Figure, the copper−nitrosyl intermediate may interact with additional NO to form the dispropotionation products NO_2 and N_2O. There is evidence that Cu−NIRs may produce N_2O when the concentration of NO becomes high,[115] and the production of N_2O might be from disproportionation.

On the basis of crystallographic results revealing amino acid residues in close proximity to the type 2 copper active sites, another mechanism first suggested by Adman and co-workers[99,101] and later supported by Suzuki and co-workers[98,116] and others[117] has been recently discussed. This mechanism involves amino acid residues Asp-98 and His-255 (in *A. cycloclastes*) as general acid−base catalysts. These two residues are in close proximity to the copper-bound water ligand in the enzyme. The mechanism, shown in Figure 7, invokes nitrite binding prior to reduction of Cu(II) to Cu(I). Initially, the aspartate residue deprotonates the copper-bound water and nitrite displaces the hydroxide ligand, with nitrite bonding in an η^2-O,O′ fashion to a Cu(II) ion. In the second step, reduction of Cu(II) to Cu(I) is followed by a third step where the bound nitrite is protonated by the aspartate residue. The reaction is completed by the breaking of an N−O bond and concomitant protonation to form water, electron donation from copper to a formally NO^+ (equivalent to NO_2^-) moiety, and subsequent release of NO(g). Finally, the

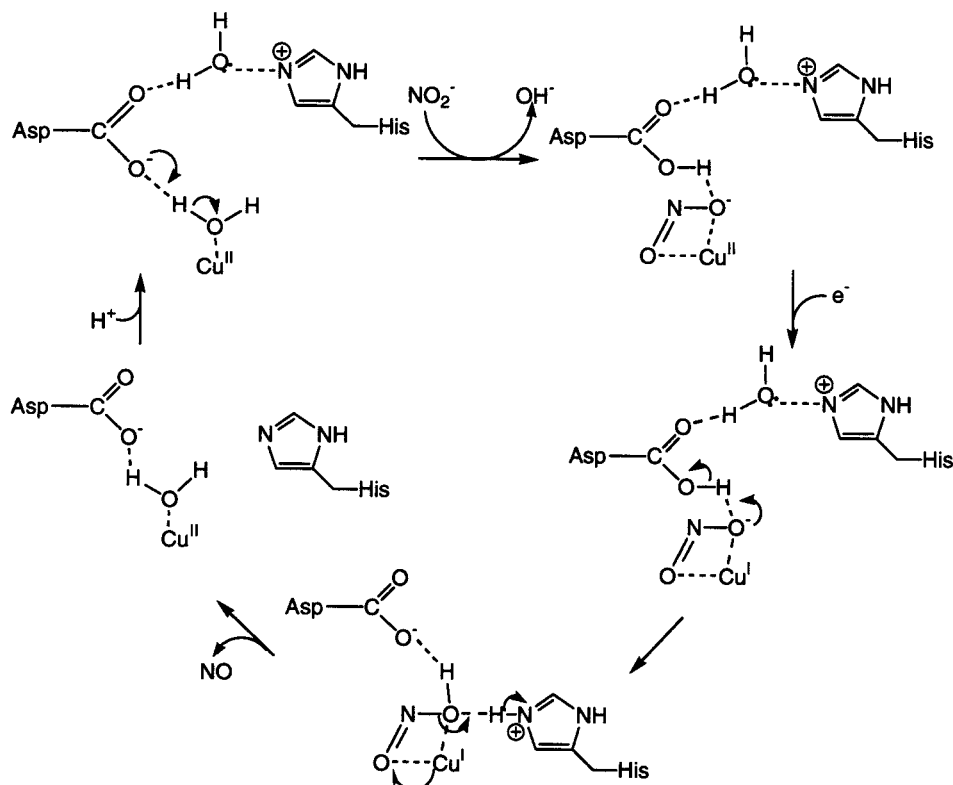**Figure 6.** General mechanism for Cu-mediated reduction of nitrite.

Figure 7. Second alternate mechanism for Cu-mediated nitrite reduction, involving both Asp-98 and His-255.

catalytic cycle is restarted by the donation of an external proton to the catalytic histidine residue.

This alternative mechanism supports the finding that oxidized Cu−NIR binds nitrite in an asymmetric η^2-O,O′ fashion.[101] In addition, recent studies by Shapleigh, Scholes, and co-workers[118,119] along with work by Hasnain and co-workers[120] have suggested that nitrite binding to the oxidized type 2 copper center might increase the redox potential at the type 2 copper site, thereby facilitating both the electron transfer from the type 1 copper and nitrite reduction. However, dehydration of the putative cuprous O-bound nitrito presupposes the formation of an O-bound Cu-nitrosyl species, which is unprecendented in inorganic copper chemistry (see section III). Moreover, mutagenesis studies that identified Asp-92 and His-255 as essential residues to the catalytic activity are being reevaluated,[116,117] although there is recent evidence that site-directed mutagenesis of His-255 to Asn results in a novel mode of nitrite binding, as determined by X-ray crystallography.[121] Using the physiological electron donor azurin, the specific activity of the D92N mutant protein was shown to be ~60% of that of the wild-type protein.[122] The conservation of NIR enzymatic activity despite the substitution of the carboxylate group by a nonionizable side chain thus casts doubt on the mechanism shown in Figure 7. Recent findings by Tolman[123,124] (also see section III.A.2) have shown that Cu(I) binds NO_2^- in an η^1-N fashion; it would seem more likely that nitrite binds to a reduced Cu(I) center during catalysis via η^1-N coordination. Such an interaction would expose the nitrite oxygen atoms to protonation and avoid a needed isomerization (from O-bound to N-bound) step in the mechanism.

B. Nitric Oxide Reductase

1. Structure

Genetic and biochemical analyses have shown that nitric oxide reductase and cytochrome oxidase have evolved from a common ancestor, assumed to be an anaerobic, NO-reducing enzyme.[125−131] The denitrifying NO reductases and the respiratory heme-copper cytochrome oxidases are members of the same superfamily, called the heme-copper oxidase superfamily. NOR is structurally most closely related to the cbb_3-type oxidases. At present, three different bacterial NORs have been characterized. All three are integral membrane metalloenzymes containing a unique non-heme iron center (Figure 8).

The best studied NORs are the cytochrome bc complexes (cNOR) purifed from gram-negative bacteria, e.g., *P. stutzeri, P. denitrificans,* and *Paracoccus halodentrificans*.[26,132−137] The purified cNORs consist of two subunits and use membrane or soluble *c*-type cytochromes or small blue copper proteins (azurin, pseudoazurin) as physiological electron donors (Figure 8).[1,5,138] Another type of NOR, qNOR, uses ubihydroquinone or menahydroquinone as an electron donor, consists of one subunit, and is not only present in soil and marine bacteria or in archaea but also in pathogenic microorganisms such as *Neisseria meningitides, Neisseria gonorrhea,* and *Corynebacterium diphteriae*, which do not denitrify.[139−141] A third type of NOR has been described recently that is present in the gram-positive bacterium *Bacillus azotoformans*.[142] This NOR uses menahydroquinone as an electron donor, consists of (at least) two subunits, and
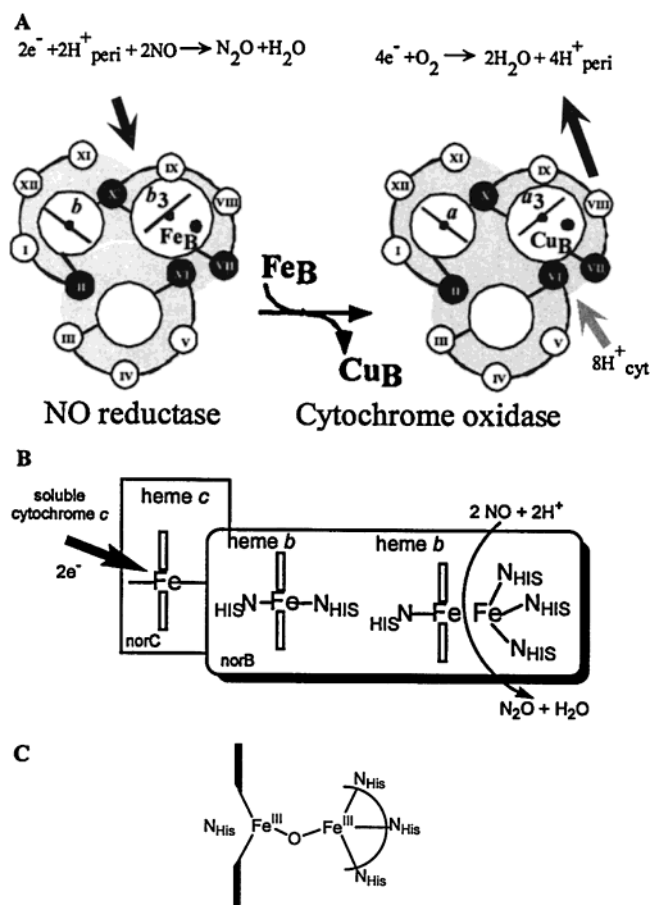
Figure 8. A: Topview of the putative structure of NorB and of SUI of cytochrome *c* oxidase.[137,140] Arrows indicate proton movements; those of the oxidase move vectorially from bottom to top crossing the cytoplasmic membrane. In contrast, the scalar protons in NO reduction move from top to the heme b_3–FeB center, located halfway in the membrane. Roman numerals refer to established and putative (NO reductase) transmembrane α-helices. Histidine ligands are located in the dark helices. B: Side view of cNOR showing the putative pathway of electron transfer from soluble electron donors via heme *c* of NorC to the binuclear center of NorB where the reduction of NO occurs (see text for further details). C: Proposed structure of the binuclear oxo-bridged heme/non-heme iron active site of NO reductase. Upon reduction, a bond is formed between the heme-iron and the histidine nitrogen atom (cf. Figure 9).

contains Cu_A.[143] It is called qCu_ANOR. The properties of these three types of NOR are treated below.

2. cNOR

Purified cNORs consist of two subunits, a smaller, heme *c* containing subunit, NorC (17 kDa), and a large, heme *b* containing subunit, NorB (53 kDa). On the basis of its amino acid sequence, NorB is homologous to the large subunit (SUI) of cytochrome oxidases.[26,132,133,135,136,144–146] Comparison of the genes present in the putative *nor* operons of various bacteria suggests that cNOR might consist of four subunits, NorE, a homologue to SUIII of cytochrome oxidases and NorF.[3,144,146] However, if the physiological protein complex includes the NorE and NorF gene products, they are lost upon extraction of the enzyme from the membrane by detergents. Similarly, purification of an active proton-pumping cytochrome aa_3 oxidase complex of *P. denitrificans* does not retain the bulk of SUIII and SUIV.[147,148] Thus, the function of these additional polypeptides is not clear. In cNOR purified from *P. denitrificans*, an equilibrium is observed between a heterodimeric NorC/NorB and a heterotetrameric form of the NorC/NorB complex.[135] Both the heterodimer and the heterotetramer exhibit comparable activities. In artificial membranes, the enzyme is heterotetrameric;[135] however, the type of complex formed in the native membrane is uncertain.

The primary sequences of the NorBC complexes and terminal cytochrome oxidases reveal the presence of six conserved hisitidine residues. In cytochrome *c* oxidases, these histidines ligate heme *a*, heme a_3, and Cu_B.[41,44,149–152] cNOR contains *b* hemes and non-heme iron in a 2:1 stoichiometric ratio.[26,135,145] In analogy to cytochrome oxidases, the six conserved histidine residues in NOR are proposed to coordinate heme *b* (bis-His) and heme b_3 (mono-His) and the non-heme iron (tris-His). The non-heme iron is labeled Fe_B and assumed to be structurally and functionally similar to Cu_B of cytochrome oxidase (cf. Figures 8 and 9).

NorB is an extremely hydrophobic subunit, which contains twelve putative transmembrane α-helices in accordance with the homologous SUI of cytochrome oxidases.[128] Electron cryomicroscopy studies of two-dimensional crystals of cNOR have shown that the three-arch structure detected in the SUI of cytochrome oxidases is also present in cNOR (cf. Figure 8)[135] and is also likely to be conserved in the qNOR and qCu_ANOR-type enzymes. The NorC subunit contains only a single, putative transmembrane α-helix. The low-spin *c* heme is most likely located in the periplasmic portion of the subunit. The binuclear center in NOR is presumed to be located within the membrane at a similar position as the binuclear center in cytochrome oxidase (cf. Figure 8A). Electrons from soluble or membrane-bound *c* cytochromes or pseudoazurin are first transferred to the heme *c* group of NorC and then via a low-spin heme *b* in NorB to the binuclear heme/non-heme iron active site where NO is reduced to N_2O (Figure 8B). If the binuclear center is accessible only for protons from the periplasmic side of the membrane, then the overall reaction catalyzed by NOR does not lead to the generation of a proton motive force because electrons and protons enter the catalytic center of the enzyme from the same, periplasmic side.

$$2NO + 2cyt\ c^{2+}_{peri} + 2H^+_{peri} \rightarrow$$
$$N_2O + H_2O + 2cyt\ c^{3+}_{peri}\ \ (5)$$
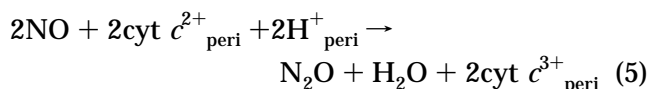
EPR, MCD, resonance Raman, and UV–vis spectroscopy methods have been used to demonstrate that one heme *b* is low-spin, while the other, heme b_3, is a pentacoordinated high-spin heme. The latter heme displays a unique absorbance at 595–600 nm in the oxidized enzyme.[26,27,135,145,153] In its reduced state, heme b_3 is pentacoordinated, high-spin, and mono-His ligated.[27] However, upon binding of CO or NO,

it becomes low-spin and hexacoordinated.[154,155] The high-spin heme b_3 and Fe_B are EPR silent in the oxidized enzyme and are suggested to form an antiferromagnetically coupled oxo-bridged heme/non-heme diiron center (Figure 8C).[27,28] The fully reduced enzyme is EPR silent, but partial reduction can lead to a loss of the magnetic coupling and the signals centered at either $g \sim 6.0$ or $g \sim 4.3$ have been assigned to high-spin heme b_3 or the non-heme iron Fe_B center, respectively.[136] However, in general, these EPR signals are weak, amounting to less than 10% of the enzyme concentration, and difficult to differentiate from signals resulting from the presence of adventitious heme and non-heme irons.

Direct evidence for the proposed μ-oxo diiron center in NOR came from resonance Raman experiments performed with the fully oxidized enzyme, in which an asymmetric Fe−O−Fe stretching mode was identified at 810 cm^{-1} that downshifts $\sim$30 cm^{-1} in $H_2^{18}O$. This assignment was confirmed by the detection of a similar signal in a synthetic oxo-bridged dinuclear model complex.[28,156,157] The pentacoordinated state of the heme iron, the strong resonance enhancement and frequency of the ν_{as}(Fe−O−Fe), and the absence of changes with D_2O are all consistent with the presence of a μ-oxo rather than a hydroxo bridge. An Fe−Fe distance of 3.5 Å and an (Fe−O−Fe) angle of $\sim$145° could be deduced from the observed frequency.[28]

3. qNOR

The first single-subunit, quinol-dependent qNOR was purified as a histidine-tagged enzyme from *Ralstonia eutropha*.[139,158] The enzyme consists of a single subunit with a molecular mass of 84 kDa. While the enzyme lacks heme c, it contains heme b and non-heme iron in an approximate 2:1 ratio, respectively. A reduced minus oxidized difference spectrum shows sharp α- and β-bands characteristic of low-spin heme and a decrease in absorbance at $\sim$580 nm assigned to a charge transfer band from a high-spin b heme. An additional transition was observed at $\sim$600 nm, but its origin is unclear. Despite the presence of some background signals from contaminants, the EPR spectrum displays resonances characteristic of a low-spin heme center. Stoichiometric signals for a high-spin heme center and a non-heme iron are lacking, suggesting an antiferromagnetic coupling between these groups as found in cNOR. The enzyme is inactive with cytochrome c as an electron donor, but can use menahydroquinone as a donor, classifying it as a qNOR. This activity is not inhibited by the quinone analogue HOQNO (2-heptyl-4-hydroxyquinolone-*N*-oxide). The most intriguing feature of qNOR is its N-terminal extension of about 280 amino acid residues. Sequence analysis indicates that this extension can fold into two transmembrane α-helices, separated by a large, relatively hydrophilic domain, which may contain the quinone binding site.[139] Although this domain has no sequence similarity to the quinol-oxidizing subunit of the terminal quinol oxidases, a thorough analysis indicates, surprisingly, sequence similarity to the

NorC subunit of cNORs.[159] Thus, qNOR is apparently a fusion of NorC and NorB. In this fusion the NorC-like domain could have lost the heme c center and obtained a quinol-binding site in the process of evolution. Alternatively, the opposite evolutionary scenario is possible, where qNOR could precede cNOR and the quinone-binding site evolved to a heme c anchoring domain.

Several archaea are capable of denitrification and were shown to reduce nitrate as in bacteria, via nitrite, NO, and N_2O to N_2.[3,5,8−12] *Pyrobaculum aerophilum* is a hyperthermophilic archaeon growing optimally at temperatures of 100 °C utilizing nitrate or oxygen as terminal electron acceptors for growth.[8,10] The NO reductase from this organism has been purified and exhibits MQH_2:NO oxidoreductase activity at temperatures as high as 95 °C.[160] The enzyme consists of a single subunit and contains heme and non-heme iron in a 2:1 ratio. Absorption spectra obtained on this enzyme indicate the presence of one low-spin and one high-spin heme. As in other NORs, the high-spin heme and non-heme iron are EPR silent due to antiferromagnetic coupling. In all these respects, the enzyme is similar to that of *R. eutropha*. However, reversed-phase chromatography of heme extracts of the pure enzyme revealed modified hemes containing a peripheral hydrophobic tail. Heme O_{p1} and O_{p2},[161] ethenylgeranylgeranyl and hydroxyethylgeranylgeranyl derivatives of protoporphyrin IX, respectively, are present in an approximate 1:1 stoichiometry. The archaeal qNOR is the first example of a NOR that contains a modified heme reminiscent of bo_3 and aa_3 oxidases rather than heme b. Whether this modification reflects an adaptation to life at high temperatures or serves another purpose remains to be established.

The presence of genes encoding qNORs in pathogenic microorganisms or marine bacteria, which do not denitrify, suggests that their physiological role may be to scavenge ambient toxic NO. As to the pathogenic bacteria, upon infection, the macrophages of the human defense system, for example, will generate micromolar concentrations of NO via the inducible NO synthase, iNOS. The toxicity of NO and the bactericidal potential of the macrophages are greatly increased because along with NO, the macrophages produce superoxide, the two compounds reacting to yield peroxynitrite, which is more toxic than either of the individual reactants.[141,162] Thus, microorganisms containing a qNOR will have a selective advantage to escape from the host's immune system. So far, none of these qNORs have been purified. A similar protective role toward high levels of NO was also assigned to bacterial flavohemoglobin and cytochrome c.[90,93,163,164]

4. qCu$_A$NOR

Recently, the first purification of a NO reductase from a gram-positive bacterium *B. azotoformans* was described.[142,143] The purified enzyme consists of two subunits and contains one non-heme iron, two copper atoms, and two b-type hemes per enzyme complex. Heme c was absent. One of the hemes is a low-spin

heme b in which the two axial hisitidine imidazole planes are positioned at an angle of 60–70° instead of the normal "parallel over meso" position in other NORs and cytochrome oxidases. The second heme b is high spin, binding CO in the reduced state. The high-spin heme center and the non-heme iron are EPR silent as in the other types of NOR. Surprisingly, the enzyme contains copper in the form of copper A, with a binuclear $Cu_2(\mu\text{-Cys})_2(His)_2$ core, which effects one-electron transfers cycling between $(Cu_2)^{2+}$ and $(Cu_2)^{3+}$ delocalized mixed-valent states,[149,151,165] a metal cofactor previously detected only in cytochrome oxidases and nitrous oxide reductases. Like the qNOR, the qCu$_A$NOR enzyme uses menahydroquinone as electron donor, while no activity could be detected with cytochrome c. Copper A and both hemes are reduced by menaquinol. On the basis of its prosthetic group composition, the *B. azotoformans* NO reductase appears to be a true hybrid between copper A containing cytochrome oxidases and NO reductases present in gram-negative bacteria.

The structural and functional variation observed in cytochrome oxidases is also present in the NORs. In both classes of enzymes, quinol and cytochrome c oxidizing variants are found. In addition, similar prosthetic groups, copper A and c-type hemes, serve as the electron entry.

5. Catalytic Mechanism and Comparisons to Heme–Copper Oxidases

Spectroscopic studies have demonstrated the presence of a heme/non-heme diiron center in the active site of cNOR. Resonance Raman data show that in the fully reduced enzyme the catalytic heme is pentacoordinated to a neutral histidine, while this histidine ligand is lost in the oxidized state. Indeed, the ferric heme remains five-coordinated and its sole axial ligand is an oxo group bridging the two irons. From the description of the oxidized and reduced state of the enzyme, a catalytic cycle was proposed (Figure 9).[26–28] Reduction of the diiron site weakens the oxo bridge and favors the formation of the heme Fe(II)–His bond. The enzyme can bind one NO molecule per ferrous iron. As observed in several hemoproteins, e.g., hemoglobin or soluble guanylyl cyclase,[166,167] the heme Fe(II)–His bond is broken after the binding of NO, forming an initial six-coordinate heme–nitrosyl, which then goes on to form a pentacoordinate heme nitrosyl complex.[168] The close proximity of the two nitrosyl groups destabilizes these otherwise poorly reactive {FeNO}^{7} species and promotes formation of the N–N bond. The product N$_2$O leaves the active site while formation of the oxo bridge completes the catalytic cycle. Redox potentiometry of the *P. denitrificans* cNOR yielded midpoint potentials of 310 and 345 mV for the heme c and low-spin heme b, respectively. The non-heme iron center was not monitored directly optically or by EPR, but its midpoint potential was inferred from a shift in the optical spectrum of the high-spin heme b center, yielding redox potentials of 60 and 320 mV for the high-spin heme b and the Fe$_B$ non-heme iron, respectively.[153] The low redox potential of heme b_3 was
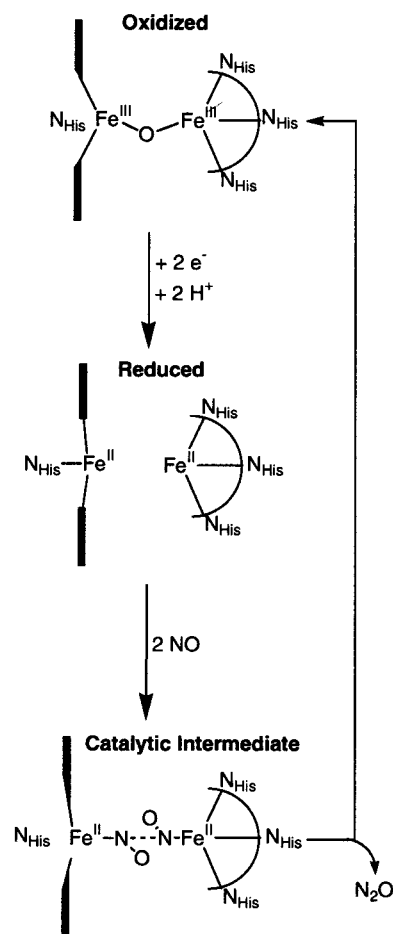

Figure 9. Putative catalytic cycle of NO reductase.

proposed to prevent the two-electron reduction of the heme b_3/non-heme iron binuclear center and avoid the formation of a stable Fe(II) heme b_3–NO complex. These authors favor an alternative catalytic mechanism where only the non-heme iron binds NO and forms a dinitrosyl complex.[5,169] However, according to this proposal, a significant catalytic role for the high-spin b heme, other than in electron transfer, is lacking.

Incubation of oxidized or reduced *P. denitrificans* cNOR with NO under turnover conditions revealed EPR signals around $g = 2.0$ and 4.0. These signals are typical for ferrous heme nitrosyl and non-heme ferrous nitrosyl complexes, respectively.[135] EPR evidence was also obtained for a pentacoordinated ferrous heme nitrosyl, in agreement with resonance Raman spectroscopy.[27,155] The concentrations represented by the $g = 2.0$ and 4.0 signals are apparently low. Formation and decay rates of these spectroscopic signatures will be needed to assign these species to true intermediates of the catalysis.

So far, there has been no pre-steady-state kinetic analyses of NOR. Steady-state turnover kinetics of cNOR yielded a sigmoidal relation between [NO] and activity, as expected for an obligatory two-substrate (i.e., two molecules of NO) reaction.[26,133,135] At high, nonphysiological concentrations of NO (about 10 μM), substrate inhibition by a single NO molecule is observed for all three types of NOR. The site of inhibition is unknown, but the inhibition is due to binding of NO to the oxidized enzyme, most likely to

the heme b_3.[26] Maximal turnover rates of purified NOR amount to about 200 NO/s, a value approximately 2-fold lower than the steady-state turnover rate during denitrification in the cellular membrane. The use of nonphysiological electron donors and the detergent extraction procedure are probable causes for the lower rates observed in the enzymatic assay. Consequently, the apparent K_m value for NO of 250−500 nM should be considered as an upper limit.[26,133] Since the free concentration of NO in soil, for example, is generally much lower, below 10 nM, the true K_m for NO may be closer to this latter value.

cNORs are also capable of catalyzing the four-electron reduction of dioxygen to water.[133,170] The rate of this reaction (40 electrons per second) is about 5-fold lower than that of NO reduction. The reported apparent K_m for dioxygen is very high (0.9 mM)[133] but was recently measured to be much lower (20 μM),[171] yielding a specificity constant (k_{cat}/K_m) of about 2×10^6 M^{-1} s^{-1}. Terminal cytochrome oxidases are capable of reducing NO to N$_2$O. Mitochondrial oxidases perform only a single or very few turnovers before becoming, reversibly, inhibited.[172,173] The prokaryotic oxidases, which may be structurally more related to the NO reductases than the mitochondrial enzymes, can sustain catalysis, but the rate is only 0.5 NO/s at 50 μM of NO, i.e., giving a specificity constant of 10^4 M^{-1} s^{-1}.[174] Thus, although NORs and oxidases each catalyze both NO and dioxygen reduction, oxidases have evolved to catalyze efficiently dioxygen reduction (250 O$_2$/s; $K_m = 5$−100 nM; specificity constant $>10^9$ M^{-1}s^{-1}) and NO reductases to efficiently catalyze the reduction of NO (specificity constant $>5 \times 10^8$ M^{-1} s^{-1}).

Sequence comparison of the primary structures of NorB subunits from several bacteria reveals several conserved glutamic acid residues that are absent from SUI of terminal heme copper oxidases.[128] These carboxylate groups of one or more of these glutamate residues may play a role in non-heme iron binding, providing a possible fifth or sixth ligand. Along with the formal charge from the porphyrinate (−2) and the μ-oxo bridge (−2), the ligation of two carboxylates would yield an electroneutral diferric active site. Alternatively, the vicinity of these charges may modulate the redox potential of the metal centers; the glutamate residues may also participate in proton binding.[170] Resonance Raman and FTIR spectroscopy of the reduced CO-binding enzyme indeed suggests a negatively charged active site.[27] Glu-198 in NorB is predicted to be located in helix VI, one helical turn away from His-194, a putative ligand to Fe$_B$. The replacement of Glu-198 by Ala caused an inactivation of the enzyme. However, the effect on the non-heme iron content was not determined.[170] Likewise, a replacement of Glu-125 by Ala rendered the enzyme inactive. This latter residue is predicted to be located on a periplasmic surface close to helix IV and, thus, distant to any of the metal centers. It is posible that this glutamate residue is involved in the binding of protons coming from the periplasm en route to the active site.[170]

The heme Fe−Fe$_B$ distance of approximately 3.5 Å in cNOR is much larger that the 5 Å heme Fe−Cu$_B$ distance in cytochrome oxidase. Instead of the diferric μ-oxo bridge observed in NOR, the binuclear center of cytochrome oxidase has been proposed to contain a peroxo bridge, or hydroxy and aqua ligands between the heme a_3 and the Cu$_B$.[44,175,176] In the ba_3-cytochrome c oxidase from *Thermus thermophilus*, the electron density between the heme a_3 and the Cu$_B$ is consistent with a single oxygen atom (oxo, hydroxo, or aqua) but the heme Fe−Cu$_B$ distance of 4.4 Å is still large.[150] Despite the difference in metal−metal distance and metal composition, NOR and cytochrome oxidase are both capable of catalyzing NO and O$_2$ reduction to N$_2$O and H$_2$O, respectively, albeit with significantly different specificities. There seems to be no a priori chemical reason iron would be preferred over copper for NO reduction.

An important feature in the active site of oxidases is the presence of a cross-linking between a tyrosine side chain and one of the histidine ligands of Cu$_B$.[41,150,152,177] The (His−Tyr) cross-link is likely to be catalyzed by Cu$_B$ itself in the premature active site. On the basis of the primary sequence of NorB, this tyrosine is absent in NORs. Requirement of copper and dioxygen for the posttranslational modification of tyrosine to topaquinone is well documented in amine oxidases.[178] In the copper-containing galactose oxidase, it is a cysteine that is cross-linked to one of the two tyrosine ligands.[179] In cytochrome c oxidases, the cross-linking of the tyrosine may secure its close proximity to the two metals and allows it to provide one of the four electrons reducing O$_2$ to H$_2$O.[180,181] Another important difference between NOR and terminal oxidases is in the conservation of the redox free energy of their respective reactions (which are quite similar in value) and in the intricate coupling of proton translocation to electron transfer.[39,42] The greater possible range of ligation states of reduced and oxidized copper as compared to iron may make copper a more suitable metal to couple proton binding and translocation to changes in the redox states of the heme iron.

III. Coordination Compounds

The synthesis of inorganic "model" complexes[182] is driven by the notion that the fundamental chemistry of a metal ion is inherently intact in a metalloenzyme or metalloprotein environment. The chemistry of a protein active site is governed by both the immediate and the second coordination shell environment around the metal ion, as provided by the protein amino acid sequence and secondary structure(s).[183,184] While the exact protein ambience cannot always be mimicked exactly in a synthetic model (or not even closely, sometimes), the local structure and geometry with the corresponding spectrochemical properties can be modeled. The overall goal is to construct synthetic analogues capable of predicting and/or reproducing key aspects of structure, spectroscopy, magnetic and electronic structure, and chemical reactivity of biological systems.[182,185] As such, first-generation models consist of reasonably reproducing metal identity, oxidation state, coordination number, and donor-ligand identity (e.g., N-donor, O-donor, S-donor) at the active site. Following structural and spectroscopic

characterization, future models are then synthesized to either corroborate or refute a given spectral or structural feature proposed in biological systems, as applicable. Finally, "functional" models that mimic biological reactivity are always exciting prospects from the standpoint of (i) the future design of efficient small molecule catalysts and (ii) providing insights into protein biochemical structures and mechanisms.[182]

A. NIR Model Compounds

The focus of this section is to discuss biologically relevant (i) copper−nitrite complexes, (ii) heme−nitrite complexes, and (iii) oxidized Fe(III)−nitric oxide species. Each of these species has been invoked as an intermediate in bacterial nitrite reductase mechanisms. A more complete treatment of copper nitric oxide interactions and chemistry (III.C) and reduced Fe(II)−nitric oxide compounds (III.D) is presented in the later sections.

1. General Considerations

A key step in Averill's proposed reaction mechanism for the reduction of nitrite to nitric oxide, applicable to both iron- and copper-containing NIRs, is the presence of a reduced enzyme metal−nitrite $(E)M-NO_2^-$ complex.[2,98] For iron enzymes, this would be $(E)Fe^{II}-NO_2^-$, while copper would present $(E)Cu^I-NO_2^-$. Subsequent protonation, dehydration, and electron transfer (not necessarily in that order) would yield an oxidized $(E)M-NO$ system. According to Enemark−Feltham notation,[53] for iron, this latter species would be $(E)Fe^{III}-NO^\bullet$, or an $\{FeNO\}^6$ complex. For copper, the species $(E)Cu^{II}-NO^\bullet$ is classified $\{CuNO\}$.[10] The MNO fragment is treated as a single, 3-atom unit that counts one electron from the π^*-orbital of NO, plus the valence-shell d-electrons from the metal (remembering that for transition metal complexes, the nd orbital resides lower in energy than either the $(n+1)$s or $(n+1)$p orbitals), yielding the total electron count n for $\{MNO\}^n$. In either the Fe or the Cu system, the "oxidized" MNO moiety is less stable than the corresponding reduced MNO system (e.g., $\{FeNO\}^6$ or $\{CuNO\}^{10}$, formally Fe(III)−NO or Cu(II)−NO, form less stable M−NO adducts when compared to the "reduced" analogues, either $\{FeNO\}^7$ or $\{CuNO\}^{11}$). Therefore, the formation of the more reactive, $(E)Fe^{III}-NO$ or $(E)Cu^{II}-NO$ reaction intermediate facilitates NO release from NIR (leaving behind either Fe(III) or Cu(II)), prohibiting the formation of a stable metal−nitrosyl complex. Incidentally, the inclusion of an $(E)M-NO$ intermediate in the reaction mechanism in some sense supports the notion of an N-bound nitrite adduct precursor during the enzyme reaction cycle; otherwise, a rearrangement would be needed to accomplish the formation of an N-bound nitrosyl, which is the normal mode of transition metal binding of nitric oxide.

A general equation for the copper(I)-mediated reduction of nitrite to nitrogen monoxide involves two protons:

$$Cu(I) + NO_2^- + 2H^+ \rightarrow Cu(II) + NO + H_2O \quad (6)$$
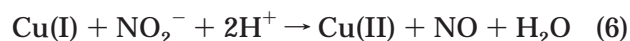
However, studying this reaction can be complicated by several other reactions, which might otherwise consume NO or yield quantities of NO that are stoichiometrically inconsistent with the proposed biomimetic reaction scheme. The two major, competing reaction pathways that can skew this reactivity are the following:

$$3H^+ + 3NO_2^- \rightarrow 2NO + HNO_3 + H_2O \quad (7)$$

$$3NO \rightarrow N_2O + NO_2 \quad (8)$$
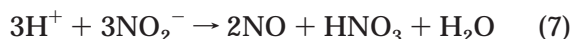
The first reaction is simple acid-catalyzed decomposition of nitrite, where (presumably) 3 equiv of nitrous acid dissociates into nitric oxide, nitric acid (or nitrate and a proton), and water.[186] The second reaction is classical nitric oxide disproportionation, to give nitrous oxide and nitrogen dioxide. As will be discussed later, copper, iron, and other transition metals may act as catalysts in NO disproportionation reactions.[186]

2. Synthetic Copper Complexes: Models for the Type 2 Cu of NIR

The modeling of the copper nitrite reductases begins with consideration of the structure around the copper ions in the native enzyme; see section II.C for full details. The active site is comprised of a type II copper center, containing a copper ion ligated by three cofacial histidine residues and a water (or possibly a hydroxide). Synthetic modeling of this active site would generally consist of three key features: (1) a mononuclear Cu ion complex, (2) a tridentate, nitrogen-donor ligand framework, and (3) an accessible $Cu(I)-NO_2^-$ adduct.
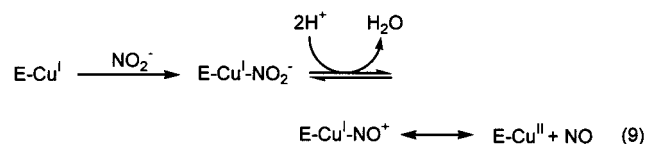
The proposed course of reaction for nitrite reduction in Cu NIRs is summarized in eq 9. A key step in this mechanism is the formation of a reduced enzyme−substrate complex, $E-Cu^I-NO_2^-$. Numerous copper(II)−nitrite complexes exist,[187−202] while none of these have demonstrated the ability to mimic the enzymatic reduction of nitrite to nitric oxide and water. Copper(II)−nitrite systems actually form rather stable complexes that do not support nitric oxide formation. The key challenge was the synthesis of a reduced Cu(I)−nitrite adduct or intermediate (possibly generated in situ) that showed biomimetic reactivity and further supported the mechanism purported by Averill (see Figure 6).[2] As will be discussed below, copper- and acid-catalyzed nitrite reduction, similar to the above mechanism, has now been accomplished by several research groups.

Structurally speaking, nitrite may coordinate to a mononuclear Cu ion in one of four ways.[187] As demonstrated in Figure 10, monodentate coordination of nitrite may occur through either nitrogen, η^1-N (**A**), or oxygen, η^1-O (**B**). Binding of nitrite in a bidentate fashion to Cu would yield either an oxygen,

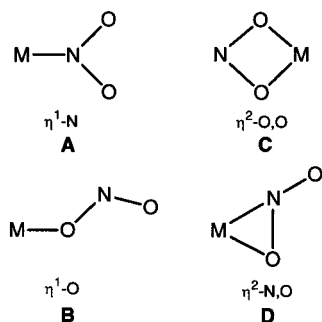**Figure 10.** Bonding modes of mononuclear metal–nitrite and metal–nitrito complexes.

oxygen bound species, η^2-O,O (**C**), or a mixed nitrogen/oxygen-coordinated complex, η^2-N,O (**D**). In addition, one must also consider the possibility of an asymmetric, η^2-O,O′-bound moiety (similar to **C**) containing only one formal M–O bond and a second, "long-contact" M–O interaction (generally with a Cu–O length >2.5 Å). On the basis of the hard–soft acid–base theory (HSAB), it should be expected that Cu(I) would prefer N-ligation, while the harder Cu(II) would prefer O-ligation, considering purely monodentate bonding modes. In fact, nearly all of the known Cu^{II}–NO_2^- crystal structures contain an O-bonded nitrito moiety,[187] while the only known Cu(I)–nitrite adduct is an N-bonded nitrite.[123,203] These are discussed below.

Functional Models: Mononuclear Copper–Nitrite Complexes. The first functional, mononuclear biomimetic model of copper NIR reactivity was developed by Tolman and co-workers.[123,203] Their system featured an isolable Cu(I)–nitrite adduct that could be reacted with acid (or acid equivalent) to yield nitric oxide and water, a reaction identical to the scheme proposed by Averill (see Figure 6).[2] As seen in Figure 11, the complex [((i-Pr)$_3$TACN)Cu(CH$_3$CN)]-PF$_6$ ((i-Pr)$_3$TACN = 1,4,7-triisopropyl-1,4,7-triazacyclononane) (**1**) reacts with sodium nitrite to afford the dinuclear, bridged dicopper(I,I)–nitrite complex [[((i-Pr)$_3$TACN)Cu]$_2$(μ-NO$_2$)]PF$_6$ (**2**). Complex **2** may be converted to a mixed-valent Cu(I,II) species **2a**, with a bridging nitrite, by oxidation using ferrocinium ion, e.g., (Cp$_2$Fe)(PF$_6$); this dinuclear copper product has been both spectroscopically (UV/vis, resonance Raman, EPR, and FTIR) and structurally characterized.[203] The subsequent reaction of the bridged Cu(I,I) complex (**2**) with triphenylphosphine, to remove one of the Cu(I) ions of the binuclear complex, yielded the mononuclear, reduced Cu(I)–nitrite adduct ((i-Pr)$_3$TACN)Cu(NO$_2$) (**3**) and the Cu(I)–phosphine complex [((i-Pr)$_3$TACN)Cu(PPh$_3$)]-PF$_6$ (**4**). Incidentally, the copper–phosphine adduct **4** may be synthesized by the direct reaction of **1** with 1 equiv of triphenylphosphine. Also of note is that the mixed-valent Cu(I,II) species **2a** may be generated by reacting complex **3** with a Cu(II) species. Compound **3** was the first example of a mononuclear copper(I)–nitrite complex, and its formulation and structure were confirmed by X-ray crystallography; nitrite was bound in an η^1-N fashion, as indicated.

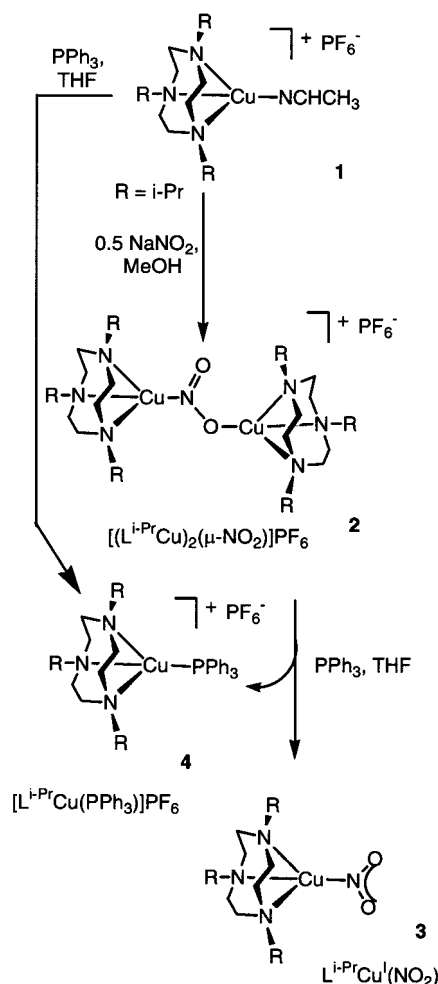To pursue nitrite reductase-like reactivity, compound **3** reacts with 2 equiv of acetic acid to yield

Figure 11. Synthesis of a stable, mononuclear η^1-N-nitrite copper(I) complex (**3**) by reaction of triphenylphosphine with a μ-NO$_2^-$ dicopper(I) complex (**2**).
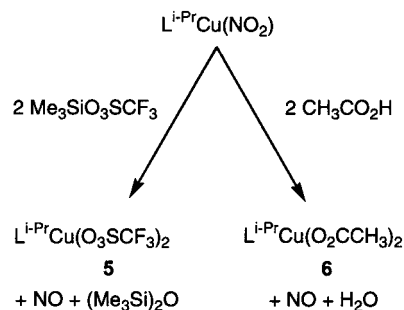

Figure 12. Evolution of NO from Cu(I)–nitrite adducts, facilitated by acid or acid equivalent.

[((i-Pr)$_3$TACN)Cu(O$_2$CCH$_3$)$_2$] (**5**) and also nitric oxide (Figure 12), as detected by gas chromatography. This reaction is biomimetic, as it models the reactivity of NIRs by converting nitrite to nitric oxide, by starting from a Cu(I)–nitrite complex and yielding an oxidized Cu(II)–nitrosyl product that dissociates NO-(g). The use of the Lewis acid Me$_3$SiO$_3$SCF$_3$ also promotes NIR activity. The copper-containing product of this reaction is [((i-Pr)$_3$TACN)Cu(O$_3$SCF$_3$)$_2$] (**6**)-(Figure 12). It is presumed that these reactions proceed by way of Lewis acid interaction with bound nitrite followed by dehydration to give a {CuNO}^{10} species, possibly a Cu(II)–nitrosyl adduct that then

dissociates to yield NO(g) and a Cu(II) ion. However, attempts to characterize the putative $\{CuNO\}^{10}$ intermediate proved to be unsuccessful.[124,203]

During the course of these studies, Tolman also reported the preparation of a mononuclear, Cu(II)−nitrite complex with a tris(pyrazolyl)borate ligand.[192] The coordination compound $[Tp^{tBu,H}]Cu(NO_2)$ (**7**) ($Tp^{t\text{-}Bu,H}$ = tris(pyrazolyl) hydroborate; substituent tBu in 3-pyrazolyl positions) was synthesized and characterized by X-ray crystallography. The most notable feature in the structure is the (nearly) symmetrically bound, η^2-O,O-bonded nitrite ligand. The overall geometry of the complex is a five-coordinate, distorted trigonal bipyramidal configuration. The reported EPR spectrum contains a rhombic EPR signal, indicative of the unusual geometry about the copper-(II) ion (in typical five-coordinate Cu(II) complexes, the observed EPR signal is generally axial). Interestingly, the nitrite ligand is quite labile, being displaced by addition of either (PPN)Cl or Me_3SiOTf (−OTf = $^-O_3SCF_3$) to afford the respective $Tp^{tBu,H}Cu^{II}Cl$ or $Tp^{tBu,H}Cu^{II}OTf$ complexes.

Casella and co-workers were also able to successfully synthesize and characterize reduced Cu(I) complexes that demonstrated biomimetic reactivity.[204−206] Copper(I) and copper(II) complexes were synthesized utilizing the six ligands shown in Figure 13. These include bis[(1-methylbenzimidazol-2-yl)methyl]-amine (1-BB), bis[(2-(1-methylbenzimidazol-2-yl)ethyl]amine (2-BB), N-acetyl-2-BB (AcBB), tris[2-(1-methylbenzimidazol-2-yl)ethyl]nitromethane (TB), bis(2-(3,5-dimethyl-1-pyrozolyl)ethyl]amine (ddah), and N,N-bis(2-ethyl-5-methyl-imidazol-4-ylmethy-l0-aminopropane (biap). Several of the corresponding Cu(II) complexes, including three Cu(II)−nitrito compounds and a bis(nitrito) Cu(II) complex, were characterized by X-ray crystallography. The mononuclear Cu(II)−nitrite complexes are coordinated in an asymmetric η^2-O,O′ fashion, with one oxygen formally bonded to copper (2.037(2) Å for Cu(ddah)(NO₂), 1.962(6) Å for $[Cu(1\text{-}BB)(DMSO)(NO_2)]^+$, and 2.008-(6) Å for $[Cu(2\text{-}BB)(NO_2)]^+$), while a long contact to the other oxygen of nitrite is observed (2.390(3) Å for Cu(ddah)(NO₂), 2.678(8) Å for $[Cu(1\text{-}BB)(DMSO)-(NO_2)]^+$, and 2.439(8) Å for $[Cu(2\text{-}BB)(NO2)]^+$).[204,206] The bis(nitrito) complex, $Cu(biap)(NO_2)_2$, features one nitrite coordinated in an asymmetric η^2-O,O′ bonding fashion, while the second nitrite is η^1-O bonded. For the asymmetric, bidentate nitrite, the formally bonded oxygen is significantly closer (2.012(5) vs 2.648(6) Å) than the long-contact oxygen. Incidentally, the Cu−O bond distance for the monodentate nitrite oxygen is exceptionally long (2.348(6) Å).[205] Unfortunately, during the course of these studies, no Cu(I)−nitrite adduct structures were successfully solved by X-ray methods. This could be due in part to extremely high reactivity of any formed Cu(I)−nitrite adducts. Nonetheless, the $[LCu^I]PF_6$ complexes were reacted with NaNO₂ and HBF₄·Et₂O in acetonitrile to yield NO and the oxidized, Cu(II) complexes (eq 10a). All six ligand systems accomplished nitrite reduction, with the best results obtained using the long-armed 2-BB ligand (overall rankings, according to ligand type: 2-BB > 1-BB > ddah > TB > AcBB). Casella
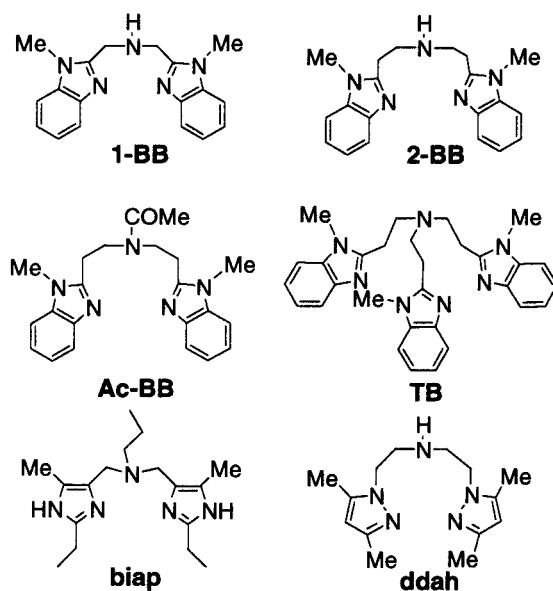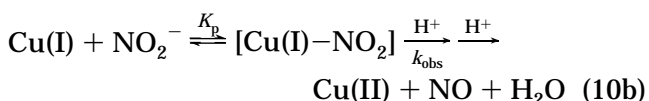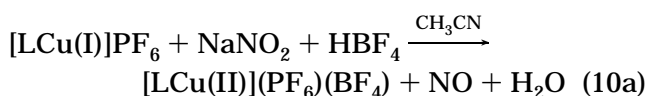

Figure 13. N-donor ligands used by Casella and co-workers to study Cu(I) and Cu(II) complexes, which are functional Cu−NIR models systems.

supposes that the two methylene spacers linking the benzimidazole to the central amine nitrogen of the 2-BB ligand are better able to accommodate the Cu(I) to Cu(II) geometric interconversion and, therefore, enhance the observed reactivity (note: ligands providing for six-membered chelate rings provide stabilization to Cu(I) (relative to Cu(II)) as deduced from measuring complex redox potentials electrochemically).[207,208] Mechanistic investigation into the reduction of nitrite supports eq 10, and the reactivity is first order in $[Cu^I]$ and $[H^+]$ and demonstrates saturation kinetics based on $[NO_2^-]$.[206] The data favors a mechanism that involves an inner-sphere electron transfer that follows protonation of the bound nitrite ligand.[204−206]

$$[LCu(I)]PF_6 + NaNO_2 + HBF_4 \xrightarrow{CH_3CN}$$
$$[LCu(II)](PF_6)(BF_4) + NO + H_2O \quad (10a)$$

$$Cu(I) + NO_2^- \underset{}{\overset{K_p}{\rightleftharpoons}} [Cu(I)\text{-}NO_2] \xrightarrow[k_{obs}]{H^+} \xrightarrow{H^+}$$
$$Cu(II) + NO + H_2O \quad (10b)$$

Casella's work is rather interesting, in terms of not only his successful biomimetic reactivity but also the reported structures of his copper(II)−nitrite complexes. These systems feature O-bonded nitrite adducts, similar to the O-bonded nitrite observed in the reaction of Cu(II) NIR with nitrite. This mode of bonding contrasts the N-bound nitrite−Cu(I) adduct determined by Tolman.[123,203] Controversy still remains as to whether the nature of the nitrite intermediate(s) is N- or O-bound in reduced biological NIR systems.

Another recent copper−nitrito complex includes work by Schugar and co-workers.[209] Use of the ligand tris[(2-(1-methyl)imidazolyl]methoxymethane (TIMM) led to the synthesis of the bis(nitrito) complex (TIMM)Cu^II(NO_2)_2 (**8**). From the X-ray crystal structure of this complex, it was revealed that both nitrito

ligands were bound in an asymmetric η^2-O,O fashion. The formal Cu−O bonds (1.990(2) and 1.993(3) Å) were considerably shorter than the Cu−O long contacts (2.488(3) and 2.513(3) Å).[209] Interestingly, the Cu(II) ion is of distorted octahedral geometry and is only coordinated by two of the three imidazoles of the tridentate TIMM ligand.
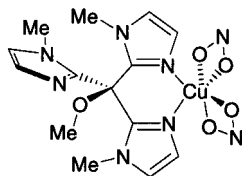

A highly interesting, solvent-induced interconversion between η^1-N-bound nitrite and asymmetric η^2-O,O′-bound nitrito was demonstrated by Tanaka and co-workers.[194] The complex [(TMPA)Cu^{II}(NO$_2$)](PF$_6$) (**9**) (TMPA = tris((2-pyridyl)-methyl)amine) recrystallizes from water to yield an η^1-N-bound nitrite that has been characterized by X-ray crystallography. However, the complex formed by recrystallization from methanol is [(TMPA)Cu^{II}(ONO)](PF$_6$) (**10**), featuring an asymmetric η^2-O,O′-bound nitrite, as also demonstrated by the X-ray crystal structure. The asymmetric η^2-O,O′-bound nitrite has a Cu−O bond length of 1.938(2) Å.
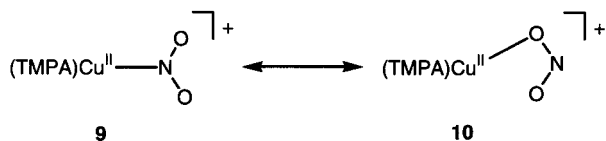

The long-contact oxygen has a Cu−O length of 2.79 Å and manifests a lengthening of the *trans*-pyridyl nitrogen-to-copper bond length (2.253 Å for the trans Cu−N$_{py}$ vs 2.039(5) and 2.049(5) Å for the other two Cu−N$_{py}$ bonds).[194] The authors go on to demonstrate the electrocatalytic reduction of NO$_2^-$ to N$_2$O (and small amounts of NO) in the presence of [(TMPA)-Cu(H$_2$O)]$^{2+}$ (**11**) at a potential of −0.40 V (vs Ag/AgCl) in H$_2$O at pH = 7.0. Interestingly, the starting material [(TMPA)Cu(H$_2$O)]$^{2+}$ (**11**) can be recovered after electrolysis. The exact mechanism of this catalytic reduction of nitrite to nitrous oxide is not fully understood. However, the authors speculate that a bound nitrite or nitrito ligand is dehydrated to give [(TMPA)Cu(NO)]$^+$, which possibly dimerizes to form a bridging N$_2$O$_2$ moiety. Decomposition of the N$_2$O$_2$ species would then yield N$_2$O.[194] This proposed dimerization is similar to the mechanism proposed by Karlin and co-workers[210] in the reaction of [(TMPA)Cu(CH$_3$CN)]$^+$ (**48**) with NO, as discussed below (see III.C).

Later work by Tanaka and co-workers involved the systematic comparison of methyl-substituted (TM-PA)Cu complexes and catalytic NO$_2^-$ reductase activity.[211] The methyl groups were introduced to the 6-position of the pyridine rings of TMPA; the ligands are designated (Me$_n$-TMPA) with n = 0, 1, 2, and 3. Reaction of the [(Me$_n$-TMPA)CuCl]$^+$ complexes with nitrite afforded only nitrito complexes, as evidenced by FTIR spectroscopy (observation of ν(N=O) near

1400 cm^{-1} and ν(N−O) near 1090 cm^{-1} for each complex), although X-ray crystal structures were not obtained. The efficiency of electrolytic catalytic reduction of nitrite was found to decrease in the order TMPA > Me$_1$-TMPA ≫ Me$_2$-TMPA ≫ Me$_3$-TMPA.[211] This loss of reactivity is not attributed to the increasing steric hindrance about the copper ions but rather is due to electronic effects and molecular structure variations imposed by the methyl substitutions.
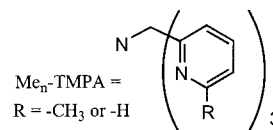
Ford and co-workers[212] report the use of nitric oxide to reduce the copper(II) complex [(dmp)$_2$Cu]$^{2+}$ (**12**) (dmp = 2,9-dimethyl-1,10-phenanthroline) to copper-(I) when dissolved in protic solvents and exposed to excess NO. In addition, when methanol was used as a solvent (or cosolvent), it was observed that CH$_3$-ONO was formed quantitatively, according to eq 11.

$$Cu(dmp)_2^{2+} + ROH + NO \rightleftharpoons$$
$$Cu(dmp)_2^{1+} + RONO + H^+ \quad (11)$$
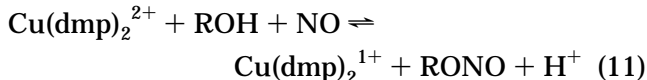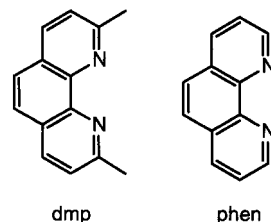
It is interesting to note that a similar reaction utilizing the closely related complex [(phen)$_2$Cu-(H$_2$O)]$^{2+}$ (**13**) (phen = 1,10-phenanthroline) is much slower, possibly due to its lower redox potential.[213] Performing the above reaction in water yielded free NO$_2^-$, presumably by the same reaction involved for R = H. The equilibrium of the above reaction is nicely demonstrated in aqueous solvents; in acidic solutions, the complex [(phen)$_2$Cu(H$_2$O)]$^+$ (**13**) reacts with NaNO$_2$ to quantitatively yield NO(g).[213] This reaction is a direct example of nitrite reductase reactivity; nitrite interacts with a reduced cuprate complex, resulting in the production of water and presumably a Cu(II)−NO (i.e., {CuNO}^{10}) species. The cupric-nitrosyl would then readily dissociate NO(g).

Binuclear Systems. Interesting and related studies employing binuclear copper complexes and NO$_x$ species have been described by Karlin and co-workers.[210,214] The dinuclear Cu(I)/Cu(I) complex, [Cu$_2$-(XYL-O)]$^+$ (**14**), reacts with nitrosonium (NO$^+$) salts (equivalent in oxidation state to NO$_2^-$) to afford the bridging nitrosyl complex [Cu$_2$(XYL-O)(NO)]$^{2+}$ (**15**) (a dicopper(II) complex with a bridging NO$^-$ ligand), which has been characterized by X-ray crystallography (Figure 14). Reaction of **14** with nitrite and two protons also gives **15** and water, a reduction and dehydration similar to the reactivity of NIR. The fact that a bridging nitrosyl is readily formed between two adjacent copper centers possibly suggests why the
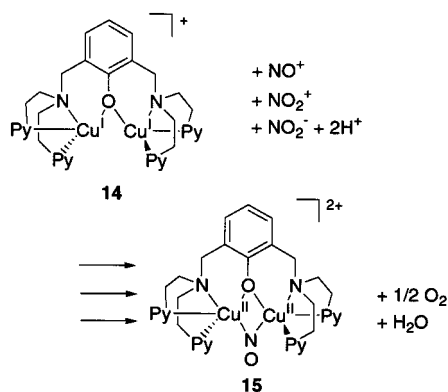
Figure 14. Reaction of dicopper (I) complex **14** with nitrite and nitrite equivalents, producing the μ-NO$^-$ dicopper(II) complex **15**.
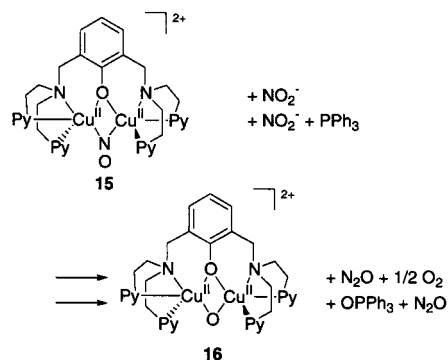

Figure 15. Reaction of bridging nitrosyl complex **15** with nitrite to yield nitrous oxide and an oxygen atom equivalent.

12.5 Å Cu⋯Cu separation in NIR is a desirable structural feature. In the enzyme, the formation of a stable, bridging nitrosyl could prevent the release of NO(g) and, therefore, make NIR less effective at nitrite reduction. The binuclear Cu(II)/Cu(II) site in **15** does not readily dissociate NO(g).

Subsequent reaction of **15** with nitrite affords the oxo-dicopper(II) complex **16**, dioxygen, and nitrous oxide (Figure 15). The stoichiometry of 0.5 equiv of O$_2$ released was confirmed by the addition of triphenylphosphine, which acts as an O-atom transfer acceptor. It is supposed that the direct attack of nitrite on the bridging nitrosyl leads to N$-$N coupling and, therefore, N$_2$O formation.

To probe the nature of nitrite binding in proteins, synthetic nitrite complexes were examined with electron spin$-$echo envelope modulation (ESEEM) spectroscopy for comparison with enzyme$-$nitrite systems.[191] The synthesis of amine-bridged polypyridyl Cu(II)$-$nitrite complexes led to the observation of the asymmetric η^2-O,O′ bonding of nitrite to copper. The complex [(TEPA)Cu^{II}(NO$_2$)]PF$_6$ (**17**) (TEPA
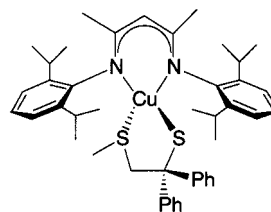

17
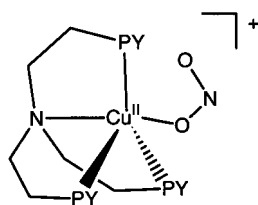
= tris((2-pyridyl)-ethyl)amine) is similar to other (TEPA)Cu^{II} complexes[215-217] with distorted square pyramidal geometries.

Interestingly, the pyridyl nitrogen in the apical position (and trans to the long-contact oxygen of bound NO$_2$$^-$) has a lengthened bond to copper relative to the equatorial pyridyl nitrogens. To probe the nature of the solution-state bonding of nitrite in **17**, ESEEM spectroscopy was utilized. In frozen solutions, ESEEM spectroscopy indicated O-ligation of nitrite to copper, as in the solid state. Subsequent attempts to observe similar ESEEM signals from nitrite-soaked hemocyanin failed to confirm the coordination of nitrite to hemocyanin in a manner consistent with the mode in complex **17**.[191]

3. Synthetic Cu Complexes: Models for the "Perturbed" Type 1 Cu Center in NIR

An advanced structural model for the type 1, blue copper center in NIR (and in other blue copper proteins)[23,218-221] has also been recently synthesized.[185,222] This complex features a copper(II) ion with an N$_2$S$_2$ donor-ligand periphery containing both a thiolate and thioether moiety. The copper complex is the first of its kind, being coordinated by a thiolate, a thioether, and two nitrogen ligands. Complex **18** contains a pseudotetrahedral coordination geometry similar to the "distorted" tetrahedral geometry of the "type 1.5" copper centers in NIR.[98] These type 1.5 centers in NIR have also been called green copper centers, with a slightly distorted geometry relative to the more familiar blue copper centers. Notable spectroscopic features, which differentiate this model from previous models, included a rhombic EPR signal, similar to the observed rhombic EPR signal in biological type 1.5 copper centers.[106] In addition, the sulfur-to-copper LMCT band appears at 691 nm in the UV/vis spectrum. As discussed in section II.A (vide supra), blue copper sites are not directly involved in NO$_x$ redox chemistry (i.e., they are not the "active site"); they are essential to the functioning of native NIR enzymes, serving an electron transport (or electron donation) role.

4. Synthetic Fe Complexes: Heme-cd$_1$ NIR Synthetic Models

This section will detail heme nitrosyl and heme nitrite complexes with direct relevance to nitrite reductase activity. A subsequent section of this review (III.D) will discuss heme$-$nitrosyls in somewhat more detail. The interested reader is referred to other reviews[223,224] for more thorough discussions of heme$-$nitrosyl compounds.

Heme Iron(III)$-$Nitrite Complexes. Early work by Scheidt and co-workers on Fe(III) porphyrin complexes and their interactions with nitrite have

shown that Fe(III)−nitrite complexes are rather unstable, indicating the suitability of hemes for mediating redox reactions on nitrite anion as a substrate.[225] Addition of nitrite to solutions of [(P)-Fe^{III}]ClO$_4$ (**19**) (P = porphyrin; tetraphenylporphyrin (TPP), octaethylporphyrin (OEP), or tetratolylporphyrin (TTP)) yielded an Fe(II)−NO complex along with nitrate anion product, eq 12.

$$[(P)Fe^{III}(NO_2)(ONO)]^- + NO_2^- \rightarrow$$
$$[(P)Fe^{II}(NO)(ONO)]^- + NO_3^- \quad (12)$$

The reaction is believed to proceed via an O-atom transfer from a bound nitrite ligand to free nitrite in solution. Subsequent use of a picket fence porphyrin allowed for the isolation of an Fe(III) bis(nitro) complex, [(TpivPP)Fe(NO$_2$)$_2$][K(18-crown-6)(H$_2$O)] (**20**).[226] Similar O-atom transfer reactions were not observed in this hindered porphyrin system, but only when used in conjunction with a potassium crown-ether counterion. The reasons for this are evident from the crystal structure, which showed two η^1-N nitrite ligands bonded to the iron porphyrin: (i) one on the picket side, situated within the picket fence, and (ii) one on the unhindered face of the porphyrin, stabilized by a tight ion-pairing interaction with the potassium crown-ether cation complex.[226] Later attempts to isolate a five-coordinate, mononitro Fe(III) porphyrin complex failed.[227] In these reactions (eqs 13 and 14), BF$_3$·OEt$_2$ was reacted with the bis(nitro) complex **20**.

$$[Fe^{III}(TpivPP)(NO_2)_2]^- + BF_3\cdot OEt_2 \rightarrow$$
$$[Fe^{III}(TpivPP)(NO_2)] + [BF_3NO_2]^- \quad (13)$$

$$2[Fe^{III}(TpivPP)(NO_2)] \rightarrow$$
$$[Fe^{III}(TpivPP)(NO_3)] + [Fe^{II}(TpivPP)(NO)] \quad (14)$$

EPR spectroscopic characterization of the reaction progression led to the postulation of a [(TpivPP)Fe-(NO$_2$)] intermediate on the basis of an observed rhombic, low-spin EPR spectrum. Decomposition of this intermediate yielded [(TpivPP)Fe(NO)] (**21**) and the O-atom transfer product [(TpivPP)Fe(NO$_3$)] (**22**), the latter of which was structurally characterized.[227]
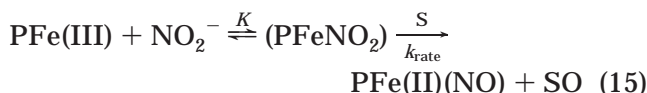
Scheidt and co-workers have also employed EPR spectroscopy (coupled with Mössbauer spectroscopic characterization) to extensively characterize heme−nitrite complexes. The bis(nitrite) complex **20** shows a very large rhombicity parameter (V/Δ) (rhombicity is described by Blumberg and Peisach).[228] Replacement of a nitrite ligand by a neutral nitrogen-donating ligand (on the nonpicket fence side of the porphyrin) leads to the complexes [(TpivPP)Fe^{III}-(NO$_2$)(Im)] (**23**) and [(TpivPP)Fe^{III}(NO$_2$)(Py)] (**24**).[229] Both of these complexes were characterized by X-ray crystallography. The loss of the second nitrite ligand, a strong π-acceptor, leads to an observed decrease in rhombicity. In addition, Mössbauer spectroscopy revealed a nuclear quadrupole splitting $\Delta E_q > 2.0$. The replacement of a second nitrite ligand from complex **20** by a sulfur-donor thiol ligand, 2,3,5,6-tetrafluorothiophenolate, led to the isolation and

structural characterization of the mononitrite complex [(TpivPP)Fe(NO$_2$)(SC$_6$HF$_4$)][K(18-crown-6)(H$_2$O)]-(**25**).[230] This possessed an increased rhombicity parameter relative to the mixed-ligand N-donor systems. Incidentally, reaction of **20** with thiols yielded not a sulfur-ligated complex but rather a ferrous nitrosyl species.[230] Mössbauer spectroscopy was used to confirm the large rhombicity of these systems, revealing a $\Delta E_q > 2.0$ mm/s for all of the studied six-coordinate ferric-nitro complexes.[229,230] These studies are extremely valuable toward understanding the electronic structure of ferric-nitrite complexes and might be applied toward understanding the electronic structure in heme-cd_1 NIRs.

Heme Iron(II)−Nitrite Compounds. Extensive studies on reduced iron−nitro compounds have also been undertaken by Scheidt and co-workers. The five-coordinate complex [(TpivPP)Fe^{II}(NO$_2$)][K(222)] (**26**) is inert to O-atom transfer reactions (and subsequent NO$_x$ redox chemistry) and has been characterized by X-ray crystallography.[231] This complex has unusually large quadrupole splitting (ΔE_q = 2.28 mm/s) as determined by Mössbauer spectroscopy and is a low-spin system. The five-coordinate ferrous-nitro complex reacts with nitric oxide to yield a six-coordinate complex, [(TpivPP)Fe^{II}(NO$_2$)(NO)]$^-$ (**27**), with diminished nuclear quadropole splitting (ΔE_q < 2.0 mm/s).[232] The low-spin, mixed (nitro)(nitrosyl) complex **27** crystallized in two forms, and X-ray structures have been obtained for each.[232] These studies revealed the coordinated nitrite ligand to be inside of the picket fence pocket. It should be noted that ferric porphyrin (nitro)(nitrosyl) complexes have also been isolated and structurally characterized,[233] and in these systems, Mössbauer spectroscopy exhibits smaller quadropole splittings (ΔE_q = 1.35−1.55 mm/s) and diamagnetic ground states compared to those of **27**.[233] Finally, mixed-ligand ferrous nitrite complexes have been synthesized using neutral nitrogen- and sulfur-donor ligands, including [(TpivPP)Fe^{II}(NO$_2$)(PMS)]$^-$ (**28**) (PMS = pentamethylene sulfide) and [(TpivPP)-Fe^{II}(NO$_2$)(Py)]$^-$ (**29**) (Py = pyridine).[234] Both complexes have been structurally characterized. In addition, Mössbauer spectroscopy indicates a normal quadropolar splitting (ΔE_q < 2.0 mm/s) for **28** and **29**, which contrasts with the five-coordinate ferrous nitrite complex [(TpivPP)Fe^{II}(NO$_2$)]$^-$ (**26**).[234] The combination of these data suggests a strong correlation between electronic structure and coordination number in ferrous nitrite complexes. The addition of a sixth, π-donor ligand to complex **26** results in the lengthening of the Fe−N(NO$_2$) bond and a weakened π-interaction between iron and nitrite. The Mössbauer data also support the notion of decreased π-bonding to nitrite when **26** is six-coordinate. These findings reveal stark contrasts in the heme Fe(II) vs heme Fe(III) chemical nature of six-coordinate nitrite complexes.
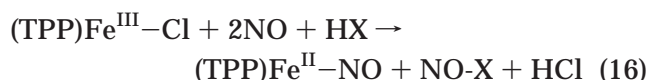
O-Atom Transfer by Heme−Nitrite Compounds. Castro and co-workers have also observed instability in interactions of Fe(III) porphyrins with nitrite ion and have utilized this to carry out interesting reactivity studies. They have shown that nitrite activation by Fe(III) porphyrins allows for the

stoichiometric transfer of an oxygen atom to a number of substrate species:[235-237]

$$PFe(III) + NO_2^- \overset{K}{\rightleftharpoons} (PFeNO_2) \xrightarrow[k_{rate}]{S}$$
$$PFe(II)(NO) + SO \quad (15)$$

Utilizing chloroiron(III) octaethylporphyrin (**30**) and potassium (crown ether) nitrite, the authors were able to achieve both selective oxygen atom insertion into allylic, benzylic, and aldehydic C–H bonds (e.g., allyl chloride, allylbenzene, cyclohexene, cyclohexanol, toluene, and propionaldehyde) and epoxidation of olefins (e.g., styrene and *cis*-stilbene).[237] In addition, the iron porphyrin nitrite complex reacted with inorganic substances to yield O-atom transfer products. Among such reactions were the conversions of (i) nitric oxide to nitrogen dioxide, (ii) carbon monoxide to carbon dioxide, (iii) triphenylphosphine to triphenylphospine oxide, and (iv) dimethyl sulfide to dimethyl sulfoxide. Ferric-nitrite complexes were also found to react with dioxygen, yielding ozone (O_3) as an O-atom transfer product. Olefins were used to trap the highly reactive ozone intermediate, and these "trapping" products were then converted to the corresponding ketones by reduction.[236] The driving force for these O-atom transfer reactions appears to be the formation of a stable, ferrous heme nitrosyl end-product, the $\{FeNO\}^7$ species. Again, the notion of ferrous nitrosyls as stable complexes further supports the idea that their formation should be precluded in NIR to allow facile release of NO(g) product. The possibility that simple ligand exchange is occurring in these systems has been ruled out by isotopic labeling experiments. Recently, the thermochemistry of O-atom transfer reactions from picket fence porphyrin iron–nitrite complexes was examined in detail,[238] revealing that the oxo-transfer free energy for the addition of oxygen to $[Fe^{II}(TpivPP(NO)(NO_2)]^-$ to form $[Fe^{III}(TpivPP)(NO_2)_2]^-$ is -50 kJ/mol, supporting the findings of Scheidt (vide supra) on the stability of dinitroiron(III) picket fence porphyrins.

Heme–Nitrosyl Complexes. To better understand and characterize the putative Fe(III)–NO intermediates, possibly formed during the catalytic cycle of NIR, it is necessary to first understand and characterize synthetic $\{FeNO\}^6$ species in the laboratory. The synthesis of $\{FeNO\}^6$ heme–nitrosyl model complexes is difficult due to the inherent instability of ferric nitrosyls with respect to reductive nitrosylation.[239,240] An example of this latter reaction is given in eq 16.

$$(TPP)Fe^{III}-Cl + 2NO + HX \rightarrow$$
$$(TPP)Fe^{II}-NO + NO-X + HCl \quad (16)$$

This reaction involves a formal reduction of iron, and an acceptor species (HX) is essential for the redox process to occur.[241] From X-ray crystallography, it is known that $\{FeNO\}^6$ complexes contain nearly linear Fe–N–O moieties with short Fe–N(NO) bond lengths (1.63–1.64 Å).[241] Infrared spectroscopy is extremely useful for the study of M–NO systems, and generally speaking, the N–O stretching frequencies of five-co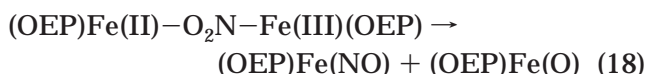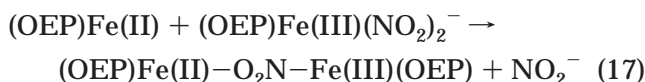ordinate $\{FeNO\}^6$ complexes range from 1665 to 1690 cm^{-1}, while those of six-coordinate $\{FeNO\}^6$ complexes fall between 1740 and 1937 cm^{-1}.[241] While these values are indicative of the coordination environment about the heme, they may not be used to definitively assign an Fe–N–O angle in these complexes.

Despite the lack of stability for $\{FeNO\}^6$ complexes (relative to that for $\{FeNO\}^7$), Scheidt and co-workers have been successful in synthesizing both five- and six-coordinate iron(III)-nitrosyl compounds. The earliest, structurally characterized examples of $\{FeNO\}^6$ complexes were $[(OEP)Fe(NO)]^+$ (**31**) and $[(TPP)Fe(NO)(H_2O)]^+$ (**32**).[242] Many years later, the six-coordinate complexes $[(OEP)Fe(NO)(1\text{-MeIm})]^+$ (**33**) (1-MeIm = 1-methylimidazole), $[(OEP)Fe(NO)(Pz)]^+$ (**34**) (Pz = pyrazole), and $[(OEP)Fe(NO)(Iz)]^+$ (**35**) (Iz = indazole) and the dimeric $[(OEP)Fe(NO)]_2(Prz)$ (**36**) (Prz = pyrazine) were synthesized and structurally characterized.[243] These four complexes featured short Fe–N(NO) bond lengths (1.627(2)–1.6465(17) Å) and nearly linear Fe–N–O bond angles (176.6(3)–177.6(3)°), typical for $\{FeNO\}^6$ systems.[243] Most recently, the five-coordinate complex $[(OEP)Fe(NO)](ClO_4)$ (**37**) was synthesized and structurally characterized.[244] This complex was found to differ structurally from an earlier reported complex $[(OEP)Fe(NO)](ClO_4)(CHCl_3)$ (**38**),[242] most notably by solvation and unit cell arrangement. It is interesting to note that both complexes have nearly linear Fe–N–O geometries (176.9(3)° for **38** and 173.19(13)° for **37**) but quite different N–O vibrational frequencies (ν_{NO} = 1838 cm^{-1} for **37** and 1868 cm^{-1} for **38**).[244]

Recently, Richter-Addo and co-workers[245] were able to observe the direct conversion of a heme–nitrosyl to a heme–nitrite, in the absence of excess NO(g). These reactions were performed using the picket fence porphyrin heme complex $[Fe(TpivPP)(NO)]$ (**39**), which directly forms $[Fe(TpivPP)(NO_2)]$ (**40**) in chloroform when exposed to pyridine in air. Exclusion of the axial base pyridine results instead in the isolation of a porphyrin ferric-chloro complex, while using nonpicket fence porphyrins leads to the formation of μ-oxo ferric porphyrin dimers. The reactions represented the first demonstrated conversion of a heme–nitrosyl to heme–nitrite complex. The biomimetic reactivity is realized upon the addition of triphenylphosphine to complex **40**, which results in O-atom transfer to form triphenylphosphine oxide and regeneration of the heme–nitrosyl complex **39**.[245]

Heme–NO and Heme–Nitrite Electrochemistry. Interest in heme–nitrosyl electrochemistry has existed for some time, due to the involvement of iron–nitrosyls in the reduction of nitrite. The electrochemistry of metalloporphyrin-NO compounds is reviewed elsewhere, by Kadish,[246] and his research group carried out early electrochemical and spectral studies on iron porphyrin nitrosyl complexes.[247-249] Meyer and co-workers[250,251] have also examined the electrocatalytic reduction of nitrite to ammonia (and nitrous oxide) using water soluble iron porphyrins. Most recently, Ryan and co-workers have extensively examined the electrochemistry of both heme–nitrosyl[252-254] and heme–nitrite[255-261] complexes, successfully characterizing various redox states in

these systems. An ongoing debate as to the stability of ferric heme nitrite complexes was recently reevaluated.[261] Under the proper reaction conditions, it was found that both ferrous and ferric heme synthetic complexes are stable in the presence of nitrite anion even in nonpicket fence porphyrin systems. Products from these reactions are suggested to be ferric- and ferrous-nitrite compounds. However, under voltammetric conditions, whereby a mixture of iron oxidation states (II/III) become present, nitrite is reduced to form a ferrous nitrosyl and μ-oxo-bridged porphyrin product, as outlined in eqs 17−19.[261]

$$(OEP)Fe(II) + (OEP)Fe(III)(NO_2)_2^- \rightarrow$$
$$(OEP)Fe(II)-O_2N-Fe(III)(OEP) + NO_2^- \quad (17)$$

$$(OEP)Fe(II)-O_2N-Fe(III)(OEP) \rightarrow$$
$$(OEP)Fe(NO) + (OEP)Fe(O) \quad (18)$$

$$(OEP)Fe(II) + (OEP)Fe(O) \rightarrow [(OEP)Fe]_2O \quad (19)$$

A detailed kinetic examination of these reactions showed no dependence upon nitrite concentration, supporting the notion of a coordinated or possibly a bridging nitrite intermediate in the first step, eq 17. Subsequent O-atom transfer to the Fe(III) moiety yields the reduced ferrous nitrosyl and an Fe(IV)=O species, eq 18. Finally, the μ-oxo porphyrin dimer is formed from the reaction of the ferryl heme with a second equivalent of ferrous heme, eq 19. This work contrasts with the findings of Scheidt and co-workers,[225] suggesting rather intricate and complicated reactivity between nitrite and iron porphyrins in synthetic systems. Invariably, this same delicate chemistry is also present in enzymatic NIRs.

It should be noted that several authors have reported in situ spectroscopic characterization of heme−nitrosyls, claiming the presence of metastable {FeNO}^{6} heme species,[247,249,262−267] although none of these cases involved structurally characterized examples. However, [(TPP)Fe(NO)(HO-i-C$_5$H$_{11}$)]$^+$ (HO-i-C$_5$H$_{11}$ = isoamyl alcohol) (**41**), a mixed nitrosyl− alcohol {FeNO}^{6} complex, was amenable to X-ray crystallography.[268] Most notable in regard to this complex is a nearly linear nitrosyl moiety (Fe−N−O 177.1(7)°) along with a relatively high N−O vibrational frequency (ν_{NO} = 1935 cm^{-1}, KBr). Kadish and co-workers have also structurally characterized the iron−corrole {FeNO}^{6} complexes [(OECor)Fe(NO)] and [(OECor)Fe(NO)](FeCl$_4$) (OECor = octaethylcorrole).[269] Both of these complexes have nearly linear Fe−N−O moieties, with Fe−N−O angles of 176.9(3)° and 171.4(9)°, respectively.[269]

Recently, Olabe and co-workers[270] have shown that the inorganic coordination complex [Fe^{II}(CN)$_5$(H$_2$O)]$^{3-}$ (**42**) demonstrates similar reactivity to the dissimilatory nitrite reductases. It is believed that **42** reacts with nitrite to form the mononitro complex [Fe^{II}-(CN)$_5$(NO$_2$)]$^{4-}$ (**43**), which is rapidly converted to a bound NO$^+$ species, [Fe^{II}(CN)$_5$(NO)]$^{2-}$ (**44**), with concomitant loss of water (presumably after the addition of two protons). It was noted that a one-electron reduction of **44** leads to the evolution of free

NO(g), although the conditions for this reaction were not evaluated in detail.[270]

B. NOR Model Systems

1. General Considerations

The modeling of the heme/non-heme diiron active site in NOR begins with a close examination of the ligand environment about each iron center in the active site of the reduced enzyme (see section II.B). The non-heme iron ion is most likely coordinated by three histidine residues and possibly a carboxylate moiety. The heme iron is coordinated by four pyrrole-nitrogen donors from the porphyrin macrocycle, along with an axial histidine residue. In the oxidized enzyme, these two metals are magnetically coupled through bridging ligand(s). On the basis of these observations, synthetic modeling of the active site consists of three key features: (1) a porphyrin ligand for the heme iron, (2) a multidentate, nitrogen donor chelate for the non-heme iron, and (3) a close proximity of the two irons.

2. Synthetic Heme/Non-Heme Diiron Complexes

Functional Models. The only model for the heme/non-heme diiron active site in NIR has been synthesized by Karlin and co-workers.[28,156,157] The complex [(^{5}L)Fe−O−Fe−Cl](ClO$_4$) (**45**) was synthesized as a mimic of the oxidized state of the enzyme and has been characterized by X-ray crystallography (see Figure 16).[157] A second analogue, [(^{5}L)Fe−O−Fe−Cl]-(BArF) (BArF = tetrakis(3,5-bis-trifluoromethyl-phenyl)borate) (**46**), was later synthesized utilizing a different counteranion for greater solubility in organic solvents.[156] The corresponding diferrous complex [(^{5}L)Fe^{II}···Fe^{II}−Cl](BArF) (**47**) was synthesized by sodium dithionite reduction of the oxo-bridged complex **46** to study the reactivity of the diiron system with nitric oxide (and dioxygen). Thorough characterization of both the oxidized and the reduced diiron complexes was performed using UV/vis and NMR spectroscopies. The oxidized model complex **46** was dissolved in a 4:1 acetonitrile/water (both ^{16}O- and ^{18}O-water) mixture for examination by resonance Raman spectroscopy. These studies identified an asymmetric Fe−O−Fe stretch at 841 cm^{-1} that downshifted to 801 cm^{-1} in ^{18}O-water. Comparison of these data with the resonance Raman characterization of NOR further supports the presence of an oxo-bridged diiron moiety in the oxidized enzyme.[28]

The reduced complex [(^{5}L)Fe^{II}···Fe^{II}−Cl](BArF) (**47**) was reacted with both high and low concentrations of NO at low temperatures. When performed on the UV/vis scale (<10 μM), complex **47** reacts with NO to afford the oxo-bridged species [(^{5}L)Fe−O−Fe−Cl]-(BArF) (**46**) and presumably N$_2$O. It has been suggested by Trogler and co-workers[271,272] (who have effected the palladium-catalyzed reduction of nitric oxide to nitrous oxide) that nitrous oxide may be produced by the electrophilic attack of free NO on the lone electron pair of a transition metal-coordinated, bent nitrosyl. This newly formed species, a hyponitrite complex, could then decompose to yield N$_2$O and H$_2$O (in the presence of protons).[271] In the
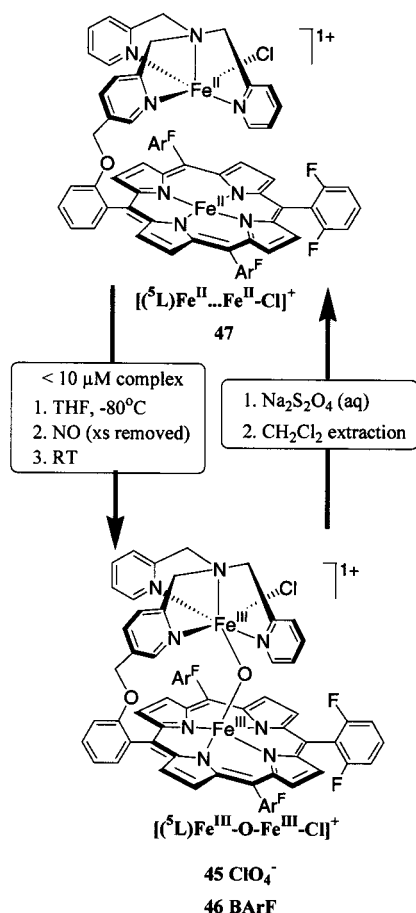
$[(^5L)Fe^{II}\cdots Fe^{II}-Cl]^+$

47

< 10 μM complex
1. THF, -80°C
2. NO (xs removed)
3. RT

1. $Na_2S_2O_4$ (aq)
2. CH_2Cl_2 extraction

$[(^5L)Fe^{III}-O-Fe^{III}-Cl]^+$

45 ClO_4^-

46 BArF

Figure 16. Heme/non-heme diiron reduced (**47**) and μ-oxo oxidized (**45**, **46**) complexes as functional models for nitric oxide reductase (NOR) reactivity.

NOR model system, described above, it is possible that both a heme−nitrosyl and a non-heme iron−nitrosyl may form, with one coordinated nitrosyl electrophilically attacking the other bound nitrosyl, resulting in a diiron-bridged hyponitrite species that ultimately decomposes to N_2O and an oxo-bridged complex. (Similar reactivity, whereby the siloxy complex $W_2(OSiMe_2Bu^t)_6$ reacts with NO to yield a bridging oxo intermediate and nitrous oxide, has been reported by Chisholm and co-workers.)[273] However, at higher complex concentrations, reaction of **47** with NO yielded a stable ferrous nitrosyl complex, in addition to both N_2O and NO_2 (as detected by gas chromatography). Exposure of $[(^5L)Fe^{II}\cdots Fe^{II}-Cl]$-(BArF) (**47**) to dioxygen in THF at room temperature generates $[(^5L)Fe-O-Fe-Cl](BArF)$ (**46**), while a spectroscopically detectable stable intermediate can be trapped at −80 °C. The reactions are summarized in Figure 16 and represent a novel, first-generation modeling of the NO_x and O_2 reactivity of the active site of bacterial NORs.

C. Copper-Mediated NO(g) Chemistry

While the interaction of nitric oxide with copper ions in biological systems is important to the global nitrogen cycle, few copper−nitrosyl species have been characterized. The first copper−nitrosyl species (a binuclear, bridging nitrosyl) was synthesized by Karlin and co-workers (section III.A.2) but was not
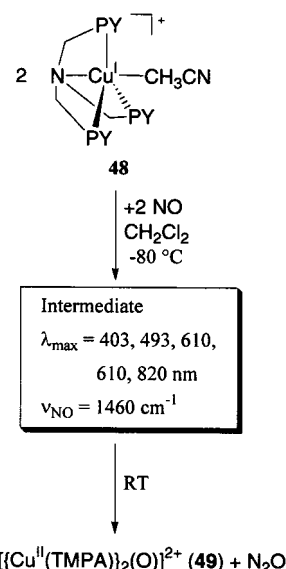

48

+2 NO
CH_2Cl_2
-80 °C

Intermediate
λ_{max} = 403, 493, 610,
610, 820 nm
ν_{NO} = 1460 cm^{-1}

RT

$[\{Cu^{II}(TMPA)\}_2(O)]^{2+}$ (**49**) + N_2O

Figure 17. Reaction of **48** with nitric oxide gives a nitrosyl−copper complex intermediate that further reacts to produce μ-oxo complex **49** and N_2O.

made by direct reaction with NO(g) but rather using NO^+ or NO_2^-.[210,214] Later efforts, also discussed below, revealed the possibility of synthesizing $\{CuNO\}^n$ species using reduced Cu(I) complexes and NO(g).

The mononuclear compound $[(TMPA)Cu^I(RCN)]^+$ (**48**) reacts with NO(g) to form a stable purple-colored intermediate at low temperature, proposed to possess a nitrosyl group (ν_{NO} = 1460 cm^{-1}) bridging the two Cu ions (Figure 17).[210] The low-energy stretching frequency (ν_{NO}) and the observed EPR silence of the intermediate species are consistent with the proposed dinuclear $Cu^{II}-(NO^-)_2-Cu^{II}$ imtermediate. This reaction intermediate was also the first example of a copper nitrosyl complex generated from a Cu(I) complex and NO(g). Warming of this intermediate yields $N_2O(g)$ and an oxo−dicopper(II) complex (**49**). It may be that the putative $Cu^{II}-(NO^-)_2-Cu^{II}$ intermediate brings together in close proximity the coordinated nitrosyl groups and facilitates (NO^-) coupling and subsequent elimination of N_2O.

In another related example from the Karlin group,[210] it was shown that the binuclear dicopper(II) complex **14** reacts with excess NO(g) in methylene chloride at low temperatures to form an unstable purple-brown intermediate (Figure 18), characterized by UV/vis spectroscopy with a λ_{max} = 380 nm.[210] The end product, the oxo−dicopper complex **16** (see Figure 15), is formed upon warming the solution to room temperature. In addition, N−N coupling and the subsequent release of $N_2O(g)$ is observed in the end products.

As has been discussed (section III.A.2), a mononuclear copper−nitrosyl species is seen as a key intermediate in biological NO_x reduction chemistry; i.e., in NIR. The first mononuclear copper−nitrosyl complex was synthesized by Tolman and co-workers, utilizing the dimeric $(Tp^{tBu,H}Cu)_2$ (**50**) complex and NO(g) (Figure 19).[274,275] The dicuprous complex reacts with nitric oxide to yield the mononuclear cuprous−nitrosyl complex $[(Tp^{tBu,H})Cu(NO)]$ (**51**), formally a
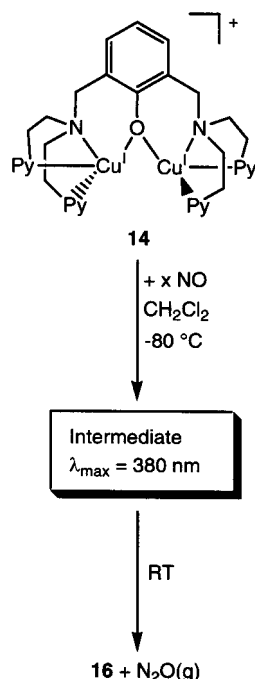
Figure 18. Reaction of xylyl dicopper(I) complex (**14**, see also Figure 14) with nitric oxide yields a low-temperature stable putative copper–nitrosyl adduct, which upon warming releases N_2O and forms the μ-oxo complex **16** (see Figure 15).

{CuNO}^{11} system. The isolated nitrosyl was characterized by X-ray crystallography and featured a bent Cu–NO moiety (163.4(6)°) and a pseudotetrahedral geometry about copper. The complex was stable for extended periods but lost NO upon application of a vacuum or an argon purge.[274]

Using bis(phenyl)-substituted tris(pyrazolyl)hydroborate ligands (**52**: **a**, diphenylimidazole ligated; **b**, acetonitrile ligated) also allowed for the observation of a mononuclear nitrosyl complex **53** (Figure 19).[276] However, **53** was not structurally characterized but nonetheless was consistent in formulation based on other spectroscopic techniques (FTIR, UV/vis, EPR, and MCD) and comparison with **51**. From a comparison of UV/vis, EPR, and MCD properties with known Cu(II) complexes (each employing the ligand Tp^{tBu}), it was confirmed that these nitrosyl complexes (**51** and **53**) indeed contain reduced Cu(I) and are best formulated as {CuNO}^{11} systems.

It was later found that reducing the steric hindrance around the CuNO moiety in [(Tp$^{R,R'}$)Cu^I(NO)] systems promoted NO disproportionation.[277] The neutral complexes [(Tp^{Ms,H})Cu^I(THF)] (**54**) (THF = tetrahydrofuran) and [(Tp^{CF_3,CH_3})Cu^I(CH$_3$CN)] (**55**) (Figure 20) were structurally characterized and the corresponding nitrosyl adducts studied by FTIR, EPR, NMR, and UV/vis spectroscopies. These complexes catalyzed disproportionation in an NO(g) environment to give N_2O (confirmed by gas chromatography) and the corresponding Cu^{II}(NO$_2^-$) complexes. The nitrito complexes [(Tp^{CF_3,CH_3})Cu^{II}(NO$_2^-$)] (**56**) and [(Tp^{CH_3,CH_3})Cu^{II}(NO$_2^-$)] (**57**) were characterized by X-ray crystallography and featured a symmetric η^2-O,O nitrite bound to square-pyramidal Cu(II) ions.[277,278] This is in sharp contrast to the X-ray structure of the independently synthesized a [(Tp^{tBu,H})-
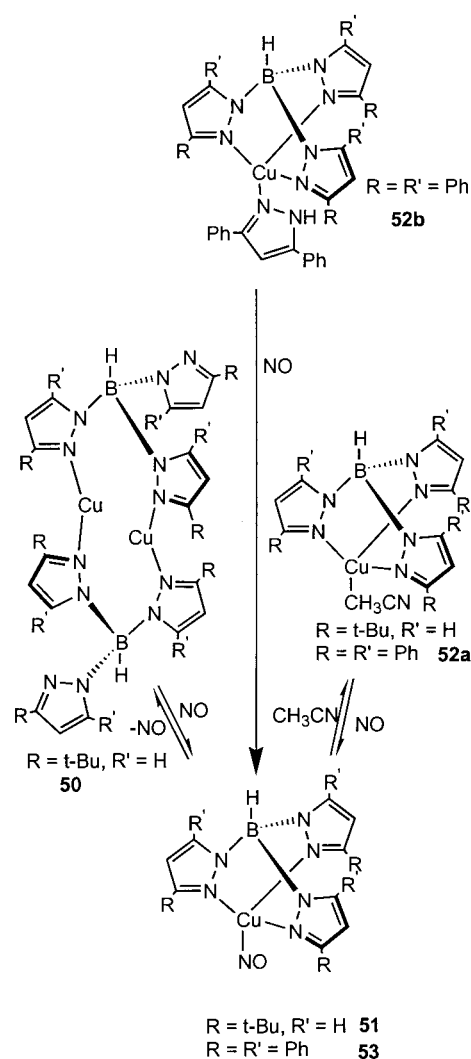

Figure 19. Reaction of pyrazolylborate copper(I) complexes with nitric oxide, yielding mononuclear Cu–NO adducts **51** and **53**.

Cu(NO$_2^-$)] (**58**) complex, which demonstrated asymmetric η^2-O,O′ coordination of nitrite to a distorted square-pyramidal copper.[192] The use of EPR spectroscopy also revealed differences in geometries between the nitric oxide adducts of [(Tp^{tBu,H})Cu^I(NO)] (**51**), [(Tp^{CF_3,CH_3})Cu^I(NO)] (**59**), and [(Tp^{CH_3,CH_3})Cu^I-(NO)] (**60**) systems; the sterically hindered Tp^{tBu,H} (**51**) and [(Tp^{Ph,Ph})Cu^I(NO)] (**53**) complexes demonstrated rhombic EPR signals with significant hyperfine splitting and low g values ($g < 2.0$), each showing distinct Cu(I)–(NO•) character. The N–O stretching frequency ν_{NO} was 1712 cm^{-1} for Tp^{tBu,H} (**51**) (Cu–N–O angle of 163.4(6) °) and 1720 cm^{-1} for Tp^{Ph,Ph} (**53**).[276] The Tp^{CH_3,CH_3} (**59**) and Tp^{CF_3,CH_3} (**60**) complexes each produced axial EPR signals, while the N–O stretching frequency ν_{NO} was 1753 cm^{-1} for **60** (but not reported for **59**). The [(Tp^{Ms,H})Cu^I(NO)] (**61**) complex was found to be EPR silent, but had sharp ^{1}H NMR signals and an N–O stretching frequency ν_{NO} of 1712 cm^{-1}.[277,278] It was concluded, on the basis of steric influence and electron donation, that the nature of substituents R and R′ greatly affected spectroscopic properties of {CuNO}^{11} systems and the NO(g) disproportionation facility of Cu(I) complexes. Stronger electron-withdrawing substituents (e.g., R
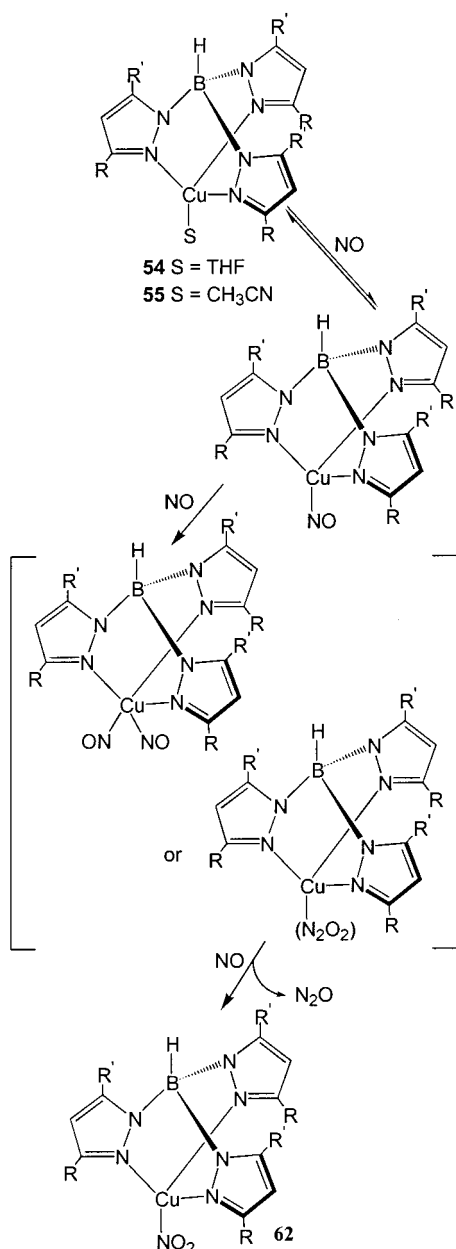
54 S = THF
55 S = CH$_3$CN

Figure 20. Scheme proposed for the reaction of mononuclear copper complexes with nitric oxide and subsequent N–N coupling to give nitrous oxide plus a nitrito copper-(II) product **62**.

= phenyl) and functional groups of greater steric bulk (e.g., R = *tert*-butyl, mesityl) slowed the rate of NO disproportionation. Mechanistic investigations suggested an electrophilic attack of a second NO molecule upon an initial Cu–NO adduct giving a Cu–(NO)$_2$ species (Figure 20), followed by N–N coupling (to yield N$_2$O) and O-atom transfer to NO to give NO$_2^-$ coordinated to copper(II) (**62**).

The synthetic copper complexes discussed thus far are ligated by either pyridyl-, pyrozolyl-, imidazolyl-, or amine-containing chelates. Recently, a complex with mixed-ligand molecular scaffolds was also reported.[279] One such Cu(I) complex (**63**) to be reacted with NO utilizes the ligand 1,4-diisopropyl-7,2-pyridylmethyl-1,4,7-triazacyclononane and is shown in Figure 21. The triflate salt of the TACN-derivatized complex disproportionates excess NO, yielding a
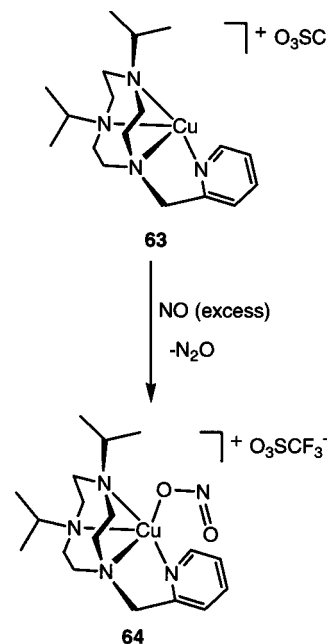

Figure 21. Reaction of mixed-ligand copper(I) complex with nitric oxide gives a nitrito copper(II) compound **64** and N$_2$O.

Cu(II)–nitrito complex (**64**). This compound was characterized by X-ray crystallography and featured an asymmetric η^2-O,O'-bound nitrito ligand. Such reductive disproportionation reactivity differed from similarly ligated R$_3$TACN systems in alcohol solvents, suggesting that both ligand denticity and ligand electronic structure, combined with solvent effects, strongly influence NO reactivity with copper ion complexes.[279]
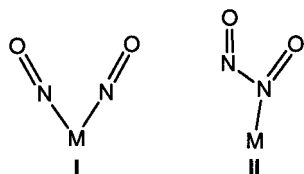
Copper complexes have also been employed for NO disproportionation in reactions using alcohols as reducing agents.[280] The complex [LCu(CH$_3$CN)]PF$_6$ (**1**), where L = (^{i}Pr)$_3$TACN, reacts with excess NO in alcohol solutions (MeOH, EtOH, ^{i}PrOH, and PhCH$_2$-OH) to yield nitrous oxide and the corresponding aldehyde or ketone products. For the related LCu^{I}Cl complex, some mechanistic information is also available. Low-temperature (−78 °C) reaction of the parent complex LCuCl in methanol, with excess NO, led to the observation of a putative hyponitrite-containing complex [(LCu)$_3$(N$_2$O$_2$)Cl]$^+$ (**65**), detected from cold solutions by electrospray ionization mass spectrometry (ESI-MS). Subsequent warming to room temperature yielded nitrous oxide. The mass spectrometry results also suggested the involvement of mutlicopper species during catalysis, on the basis of the identification of a multinuclear complex such as **65**.[280]

It should be noted that two distinct forms of copper–nitrosyl chemistry are evidenced by Karlin and Tolman. In the Karlin systems, the formation of nitrous oxide from nitric oxide is accompanied by the assembly of oxo-bridged copper species, while there is no evidence for nitrite or nitrogen dioxide production. Tolman's systems present the formation of nitric oxide and concomitant formation of a copper–nitrite adduct, with reactivity similar to classic nitric oxide disproportionation. Clearly, more Cu(I) and Cu(II) nitrosyl complexes need to be studied to gain a better

understanding of the subtleties that underlie Cu−NO interactions and reactivity patterns.

D. Iron Complex-Mediated NO(g) Reactivity

Heme Complexes. The catalytic disproportionation of NO to N_2O and NO_2 requires an N−N coupling to form the required N_2O product. It has been proposed that two intermediates are plausible precursors to formal N−N coupling:[281]

In form **I**, a dinitrosyl, the metal center and corresponding ligand framework would have to accommodate a *cis*-dinitrosyl, a scenario precluded in heme systems. Form **II**, termed hyponitrite or hyponitrous, is formed by electrophilic attack of NO to a bound metal−nitrosyl. Following N−N coupling, the next step would be O-atom abstraction (by NO) to yield NO_2 and N_2O.

Ford and co-workers[282,283] have used laser flash photolysis techniques to study NO binding kinetics with heme systems; a recent review on the photochemistry of metal nitrosyl complexes has also appeared.[284] Specifically, they measured rate constants for NO coordination (k_{on}) and NO dissociation (k_{off}) and, therefore, determined the corresponding entropies of activation for the association ($\Delta S_{on}^{\ddagger}$) and dissociation ($\Delta S_{off}^{\ddagger}$) processes. These experiments, using the water soluble porphyrin (Fe(II) or Fe(III)) complexes [(TPPS)Fe]$^{0/+}$ (**66**) and [(TMPS)Fe]$^{0/+}$ (**67**), further demonstrated the greater affinity of Fe(II) for NO bonding, as compared to Fe(III) bonding with NO (see section III.A.4). The ferric complexes are believed to be six-coordinate with axial water ligation. As such, ligand dissociation is required prior to NO binding; this dissociative process yields large calculated $\Delta S_{on}^{\ddagger}$ values for overall NO binding (100 ± 4 J mol^{-1} K^{-1} for TPPS and 86 ± 2 J mol^{-1} K^{-1} for TMPS). However, the ferrous systems, which are typically five-coordinate in water and, therefore, do not require ligand dissociation prior to NO bonding, have much smaller entropies of activation, $\Delta S_{on}^{\ddagger}$ (12 ± 10 J mol^{-1} K^{-1} for TPPS and 16 ± 20 J mol^{-1} K^{-1} for TMPS). The observed rate constants for NO bonding for the ferrous porphyrins are 3 orders of magnitude greater than the rate constants for NO bonding to ferric porphyrins. These results add quantitation to the generally accepted views that (i) NO requires a free coordination site prior to bonding to heme and (ii) NO bonds to Fe(II) with a greater affinity as compared to NO bonding to Fe(III).

Recently, Farmer and co-workers[285] were able to demonstrate N−N coupled intermediates in (TPP)-Fe systems. While the end product from the reaction of [(TPP)Fe(NO)] (**68**) (see also eq 16) and excess NO is the nitrosyl−nitrite complex (TPP)Fe(NO)(NO$_2$) (**69**), limiting the amount of free NO in the reaction allowed for the observation of transient N_xO_x species

$$(TPP)Fe\text{-}NO + NO \rightleftharpoons (TPP)Fe\text{-}N_2O_2$$
$$\quad\quad\text{A}\quad\quad\quad\quad\quad\quad\quad\quad\text{B}$$

$$(TPP)Fe\text{-}N_2O_2 + NO \longrightarrow (TPP)Fe + N_2O + NO_2$$
$$\quad\quad\text{B}\quad\quad\quad\quad\quad\quad\quad\quad\quad\text{C}$$

$$(TPP)Fe + NO \longrightarrow (TPP)Fe\text{-}NO$$
$$\quad\quad\text{C}\quad\quad\quad\quad\quad\quad\quad\text{A}$$

$$(TPP)Fe\text{-}NO + NO_2 \longrightarrow (TPP)Fe(NO)(NO_2)$$
$$\quad\quad\text{A}\quad\quad\quad\quad\quad\quad\quad\quad\quad\text{D}$$

$$(TPP)Fe(NO)(NO_2) \rightleftharpoons (TPP)Fe(NO_2) + NO$$
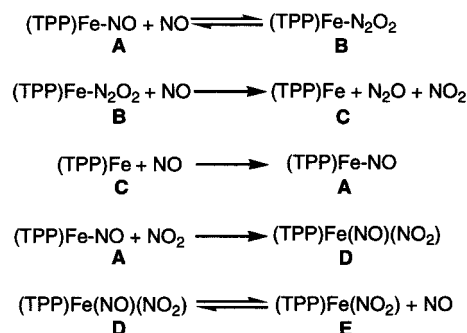$$\quad\quad\text{D}\quad\quad\quad\quad\quad\quad\quad\quad\text{E}$$

Figure 22. Proposed reaction mechanism for the disproportionation of nitric oxide using heme−nitrosyls.

during the course of the reaction by utilizing FTIR spectroscopy. The overall, proposed course of reaction is given in Figure 22.

In step 1, the iron nitrosyl reacts reversibly with an additional equivalent of NO to yield an N−N coupled intermediate (**B**). Subsequent O-atom transfer to NO yields the ferrous-heme complex **C**, N_2O, and NO_2 products. Reaction with additional NO, can reform the mononitrosyl (**A**). However, in the presence of NO_2 gas (generated in the second step), the heme nitrosyl nitrite complex **D** is formed, which reversibly binds NO, as shown in the final reaction equilbrium step.[285]

The above mechanism was further supported by the use of PPh$_3$ as a competitive O-atom acceptor. In the presence of a 100-fold excess of PPh$_3$, N_2O production becomes catalytic with concomitant formation of OPPh$_3$. In effect, the generation of N_2O has been uncoupled to the formation of NO_2. The mechanism of O-atom transfer was examined by in situ FTIR spectroscopy. By using $^{14}N/^{15}N$ mixed labels, it was possible to identify isotope-sensitive bands that are consistent with each proposed intermediate, including an N−N coupled hyponitrite (e.g., **II**, vide supra).[285]

However, Ford and co-workers[286,192] have reported that heme−nitrosyls such as [(TPP)Fe(NO)] (**68**) do not react with excess NO(g) at room temperature, contrasting intermediate **B**, Figure 22, and Farmer's observations.[285] Ford further suggests that the observation of a mixed nitrosyl/nitrite product is due to trace NO_2 contamination from commercial NO(g) cylinders. Researchers typically purify NO(g) streams with cold traps to "freeze out" contaminants such as N_2O, NO_2, and N_2O_3, so it is uncertain how NO_2 contamination would occur. Thus, controversy still remains as to the NO disproportionation ability of **68**; it seems that the exact reaction conditions (e.g., solvent, presence of water, temperature, and purification efficiency) dictate the observed heme−nitrosyl chemistry.

Ford and co-workers[287] describe the reversible formation of trans(dinitrosyl) complexes, [(TPP)Fe-(NO)$_2$] (**70**) (TPP = 5,10,15,20-tetrakis(phenyl)porphyrin) and [(TmTP)Fe(NO)$_2$] (**71**) (TmTP = *meso*-tetra-*m*-tolyl-porphyrin), which are not susceptible to NO disproportionation. Such dinitrosyl compounds are formed at low temperatures and exist in thermal equilibrium with the corresponding mononitrosyl complexes, [(TPP)Fe(NO)] (**68**) and [(TmTP)Fe(NO)]

(**72**), which predominate at room temperature. The equilibrium in these systems has been nicely followed with the use of variable-temperature ^{1}H NMR, UV/vis, and FTIR spectroscopic experiments.

Non-Heme Iron Nitrosyls. It has been found that non-heme, high-spin Fe(II) containing enzymes are typically EPR silent, using common EPR spectrometers.[288,289] Thus, nitric oxide has been employed as an EPR "probe", as it readily binds to Fe(II) sites in enzymes and coordination complexes. The bonding of NO to ferrous ions allows for the direct EPR examination (and comparison) of $S = 3/2$, {FeNO}^{7} systems in both metalloenzymes and synthetic compounds. A recent examination by Solomon and co-workers[289] suggested that these systems are best described as Fe^{3+} ($S = 5/2$) antiferromagnetically coupled to NO$^-$ ($S = 1$), for a net spin of $S = 3/2$. Examination of two model complexes, [(Me$_3$TACN)-Fe(NO)](N$_3$)$_2$ (**73**) and [(EDTA)Fe(NO)] (**74**) by X-ray absorption, resonance Raman, UV/vis, MCD, and EPR spectroscopies, combined with magnetic susceptibility data from SQUID susceptometry, yielded a picture consistent with the overall $S = 3/2$, {FeNO}^{7} system.[289] Subsequent examination of the non-heme Fe enzyme (coordinated to NO) soybean lipoxygenase by MCD spectroscopy yielded similar electronic structural findings.

Recently, a systematic study of NO and O$_2$ bonding to Fe(II) complexes chelated by EDTA-derivatized ligands (aminocarboxylates) was completed.[290] The EDTA-based ligands were systematically varied, resulting in a total of thirty eight ferrous-chelate complexes used for the investigations. The complexes all formed stable nitrosyl adducts (as observed by UV/vis and FTIR spectroscopies), and the reversibility of NO binding was explored. The results of this work suggested that the more electron-rich chelates favored the conversion of Fe(II) to Fe(III), creating a more O$_2$-reactive and NO-reactive species. It is of interest to note that the rate of nitrosylation was typically found to be nearly 3 orders of magnitude faster than that of corresponding oxygenation reactions. Several of the ferrous nitrosyl complexes were reported to decompose, over the course of hours, to yield nitrous oxide and a ferric ion complex.[290]

Iron complexes utilizing the ligand H$_2$TC-5,5, a tropocoronand ligand, have been employed in studies involving the catalytic disproportionation of NO. This macrocyclic ligand is bis-anionic and contains four nitrogen donors, similar to porphyrins. However, the tropocoronand ligand is nonplanar and tends to favor a trigonal bipyramidal metal ion geometry.

H$_2$TC-*n,m*
n = m = 5
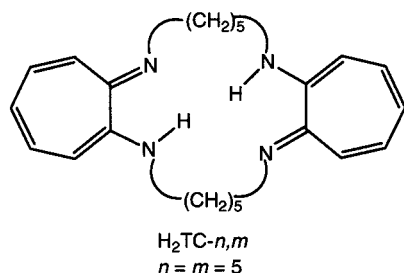
The complex [Fe(TC-5,5)] (**75**) reacted with 1 equiv of NO to yield an isolable ferrous nitrosyl (**76**), Figure
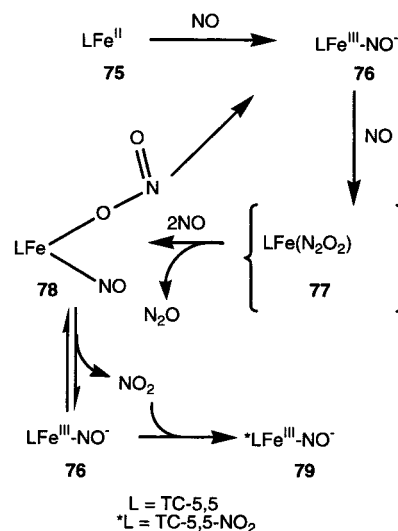

Figure 23. Summary of the reactivity of Fe(II)TC-5,5 (**75**) with nitric oxide.

23.[291] The structure of compound **76** was confirmed by X-ray crystallography, while Mössbauer and EPR spectroscopy, combined with SQUID susceptometry, identified the complex as a low-spin Fe(III)−NO$^-$ species. This iron nitrosyl (**76**) reacts with excess NO to form an intermediate species (**77**), which further reacts with additional NO to give N−N coupling (and N$_2$O) along with a mixed nitrosyl−nitrito complex (**78**). Species **78** was monitored by in situ FTIR spectroscopy at −78 °C ($\nu_{NO} = 1850$ cm^{-1}) but decomposed upon warming to room temperature. However, warming reforms the ferrous nitrosyl (**76**), which continues to react with NO (to produce N$_2$O and NO$_2$). The formation of free NO$_2$ in the reaction mixture eventually induced ligand nitration (of the aromatic tropolone rings) to yield a catalytically inactive nitrosyl compound **79**.

Complexes were also prepared utilizing the H$_2$TC-5,5 ligand and manganese(II) to form [Mn(THF)(TC-5,5)] (**80**) (Figure 24), a trigonal bipyramidal complex with coordinated tetrahydrofuran in the equatorial plane.[292] Reaction of **80** with 1 equiv of NO forms a stable manganese nitrosyl (**81**), an {MnNO}^{6} system that has been characterized by X-ray crystallography. As depicted in Figure 24, compound **81** is believed to react with 1 additional equiv of NO to form a dinitrosyl or hyponitrito intermediate. Mixed labeling studies, using both ^{14}NO and ^{15}NO, support a dinitrosyl that rearranges to a hyponitrite intermediate (**82**) (although they could not rule out the formation of intermediates such as **83**). Finally, N$_2$O is produced once 1 or 2 more equiv of NO is added, with concomitant isomerization to an O-bonded nitrito, nitrosyl complex (**84**). It is also noted that **80** reacts with AgNO$_2$ to afford **85** directly, and reaction of **85** with NO leads to the observed formation of **84**, further supporting the equilibrium suggested in the final step of the proposed mechanism. Analysis of the reaction headspace using gas chromatography supported the 1:4 manganese to NO stoichiometry described in the reaction scheme.

Additional attempts to model nitric oxide binding to non-heme ferrous ions have employed tetradentate nitrogen-donor chelates. Borovik and co-workers[293,294]
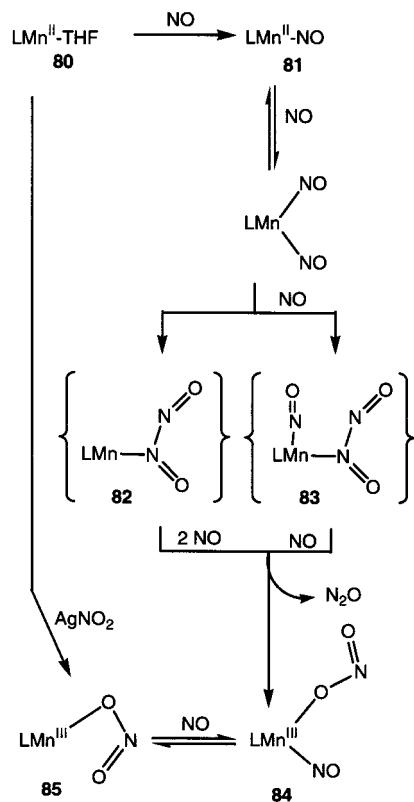
Figure 24. Summary of the reactivity of MnTC-5,5 (**80**) with nitric oxide.

have synthesized a series of iron nitrosyl complexes **86**−**89** utilizing derivatives of the tripodal ligand tris-(N-R-carbamoylmethy)amine. Variations in R allowed for refinement of steric interactions with bound NO, based upon the cavity size around the iron ion. Each of the systems exhibited a net $S = 3/2$ spin state with a formal assignment of Fe(III) supported by Mössbauer spectroscopy for complexes **87**−**89**. Each of the nitrosyl complexes has been characterized by X-ray crystallography, revealing trigonal bipyramidal geometries with nitric oxide bound in the apical position. Compound **86** was found to crystallize with four crystallographically distinct species in the asymmetric unit. Interestingly, each of these Fe−NO moieties in the structure had a different Fe−N−O angle, ranging from 157.5(5) to 175.6(5)°. It was found that the more symmetrically formed cavities (and presumably smaller-diameter cavities) supported linear NO coordination, while deviations from C_3 symmetry allowed for Fe−NO bending. In complexes **87**−**89**, the Fe−NO angles varied from

R = N-(S)-(-)-(a)-methylbenzyl **86**
R = isopropyl **87**
R = cyclopentyl **88**
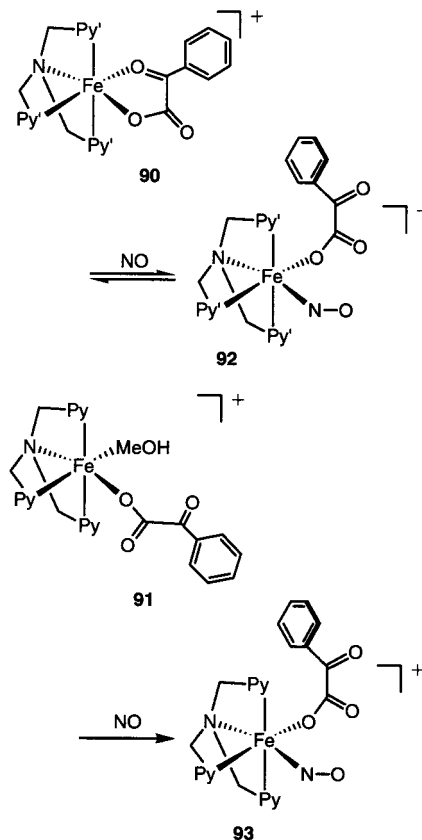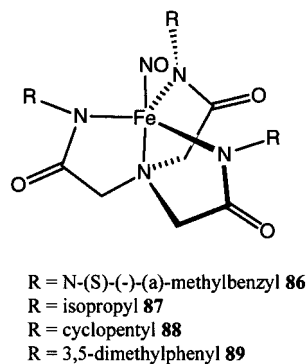R = 3,5-dimethylphenyl **89**

Figure 25. Reaction of Que's non-heme iron complexes (**90** and **91**) with nitric oxide, as model systems for α-keto acid dependent non-heme iron enzyme reactions with nitric oxide.

160.3(2)° (in **89**) to 178.2(5)° (in **87**). These angular differences were directly attributed to cavity size, which was measured to be ∼3 Å in diameter for **87** and **88**, while compound **89** was much larger (∼8 Å in diameter). The general preference for five-coordinate nitrosyls is to have an equatorial-bound NO; however, as demonstrated in these systems, NO may be forced into an apical (and linear) position by steric constraints.

Coordinatively saturated non-heme iron−nitrosyl complexes have been synthesized by Que, Jr. and co-workers.[295] In an attempt to model mononuclear NO adducts for α-keto acid dependent non-heme iron enzymes, ferrous complexes were synthesized using the tetradentate ligands TPA (TPA = tris((2-pyridyl)-methyl)amine) and 6-TLA (6-TLA = tris((2-pyridyl-6-methyl)-methyl)amine), along with the added coligand benzoylformate for both systems (Figure 25). These complexes were found to react with nitric oxide, yielding characteristic $S = 3/2$ EPR signals.

Iron(II) compound **90** was found to reversibly bind NO but was not amenable to X-ray crystallography. Compound **91** irreversibly binds NO, forming **93**. The X-ray structure revealed two conformers, with Fe−N−O angles of 155(2) and 162(2)°; in each, the overall geometry was a distorted octahedron with NO bonded equatorially, trans to the amine nitrogen. The Fe^{III}/Fe^{II} redox potentials measured for ferrous complexes **90** (+0.87 V vs NHE) and **91** (+0.34 V vs NHE) might explain why the latter irreversibly binds NO, if we consider that binding NO involves redox chem-

istry with the iron(II) precursor complexes leading to an {FeNO}^{7} product fragment, formally considered Fe(III)−NO$^-$.


94
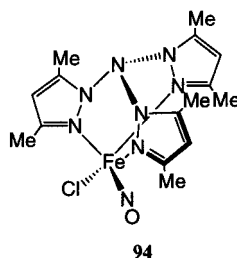
Another model for non-heme iron enzymes that is relevant to non-heme iron−nitrosyls that are proposed in the catalytic mechanism of NOR was prepared and characterized by Que, Jr. and co-workers.[296] The enzyme isopenicillin N-synthase (IPNS) contains a single non-heme Fe(II) center and catalyzes an oxidative ring closure of δ-(L-α-aminoadipoyl)-L-cysteinyl-D-valine (ACV; effectively a sulfur-donor ligand to Fe(II)) to isopenicillin N. The synthetic model complex [(TpzA)Fe^{II}(NO)(Cl)](BPh$_4$) (**94**), a high-spin, $S = 3/2$ ferrous nitrosyl, was examined by Fe K-edge X-ray absorption spectroscopy (XAS), and the results were compared with the nitrosyl-bound IPNS enzyme complex. The results of these EXAFS observations further supported the Fe(II) coordination environment in IPNS.[296] The reduced iron(II)−nitrosyl complex (**94**) was also characterized by X-ray crystallography, revealing an Fe−N−O angle of 157.1(8)°. Additional synthetic Fe(II) complexes were synthesized to model the Fe^{II}IPNS−ACV complex and their reactivities with NO examined.[297] The complexes [Fe(TPA)(SAr)]$^+$ (**95−98**) (Ar = C$_6$H$_2$-2,4,6-Me$_3$; C$_6$H$_4$-4-Me; C$_6$H$_5$; C$_6$H$_4$-4-Cl) were each synthesized and reacted with NO in order to model aspects of the enzymatic active site thiolate coordination under turnover. Characterization of the NO adducts revealed $S = 3/2$ signals by EPR spectroscopy and large rhombicity parameters that were attributed to thiolate ligation.[297]

Another model claiming NOR reactivity that did not include a heme/non-heme diiron system was presented by Jabs and co-workers.[298] The polymeric complex [(ascorbate)Fe^{II}]$_x$ (**99**) reacts with NO in ethanol or methanol to yield a dinitrosyl complex [(ascorbate)Fe^{III}(NO)$_2$]$_x$ (**100**) and both N$_2$O and NO$_2$. A mechanistic possibility that was put forth to explain the formation of nitric oxide and nitrogen dioxide was an electrophilic attack of free NO on a coordinated nitrosyl to produce both N$_2$O and NO$_2$. This reactivity may be suppressed by the addition of nitrogen-donor (π-acceptor) ligands, presumably by reducing the negative charge on coordinated NO.[298]

Diiron Non-Heme Nitrosyls. Que, Jr. and co-workers[299−303] have also synthesized non-heme diiron complexes as models for proteins such as hemerythrin, methane monooxygenase, and ribonucleotide reductase. The diferrous complex, [(6-Me$_3$-TPA)Fe^{II}$_2$-(μ-OH)$_2$]$^{2+}$ (**101**), was found to react with NO and form mononuclear ferrous nitrosyls, as ascertained from their $S = 3/2$ EPR signal.[304] UV/vis spectroscopic properties similar to those of the monoiron nitrosyl

complex **93** (Figure 25) were found for the nitrosyl adduct of **101**, supporting the formulation of an [Fe-(6-Me$_3$-TPA)(NO)(OH)]$^+$ complex (**102**), presumably with a structure similar to **93**. The reaction of **101** with NO was performed using stopped-flow UV/vis spectroscopy, and kinetic information was obtained to compare the relative affinity of Fe(II) binding of both NO and O$_2$. It was found that the diiron complex **101** reacts with NO nearly 10^3 times faster than with O$_2$, similar to the findings of Schneppensieper et al.[290]

104
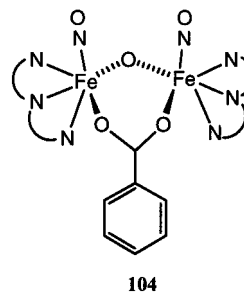
As model compounds for the same protein active sites, Lippard and co-workers[305−309] have synthesized non-heme diiron complexes, including [(Et-HPTB)-Fe$_2$(O$_2$CPh)](BF$_4$)$_2$ (**103**).[310] It should be noted that both the diiron-containing enzymes methane monooxygenase[311] and ribonucleotide reductase[312] are known to react with NO to produce nitrous oxide. The nitric oxide intermediate (in ribonucleotide reductase), believed to be a dinitrosyl complex, is EPR silent because the {FeNO}^{7} moieties are antiferromagnetically coupled.[312] Complex **103** reacts with nitric oxide to form a dinitrosyl species, [(Et-HPTB)-Fe$_2$(NO)$_2$(O$_2$CPh)](BF$_4$)$_2$ (**104**), which was structurally characterized. The Fe−N−O angles are nearly linear (166.6(7) and 168.3(7)°), while the NO is found to bind trans to the amine nitrogen of the chelates. The use of EPR spectroscopy revealed that the nitrosyl adduct is EPR silent, presumably from the antiferromagnetic coupling of the diiron nitrosyls. From SQUID susceptometry, it was found that each iron was a net $S = 3/2$ spin center, with $\nu_{NO} = 1785$ cm^{-1} as determined by FTIR spectroscopy. These results, combined with Mössbauer data, suggest an {FeNO}^{7} system. The dinitrosyl complex did not react to produce N$_2$O and a corresponding Fe−O−Fe bridged complex, as mentioned above and proposed in the reaction of ribonucleotide reductase with NO.[312] However, it is interesting to note that the exposure of **104** to dioxygen led to the formation of a bis(nitrato) complex, [(Et-HPTB)Fe$_2$(NO$_3$)$_2$(OH)](BF$_4$)$_2$ (**105**), possibly via a peroxynitrite intermediate.[310]

E. Transition Metal Nitric Oxide Sensors, Scavengers, and Delivery Agents

NO Sensors. Free nitric oxide in biological systems and its detection have become a hot topic in recent years.[313−315,333] One of the ways being developed for the in vivo detection of NO has been the use of transition metal-based NO sensors. Lippard and co-workers[292] have recently developed a novel NO sensor using Co^{II} and a fluorescent ligand H$_2$DATI-
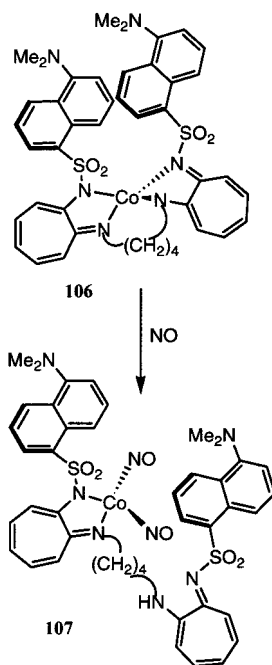
Figure 26. Cobalt complex nitric oxide sensor, complex **106**, involving a ligand with appended fluorescent dansyl groups.

Figure 27. The monomeric cobalt complex unit (**108**) within a polymeric matrix, employed in reversible NO binding.

4, complex **106** (Figure 26). The ligand features two nitrogen donors from each aminotroponiminate ring, and each ring is linked to dansyl fluorophores (dansyl = 5-(dimethylamino)naphthalenesulfonamide). The aminotroponiminate rings are linked by a 4-methylene spacing bridge. The cobalt(II) ion has a partially filled d orbital, and when the metal ion and ligand are fully bonded, the dansyl group fluorescence is quenched. In the presence of nitric oxide, NO binds to the Co ion to form a dinitrosyl species (**107**) and subsequently displaces two nitrogen donors of the tetradentate ligand. This dissociation, as depicted in Figure 26, results in fluorescence enhancement (λ_{ex} = 350 nm; λ_{fluor} = 505 nm) and, therefore, NO detection. Several unlinked systems, of the general formula [Co(DATI)$_2$] (DATI = dansyl-substituted aminotroponimate), have also been synthesized and evaluated for NO-sensing abilities.[316] These systems bind two NO molecules and show an increase in fluorescence upon NO binding and ligand dissociation. However, the nontethered systems react slower with NO, over the course of days, compared to the faster [Co(DATI-4)] systems.[316]

NO Scavengers. Transition metal−nitrosyl complexes have also been prepared with the potential to afford the controlled release (or capture) of nitric oxide in vivo. Borovik and co-workers[317] have synthesized a porous methyacrylate copolymer incorporating a classical Schiff base N$_2$O$_2$ ligand that ligates cobalt(II), forming compound **108** (Figure 27). These cobalt centers, which are stable to air, reversibly bind NO to form mononitrosyl adducts (Figure 27) that have been characterized by EPR, UV/vis, and X-ray absorption spectroscopies.[317] The systems readily lose NO upon application of a vacuum at high temperatures but, more importantly, slowly evolve free NO(g) at room temperature over the course of a
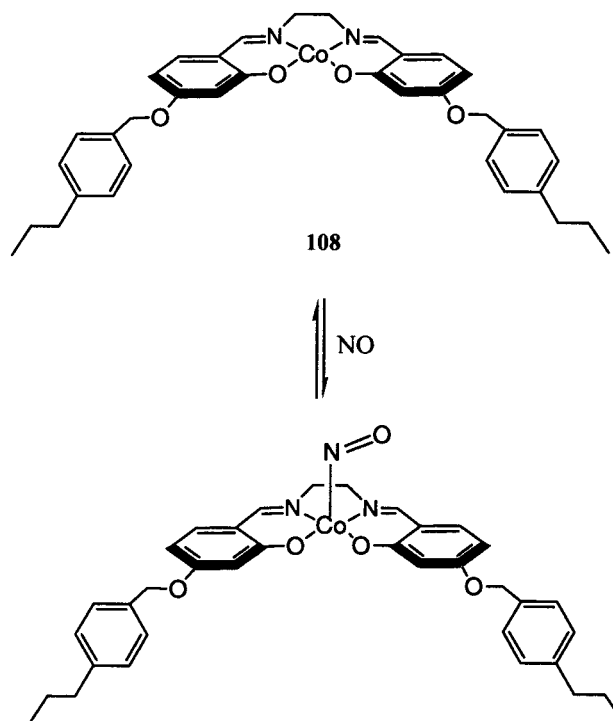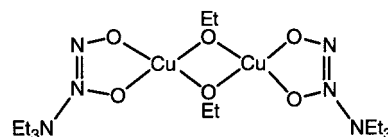
month. Such compounds might be useful in vivo for the slow release of NO and/or as an NO scavenger.

NO Delivery: NONOates. The controlled release of NO using non-nitrosyl transition metal species in reactions with other potential NO• sources has also been explored. The use of N-nitroso compounds, namely, the diazeniumdiolate X−N$_2$O$_2^-$ (NONOate) ligands, is promising due to the potential for releasing 2 equiv of NO (when X is a secondary amine). Keefer and co-workers[318−326] have examined the possibility of using transition metals coordinated to NONOates as potential pharmacological NO delivery agents. Using the secondary amine NONOate Et$_2$N−N$_2$O$_2^-$ as a ligand for copper ions led to several complexes of the general formula Cu$_x$(L)$_y$(Et$_2$N−N$_2$O$_2$)$_2^{z-}$ (where L = OMe or OEt).[319,320] The N$_2$O$_2^-$ fragments are coordinated to Cu in an η^2-O,O fashion, as revealed by X-ray crystallography. Examination of the NO-releasing ability in these compounds revealed that copper coordination enhances the quantity of NO release from NONOates, relative to the sodium salts. The vasorelaxant effects of these complexes were examined in vitro using rabbit aorta, demonstrating an increased vasorelaxant potency relative to that of the sodium NONOates.[320]

Tolman and co-workers have synthesized copper−NONOate complexes using the (^{i}Pr)$_3$TACN ligands in an attempt to probe how the copper ion complex environment may control or influence the release of NO from copper−NONOate compounds.[327,328] The

complex [((^{i}Pr)$_3$TACN)Cu(Et$_2$N(N$_2$O$_2$)](OSCF$_3$) (**109**) was synthesized and characterized by X-ray crystallography.[327] The NONOate was found to bond to copper in a symmetrical η^2-O,O fashion. Complex **109** was found to be stable for extended periods of time at ambient temperatures. However, upon addition of protic acids or thiols, NO is released (~80% yield of NO).[327] The evolution of NO was found to be slower than that for sodium NONOate, suggesting a stabilizing influence from the copper ion supported by a tridentate ligand. Extending these investigations and using TACN-derivatized ligands with pyridine, amide, or phenolate pendant tethers allowed for the study of tetradentate mixed-ligand systems. In the pyridine-tethered and amide-tethered ligand systems, [Et$_2$N(N$_2$O$_2$)]$^-$ was also found to coordinate to copper in the usual η^2-O,O bidentate bonding mode, as revealed by X-ray crystallography. Interestingly, the phenolate-tethered TACN ligand was revealed to have a monodentate-bound [Et$_2$N(N$_2$O$_2$)]$^-$ ligand.[328] However, these structural variations had little effect on the rate of NO release from these tetradentate compounds.

Metalloporphyrin complexes have also been prepared with X[N$_2$O$_2$]$^-$ ligands. Richter-Addo and co-workers[329] have utilized the NONOate analogue Cupferron, where X = Ph (as opposed to the secondary amine in NONOates). They successfully synthesized both [(TPP)Fe(η^2-ON(Ph)NO)] (**110**) and the methoxy-derivatized [(T(p-OCH$_3$)PP)Fe(η^2-ON(Ph)NO)] (**111**) complexes, the first structurally characterized stable metalloporphyrins with an X[N$_2$O$_2$]$^-$ functionality. It is interesting to note that protonation of **110** with triflic acid yielded the corresponding heme−nitrosyl complex **68** (see section III.D). Scheidt and co-workers[330] have also employed NONOates as nitrosylating agents in the synthesis of heme−nitrosyls.

IV. Concluding Remarks

In this article, we have presented a current view of bacterial denitrification and the metal sites involved in these enzymatic processes, with a particular focus on the catalytic metal centers that interact directly with nitric oxide. We have discussed the bioenergetics of denitrification with a particular emphasis on the parallels and the contrasts between denitrification and aerobic respiration. The fact that nature may accomplish three of the four steps of biological denitrification with the involvement of only two transition metals, iron and copper, can in part be rationalized in terms of the known coordination chemistry and reactivity of these metal ions. Both of these metals have two readily accessible and stable oxidation states, are capable of binding and activating nitric oxide (and dioxygen), and may participate in electron-transfer processes. It is rather remarkable that both iron and copper NIRs can perform the exact same reductions, while there is no clear evidence why some organisms prefer one over the other. It is also perplexing that both the heme/non-heme active site of NOR and the heme/copper active site of cytochrome c oxidase can perform the same reactions reducing either nitric oxide or dioxygen. Clearly, nature has

evolved the appropriate enzymes and active site chemistries to deliver the optimum function in a given organism, but it appears that an initial choice in metal ions is available. The associated research problems relevant to the iron/copper-mediated steps in denitrification are of profound interest to both chemists and biologists. As such, attempts to completely understand the nature of these enzymatic transformations employing the quite limited set of metals and ligands available to living organisms requires a close collaboration between scientists in the disciplines of microbiology, bioenergetics, biochemistry, biophysics, bioinorganic chemistry, and inorganic coordination chemistry.

The reduction of nitrite by the heme-cd_1 and the copper-containing NIRs is proposed to proceed via a common mechanism. It involves the binding of nitrite to a reduced metal (Fe^{II} or Cu^I) center with concomitant dehydration/oxidation to yield a putative "oxidized" M−NO moiety (Fe^{III}−NO or Cu^{II}−NO) that then dissociates NO(g). From relevant synthetic chemistry, it is known that both copper(I) and iron(II) ions may in fact participate, in various ways, to yield nitrosyl complexes and, in some cases, free NO(g). Several novel nitrosyl complexes have been discovered in recent years, including the elusive {CuNO}^{10} and {CuNO}^{11} species, which had not been characterized prior to "model" investigations of NIR reactivity. Alternatively, a catalytic cycle in which substrate binding occurs before reduction of the E−S complex is also possible. In this proposal, nitrite ion binds in an η^1-O fashion to the oxidized metal center rather than in an η^1-N fashion to the reduced center. A better assessment of the reaction steps implied in these two very distinct proposals and their relevance to the physiological cycle of these enzymes are challenging goals for the coming years.

The NO reductases and cytochrome oxidases are evolutionarily related. Recent developments indicate that the structural and functional diversity observed in cytochrome oxidases is also present in NORs. In both classes of enzymes, substrate quinol and cytochrome c oxidizing variants are found. In addition, similar prosthetic groups, copper A and c-type hemes, serve in electron entry. However, all NORs characterized so far contain a non-heme iron instead of copper at the active site. It is not known what determines the metal specificity; both enzymes have three conserved histidines. Future research may entail metal substitutions at the enzyme active site to study the changes in chemistry. The synthesis of model compounds will provide further insight into the roles played by both the non-heme iron and copper ions in catalyzing NO or O$_2$ reduction. For instance, the synthetic NOR analogue **47** (section III.B.2) may be synthesized with either Fe^{II} or Cu^I in the non-heme tether, allowing for a direct comparison of copper vs iron reactivity using both nitric oxide and dioxygen as substrates.

We have also tried to cover recent developments in the coordination chemistry of M−NO$_x$ species, particularly those involved in NO$_x$ redox processes. Such chemistry is relevant to fundamental issues of structure, spectroscopy, bonding, and reactivity in

both the limited coordination environments of synthetic compounds and may often be applied and/or compared with the metal site properties in the native proteins and enzymes. Particular attention has been paid to heme−nitrite compounds and heme iron(III)-nitrosyl species, both relevant to the putative NIR reaction mechanism. A large body of electronic structural information is now available on such species, including EPR and Mössbauer spectroscopic characterization, for numerous heme systems with varying axial ligand environments. From these studies, we have a better understanding of the delicate nature of iron(III)−nitrite interactions. Attention was also given to copper−nitrite complexes, particularly those copper(I) species that were found to reduce nitrite to nitric oxide. A section has also been devoted to Cu−NO(g) interactions, an area of chemistry that has received virtually no attention until the last 10 years. From these studies, it has been clearly defined that the detailed nature of the ligand environment and the solvent dictate nitric oxide redox chemistry. Several non-heme mono- and diiron complexes were considered on the basis of their interesting interactions with NO(g). Special attention was given to NO delivery agents; for instance, the copper-coordinated NONOates release free NO(g) in solution. Finally, we have mentioned transition metal complexes that may be used as (potential) in vivo nitric oxide sensors. Clearly, while a good start has been made in synthesizing and characterizing both iron and copper nitrite and nitrosyl complexes, much work remains ahead.

Obviously, understanding bacterial denitrification is relevant to the complex role of NO in human health. It can also be so in the design of iron and copper coordination complex-based systems with the abilities to limit or reduce NO_x emission in the environment. Nitric oxide, produced in automotive exhaust, readily reacts with dioxygen to yield NO_2, an active component in smog. In addition, nitrous oxide is a known greenhouse gas that is also responsible for ozone depletion. Hence, the careful design and synthesis of NO_x selective iron or copper complexes might be extremely useful in the production of pollution-reducing components that might be employed at the source of NO_x emissions (e.g., in an automobile muffler).

V. Acknowledgments

VI. Abbreviations

1-MeIm	1-methylimidazole
BarF	terakis(3,5-bis-trifluoromethyl-phenyl)borate
dmp	2,9-dimethyl-1,10-phenanthroline
EDTA	ethylenediaminetetraacetic acid
Et-HPTB	N,N,N′,N′-tetrakis(N-ethyl-2-benzimidazolyl-methyl)-1,3-diaminopropane
Iz	indazole
MS	mesityl
NOx	gaseous substrates related to NO by way of a redox process, including NO_2 and N_2O
NAR	nitrate reductase
NIR	nitrite reductase
NOR	nitric oxide reductase
N$_2$OR	nitrous oxide reductase
OEP	2,3,7,8,12,13,17,18-octaethylporphine
OTf	trifluoromethanesulfonate
phen	1,10-phenanthroline
PMS	pentamethylene sulfide
Prz	pyrazine
Py	pyridine
Pz	pyrazole
TEPA	tris((2-pyridyl)-ethyl)amine
TMPA	tris((2-pyridyl)-methyl)amine
TpzA	tris(3,5-dimethylpyrazolyl-1-ylmethyl)-amine
TMPS	*meso*-tetrakis(sulfonatomesityl)porphyrin
TmTP	*meso*-tetra-*m*-tolyl-porphinato
TpivPP	5,10,15,20-tetrakis(o-pivalamidophenyl)porphyrin
TPP	5,10,15,20-tetrakis(phenyl)porphyrin
TPPS	*meso*-tetrakis(4-sulfonatophenyl)porphyrin
Tp$^{RR'}$	tris(pyrazolyl) hyrdroborate; substituent R in 3-pyrazolyl position, substituent R′ in 5-pyrazolyl position
TTP	5,10,15,20-tetrakis(tolyl)porphyrin

VII. References

(1) Berks, B. C.; Ferguson, S. J.; Moir, J. W.; Richardson, D. J. *Biochim. Biophys. Acta* **1995**, *1232*, 97.
(2) Averill, B. A. *Chem. Rev.* **1996**, *96*, 2951.
(3) Zumft, W. G. *Microbiol. Mol. Biol. Rev.* **1997**, *61*, 533.
(4) Moura, I.; Moura, J. J. G. *Curr. Opin. Chem. Biol.* **2001**, *5*, 168.
(5) Richardson, D. J.; Watmough, N. J. *Curr. Opin. Chem. Biol.* **1999**, *3*, 207.
(6) Ferguson, S. J. *Antonie Van Leeuwenhoek* **1994**, *66*, 89.
(7) Stouthamer, A. H. *Antonie Van Leeuwenhoek* **1992**, *61*, 1.
(8) Afshar, S.; Kim, C.; Monbouquette, H. G.; Schroder, I. I. *Appl. Environ. Microbiol.* **1998**, *64*, 3004.
(9) Tomlinson, G. A.; Jahnke, L. L.; Hochstein, L. I. *Int. J. Syst. Bact* **1986**, *36*, 66.
(10) Volkl, P.; Huber, R.; Drobner, E.; Rachel, R.; Burggraf, S.; Trincone, A.; Stetter, K. O. *Appl. Environ. Microbiol.* **1993**, *59*, 2918.
(11) Vorholt, J. A.; Hafenbradl, D.; Stetter, K. O.; Thauer, R. K. *Arch. Microbiol.* **1997**, *167*, 19.
(12) Werber, M. M.; Mevarech, M. *Arch. Biochem. Biophys.* **1978**, *186*, 60.
(13) Park, S. Y.; Shimizu, H.; Adachi, S.; Nakagawa, A.; Tanaka, I.; Nakahara, K.; Shoun, H.; Obayashi, E.; Nakamura, H.; Iizuka, T.; Shiro, Y. *Nat. Struct. Biol.* **1997**, *4*, 827.
(14) Shimizu, H.; Obayashi, E.; Gomi, Y.; Arakawa, H.; Park, S. Y.; Nakamura, H.; Adachi, S.; Shoun, H.; Shiro, Y. *J. Biol. Chem.* **2000**, *275*, 4816.
(15) Shoun, H.; Kim, D. H.; Uchiyama, H.; Sugiyama, J. *FEMS Microbiol. Lett.* **1992**, *73*, 277.
(16) Shoun, H.; Tanimoto, T. *J. Biol. Chem.* **1991**, *266*, 11078.
(17) Tsuruta, S.; Takaya, N.; Zhang, L.; Shoun, H.; Kimura, K.; Hamamoto, M.; Nakase, T. *FEMS Microbiol. Lett.* **1998**, *168*, 105.
(18) Denninger, J. W.; Marletta, M. A. *Biochim. Biophys. Acta* **1999**, *1411*, 334.
(19) Fukuto, J. M.; Wink, D. A. In *Metal Ions in Biological Systems*; Sigel, A. S. H., Ed.; Marcel Dekker: New York, 1999; Vol. 36, p 547.
(20) Walker, F. A.; Ribeiro, J. M. C.; Montfort, W. R. In *Metal Ions in Biological Systems*; Sigel, A. S. H., Ed.; Marcel Dekker: New York, 1999; Vol. 36, p 621.
(21) Ding, X. D.; Weichsel, A.; Andersen, J. F.; Shokhireva, T. K.; Balfour, C.; Pierik, A. J.; Averill, B. A.; Montfort, W. R.; Walker, F. A. *J. Am. Chem. Soc.* **1999**, *121*, 128.

(22) Maes, E. M.; Walker, F. A.; Montfort, W. R.; Czernuszewicz, R. S. *J. Am. Chem. Soc.* **2001**, *123*, 11664.

(23) Adman, E. T. *Adv. Protein Chem.* **1991**, *42*, 145.

(24) Godden, J. W.; Turley, S.; Teller, D. C.; Adman, E. T.; Liu, M. Y.; Payne, W. J.; LeGall, J. *Science* **1991**, *253*, 438.

(25) Murphy, M. E. P.; Turley, S.; Kukimoto, M.; Nishiyama, M.; Horinouchi, S.; Sasaki, H.; Tanokura, M.; Adman, E. T. *Biochemistry* **1995**, *34*, 12107.

(26) Girsch, P.; de Vries, S. *Biochim. Biophys. Acta* **1997**, *1318*, 202.

(27) Moënne-Loccoz, P.; de Vries, S. *J. Am. Chem. Soc.* **1998**, *120*, 5147.

(28) Moënne-Loccoz, P.; Richter, O.-M. H.; Huang, H.-W.; Wasser, I. M.; Ghiladi, R. A.; Karlin, K. D.; de Vries, S. *J. Am. Chem. Soc.* **2000**, *122*, 9344.

(29) Rasmussen, T.; Berks, B. C.; Sanders-Loehr, J.; Dooley, D. M.; Zumft, W. G.; Thomson, A. J. *Biochemistry* **2000**, *39*, 12753.

(30) Brown, K.; Djinovic-Carugo, K.; Haltia, T.; Cabrito, I.; Saraste, M.; Moura, J. J. G.; Moura, I.; Tegoni, M.; Cambillau, C. *J. Biol. Chem.* **2000**, *275*, 41133.

(31) Alvarez, M. L.; Ai, J.; Zumft, W.; Sanders-Loehr, J.; Dooley, D. M. *J. Am. Chem. Soc.* **2001**, *123*, 576.

(32) Babcock, G. T.; Wikstrom, M. *Nature* **1992**, *356*, 301.

(33) Mitchell, P. *Nature* **1961**, *191*, 144.

(34) Mitchell, P. *Biol. Rev.* **1966**, *41*, 445.

(35) Mitchell, P. *J. Theor. Biol.* **1976**, *62*, 327.

(36) Trumpower, B. L.; Gennis, R. B. *Annu. Rev. Biochem.* **1994**, *63*, 675.

(37) Brandt, U. *Biochim. Biophys. Acta* **1997**, *1318*, 79.

(38) Fei, M. J.; Yamashita, E.; Inoue, N.; Yao, M.; Yamaguchi, H.; Tsukihara, T.; Shinzawa-Itoh, K.; Nakashima, R.; Yoshikawa, S. *Acta Crystallogr., Sect. D* **2000**, *56*, 529.

(39) Michel, H. *Nature* **1999**, *402*, 602.

(40) Michel, H. *Biochemistry* **1999**, *38*, 15129.

(41) Ostermeier, C.; Harrenga, A.; Ermler, U.; Michel, H. *Proc. Natl. Acad. Sci. U.S.A.* **1997**, *94*, 10547.

(42) Wikstrom, M. *Biochim. Biophys. Acta* **2000**, *1458*, 188.

(43) Wikstrom, M. *Biochemistry* **2000**, *39*, 3515.

(44) Yoshikawa, S.; Shinzawa-Itoh, K.; Nakashima, R.; Yaono, R.; Yamashita, E.; Inoue, N.; Yao, M.; Fei, M. J.; Libeu, C. P.; Mizushima, T.; Yamaguchi, H.; Tomizaki, T.; Tsukihara, T. *Science* **1998**, *280*, 1723.

(45) Shapleigh, J. P.; Payne, W. J. *J. Bacteriol.* **1985**, *163*, 837.

(46) Jordan, P. A.; Thomson, A. J.; Ralph, E. T.; Guest, J. R.; Green, J. *FEBS Lett.* **1997**, *416*, 349.

(47) Melville, S. B.; Gunsalus, R. P. *J. Biol. Chem.* **1990**, *265*, 18733.

(48) Schroder, I.; Darie, S.; Gunsalus, R. P. *J. Biol. Chem.* **1993**, *268*, 771.

(49) Baker, S. C.; Ferguson, S. J.; Ludwig, B.; Page, M. D.; Richter, O. M.; van Spanning, R. J. *Microbiol. Mol. Biol. Rev.* **1998**, *62*, 1046.

(50) Chang, C. K. *J. Biol. Chem.* **1985**, *260*, 533.

(51) Chang, C. K.; Barkigia, K. M.; Hanson, L. K.; Fajer, J. *J. Am. Chem. Soc.* **1986**, *108*, 1352.

(52) Averill, B. A.; Tiedje, M. *FEBS Lett.* **1982**, *138*, 8.

(53) Enemark, J. H.; Feltham, R. D. *Coord. Chem. Rev.* **1974**, *13*, 339.

(54) Williams, P. A.; Fülöp, V.; Garman, E. F.; Saunders, N. F. W.; Ferguson, S. J.; Hajdu, J. *Nature* **1997**, *389*, 406.

(55) Silvestrini, M. C.; Tordi, M. G.; Musci, G.; Brunori, M. *J. Biol. Chem.* **1990**, *265*, 11783.

(56) Wang, Y.; Averill, B. A. *J. Am. Chem. Soc.* **1996**, *118*, 3972.

(57) George, S. J.; Allen, J. W. A.; Ferguson, S. J.; Throneley, R. N. F. *J. Biol. Chem.* **2000**, *275*, 33231.

(58) Fülöp, V.; Moir, J. W. B.; Ferguson, S. J.; Hajdu, J. *Cell* **1995**, *81*, 369.

(59) Horowitz, P. M.; Muhoberac, B. B.; Falksen, K.; Wharton, D. C. *J. Biol. Chem.* **1982**, *257*, 2140.

(60) Kobayashi, K.; Koppenhöfer, A.; Ferguson, S. J.; Tagawa, S. *Biochemistry* **1997**, *36*, 13611.

(61) Wilson, E. K.; Bellelli, A.; Liberti, S.; Arese, M.; Grasso, S.; Cutruzzola, F.; Brunori, M.; Brzezinski, P. *Biochemistry* **1999**, *38*, 7556.

(62) Kobayashi, K.; Koppenhöfer, A.; Ferguson, S. J.; Watmough, N. J.; Tagawa, S. *Biochemistry* **2001**, *40*, 8542.

(63) Jafferji, A.; Allen, J. W. A.; Ferguson, S. J.; Fülöp, V. *J. Biol. Chem.* **2000**, *275*, 25089.

(64) Huynh, B. H.; Lui, M. C.; Moura, J. J. G.; Moura, I.; Ljungdahl, P. O.; Münck, E.; Payne, W. J.; Peck, H. D.; Vandervartanian, D.; Legall, J. *J. Biol. Chem.* **1982**, *257*, 9576.

(65) Timkovich, R.; Cork, M. S.; Talor, P. V. *Arch. Biochem. Biophys.* **1985**, *240*, 689.

(66) Silvestrini, M. C.; Galeotti, C. L.; Gervais, M.; Schinina, E.; Barra, D.; Bossa, F.; Brunori, M. *FEBS Lett.* **1989**, *254*, 33.

(67) Jüngst, A.; Wakabayashi, S.; Matsubara, H.; Zumft, W. G. *FEBS Lett.* **1991**, *279*, 205.

(68) Weeg-Aerssens, E.; Wu, W.; Ye, R. W.; Tiedje, J. M.; Chang, C. K. *J. Biol. Chem.* **1991**, *266*, 7496.

(69) Sann, R.; Kostka, S.; Friedrich, B. *Arch. Microbiol.* **1994**, *161*, 453.

(70) Cheesman, M. R.; Ferguson, S. J.; Moir, J. W. B.; Richardson, D. J.; Zumft, W. G.; Thomson, A. J. *Biochemistry* **1997**, *36*, 16267.

(71) Allen, J. W. A.; Watmough, N. J.; Ferguson, S. J. *Nat. Struct. Biol.* **2000**, *7*, 885.

(72) Nurizzo, D.; Silvestrini, M.-C.; Mathieu, M.; Cutruzzola, F.; Bourgeois, D.; Fülöp, V.; Hajdu, J.; Brunori, M.; Tegoni, M.; Cambillau, C. *Structure* **1997**, *5*, 1157.

(73) Nurizzo, D.; Cutruzzola, F.; Arese, M.; Bourgeois, D.; Brunori, M.; Cambillau, C.; Tegoni, M. *Biochemistry* **1998**, *37*, 13987.

(74) Cutruzzolá, F.; Arese, M.; Grasso, S.; Bellelli, A.; Brunori, M. *FEBS Lett.* **1997**, *412*, 365.

(75) Besson, S.; Carneiro, C.; Moura, J. J. G.; Moura, I.; Fauque, G. *Anaerobe* **1995**, *1*, 219.

(76) Kopenhöfer, A.; Turner, K. L.; Allen, J. W. A.; Chapman, S. K.; Ferguson, S. J. *Biochemistry* **2000**, *39*, 4243.

(77) Lopes, H.; Besson, S.; Moura, I.; Moura, J. J. G. *J. Biol. Inorg. Chem.* **2001**, *6*, 55.

(78) Churg, A. K.; Warshel, A. *Biochemistry* **1986**, *25*, 1675.

(79) Varadarajan, R.; Zewert, T. E.; Gray, H. B.; Boxer, S. G. *Science* **1989**, *243*, 69.

(80) Rivera, M.; Seetharaman, R.; Girdhar, D.; Wirtz, M.; Zhang, X.; Wang, X.; White, S. *Biochemistry* **1998**, *37*, 1485.

(81) Tezcan, F. A.; Winkler, J. R.; Gray, H. B. *J. Am. Chem. Soc.* **1998**, *120*, 13383.

(82) Shelnutt, J. A.; Song, X.-Z.; Ma, J.-G.; Jia, S.-L.; Jentzen, W.; Medforth, C. J. *Chem. Soc. Rev.* **1998**, *27*, 31.

(83) Ma, J.-G.; Vanderkooi, J. M.; Zhang, J.; Jia, S.-L.; Shelnutt, J. A. *Biochemistry* **1999**, *38*, 2787.

(84) Das, T. K.; Wilson, E. K.; Cutruzzola, F.; Brunori, M.; Rousseau, D. L. *Biochemistry* **2001**, *40*, 10774.

(85) Cutruzzolá, F.; Brown, K.; Wilson, E. K.; Bellelli, A.; Arese, M.; Tegoni, M.; Cambillau, C.; Brunori, M. *Proc. Natl. Acad. Sci. U.S.A.* **2001**, *98*, 2232.

(86) Montfort, W. R.; Weichsel, A.; Anderson, J. F. *Biochim. Biophys. Acta* **2000**, *1482*, 110.

(87) Weichsel, A.; Andersen, J. F.; Champagne, D. E.; Walker, F. A.; Montfort, W. R. *Nat. Struct. Biol.* **1998**, *5*, 304.

(88) Andersen, J. F.; Ding, X. D.; Balfour, C.; Shokhireva, T. K.; Champagne, D. E.; Walker, F. A.; Montfort, W. R. *Biochemistry* **2000**, *39*, 10118.

(89) Moir, J. W. *Biochim. Biophys. Acta* **1999**, *1430*, 65.

(90) Cross, R.; Lloyd, D.; Poole, R. K.; Moir, J. W. B. *J. Bacteriol.* **2001**, *183*, 3050.

(91) Yoshimura, T.; Iwasaki, H.; Shidara, S.; Suzuki, S.; Nakahara, A.; Matsubara, T. *J. Biochem.* **1988**, *103*, 1016.

(92) Yoshimura, T.; Shidara, S.; Ozaki, T.; Kamada, H. *Arch. Microbiol.* **1993**, *160*, 498.

(93) Cross, R.; Aish, J.; Paston, S. J.; Poole, R. K.; Moir, J. W. B. *J. Bacteriol.* **2000**, *182*, 1442.

(94) Kopenhöfer, A.; Little, R. H.; Lowe, D. J.; Ferguson, S. J.; Watmough, N. J. *Biochemistry* **2000**, *39*, 4028.

(95) Kim, Y.; Shinzawa-Itoh, K.; Yoshikawa, S.; Kitagawa, T. *J. Am. Chem. Soc.* **2001**, *123*, 757.

(96) Coyne, M. S.; Arunakumari, A.; Averill, B. A.; Tiedje, J. M. *Appl. Environ. Microbiol.* **1989**, *55*, 2924.

(97) Suzuki, S.; Kataoka, K.; Yamaguchi, K.; Inoue, T.; Kai, Y. *Coord. Chem. Rev.* **1999**, *190–192*, 245.

(98) Suzuki, S.; Kataoka, K.; Yamaguchi, K. *Acc. Chem. Res.* **2000**, *33*, 728.

(99) Adman, E. T.; Godden, J. W.; Turley, S. *J. Biol. Chem.* **1995**, *270*, 27458.

(100) Kukimoto, M.; Nishiyama, M.; Murphy, M. E.; Turley, S.; Adman, E. T.; Horinouchi, S.; Beppu, T. *Biochemistry* **1994**, *33*, 5246.

(101) Murphy, M. E. P.; Turley, S.; Adman, E. T. *J. Biol. Chem.* **1997**, *45*, 28455.

(102) Dodd, F. E.; Hasnain, S. S.; Abraham, Z. H. L.; Eady, R. R.; Smith, B. E. *Acta Crystallogr., Sect. D* **1997**, *57*, 406.

(103) Dodd, F. E.; Van Beeumen, J.; Eady, R. R.; Hasnain, S. S. *J. Mol. Biol.* **1998**, *282*, 369.

(104) Inoue, T.; Gotowda, M.; Deligeer; Kataoka, M.; Yamaguchi, K.; Suzuki, S.; Watanabe, H.; Gohow, M.; Kai, Y. *J. Biochem.* **1998**, *124*, 876.

(105) Han, J.; Loehr, T. M.; Lu, Y.; Selverstone-Valentine, J.; Averill, B. A.; Sander-Loehr, J. *J. Am. Chem. Soc.* **1993**, *115*, 4256.

(106) LaCroix, L. B.; Shadle, S. E.; Wang, Y.; Averill, B. A.; Hedman, B.; Hodgson, K. O.; Solomon, E. I. *J. Am. Chem. Soc.* **1996**, *118*, 7755.

(107) Suzuki, S.; Deligeer; Yamaguchi, K.; Kataoka, K.; Kobayashi, K.; Tagawa, S.; Kohzuma, T.; Shidara, S.; Iwasaki, H. *J. Biol. Inorg. Chem.* **1997**, *2*, 265.

(108) Suzuki, S.; Kohzuma, T.; Deligeer; Yamaguchi, K.; Nakamura, N.; Shidara, S.; Kobayashi, K.; Tagawa, S. *J. Am. Chem. Soc.* **1994**, *116*, 11145.

(109) Kobayashi, K.; Tagawa, S.; Deligeer; Suzuki, S. *J. Biochem.* **1999**, *126*, 408.

(110) Farver, O.; Eady, R. R.; Abraham, Z. H. L.; Pecht, I. *FEBS Lett.* **1998**, *436*, 239.

(111) Libby, E.; Averill, B. A. *Biochem. Biophys. Res. Commun.* **1992**, *187*, 1529.
(112) Strange, R. W.; Dodd, F. E.; Abraham, Z. H. L.; Grossmann, J. G.; Bruser, T.; Eady, R. R.; Smith, B. E.; Hasnain, S. S. *Nat. Struct. Biol.* **1995**, *2*, 287.
(113) Howes, B. D.; Abraham, Z. H. L.; Lowe, D. J.; Brüser, T.; Eady, R. R.; Smith, D. E. *Biochemistry* **1994**, *33*, 3171.
(114) Hulse, C. L.; Averill, B. A. *J. Am. Chem. Soc.* **1989**, *111*, 2322.
(115) Jackson, M. A.; Tiedje, J. M.; Averill, B. A. *FEBS Lett.* **1991**, *291*, 41.
(116) Kataoka, K.; Furusawa, H.; Takagi, K.; Yamaguchi, K.; Suzuki, S. *J. Biochem.* **2000**, *127*, 345.
(117) Boulanger, M. J.; Kukimoto, M.; Nishiyama, M.; Horinouchi, S.; Murphy, M. E. P. *J. Biol. Chem.* **2000**, *275*, 23957.
(118) Veselov, A.; Olesen, K.; Sienkiewicz, A.; Shapleigh, J. P.; Scholes, C. P. *Biochemistry* **1998**, *37*, 6095.
(119) Olesen, K.; Veselov, A.; Zhao, Y.; Wang, Y.; Danner, B.; Scholes, C. P.; Shapleigh, J. P. *Biochemistry* **1998**, *37*, 6086.
(120) Strange, R. W.; Murphy, L. M.; Dodd, F. E.; Abraham, Z. H. L.; Eady, R. R.; Smith, B. E.; Hasnain, S. S. *J. Mol. Biol.* **1999**, *287*, 1001.
(121) Boulanger, M. J.; Murphy, M. E. P. *Biochemistry* **2001**, *40*, 9132.
(122) Prudêncio, M.; Eady, R. R.; Sawers, G. *Biochem. J.* **2001**, *353*, 259.
(123) Halfen, J. A.; Mahapatra, S.; Olmstead, M. M.; Tolman, W. B. *J. Am. Chem. Soc.* **1994**, *116*, 2173.
(124) Halfen, J. A.; Tolman, W. B. *J. Am. Chem. Soc.* **1994**, *116*, 5475.
(125) Castresana, J.; Lubben, M.; Saraste, M.; Higgins, D. G. *Embryo. J.* **1994**, *13*, 2516.
(126) Castresana, J.; Moreira, D. *J. Mol. Evol.* **1999**, *49*, 453.
(127) Garcia-Horsman, J. A.; Barquera, B.; Rumbley, J.; Ma, J.; Gennis, R. B. *J. Bacteriol.* **1994**, *176*, 5587.
(128) Hendriks, J. H. M.; Gohlke, U.; Saraste, M. *J. Bioenergetics Biomembranes* **1998**, *30*, 15.
(129) Saraste, M. *Antonie Van Leeuwenhoek* **1994**, *65*, 285.
(130) Saraste, M.; Castresana, J. *FEBS Lett.* **1994**, *341*, 1.
(131) van der Oost, J.; de Boer, A. P.; de Gier, J. W.; Zumft, W. G.; Stouthamer, A. H.; van Spanning, R. J. *FEMS Microbiol. Lett.* **1994**, *121*, 1.
(132) Carr, G. J.; Ferguson, S. J. *Biochem. J.* **1990**, *269*, 423.
(133) Fujiwara, T.; Fukumori, Y. *J. Bacteriol.* **1996**, *178*, 1866.
(134) Heiss, B.; Frunzke, K.; Zumft, W. G. *J. Bacteriol.* **1989**, *171*, 3288.
(135) Hendriks, J.; Warne, A.; Gohlke, U.; Haltia, T.; Ludovici, C.; Lubben, M.; Saraste, M. *Biochemistry* **1998**, *37*, 13102.
(136) Kastrau, D. H.; Heiss, B.; Kroneck, P. M.; Zumft, W. G. *Eur. J. Biochem.* **1994**, *222*, 293.
(137) Sakurai, N.; Sakurai, T. *Biochem. Biophys. Res. Commun.* **1998**, *243*, 400.
(138) Richardson, D. J. *Microbiology* **2000**, *146*, 551.
(139) Cramm, R.; Siddiqui, R. A.; Friedrich, B. *J. Bacteriol.* **1997**, *179*, 6769.
(140) Hendriks, J.; Oubrie, A.; Castresana, J.; Urbani, A.; Gemein-hardt, S.; Saraste, M. *Biochim. Biophys. Acta* **2000**, *1459*, 266.
(141) Householder, T. C.; Fozo, E. M.; Cardinale, J. A.; Clark, V. L. *Infect. Immun.* **2000**, *68*, 5241.
(142) Pichinoty, F.; Mandel, M.; Garcia, J.-L. *J. Gen. Microbiol.* **1979**, *115*, 419.
(143) Suharti, S.; Strampraad, M. J.; Schroder, I.; de Vries, S. *Biochemistry* **2001**, *40*, 2632.
(144) de Boer, A. P.; van der Oost, J.; Reijnders, W. N.; Westerhoff, H. V.; Stouthamer, A. H.; van Spanning, R. J. *Eur. J. Biochem.* **1996**, *242*, 592.
(145) Sakurai, N.; Sakurai, T. *Biochemistry* **1997**, *36*, 13809.
(146) Zumft, W. G.; Braun, C.; Cuypers, H. *Eur. J. Biochem.* **1994**, *219*, 481.
(147) Ludwig, B.; Grabo, M.; Gregor, I.; Lustig, A.; Regenass, M.; Rosenbusch, J. P. *J. Biol. Chem.* **1982**, *257*, 5576.
(148) Solioz, M.; Carafoli, E.; Ludwig, B. *J. Biol. Chem.* **1982**, *257*, 1579.
(149) Iwata, S.; Ostermeier, C.; Ludwig, B.; Michel, H. *Nature* **1995**, *376*, 660.
(150) Soulimane, T.; Buse, G.; Bourenkov, G. P.; Bartunik, H. D.; Huber, R.; Than, M. E. *Embo. J.* **2000**, *19*, 1766.
(151) Tsukihara, T.; Aoyama, H.; Yamashita, E.; Tomizaki, T.; Yamagu-chi, H.; Shinzawa-Itoh, K.; Nakashima, R.; Yaono, R.; Yoshika-wa, S. *Science* **1995**, *269*, 1069.
(152) Tsukihara, T.; Aoyama, H.; Yamashita, E.; Tomizaki, T.; Yamagu-chi, H.; Shinzawa-Itoh, K.; Nakashima, R.; Yaono, R.; Yoshika-wa, S. *Science* **1996**, *272*, 1136.
(153) Gronberg, K. L. C.; Roldan, M. D.; Prior, L.; Butland, G.; Cheesman, M. R.; Richardson, D. J.; Spiro, S.; Thomson, A. J.; Watmough, N. J. *Biochemistry* **1999**, *38*, 13780.
(154) Cheesman, M. R.; Zumft, W. G.; Thomson, A. J. *Biochemistry* **1998**, *37*, 3994.
(155) Sakurai, T.; Sakurai, N.; Matsumoto, H.; Hirota, S.; Yamauchi, O. *Biochem. Biophys. Res. Commun.* **1998**, *251*, 248.
(156) Ju, T. D.; Woods, A. S.; Cotter, R. J.; Moënne-Loccoz, P.; Karlin, K. D. *Inorg. Chim. Acta* **2000**, *297*, 362.

(157) Martens, C. F.; Murthy, N. N.; Obias, H. V.; Karlin, K. D. *J. Chem. Soc., Chem. Commun.* **1996**, 629.
(158) Cramm, R.; Pohlmann, A.; Friedrich, B. *FEBS Lett.* **1999**, *460*, 6.
(159) Hendriks, J.; Oubrie, A.; Castresana, J.; Urbani, A.; Gemein-hardt, S.; Saraste, M. *Biochim. Biophys. Acta* **2000**, *1459*, 266.
(160) de Vries, S.; Schröder, I. Unpublished results.
(161) Lubben, M.; Morand, K. *J. Biol. Chem.* **1994**, *269*, 21473.
(162) Butler, A. R.; Williams, D. L. H. *Chem. Soc. Rev.* **1993**, 233.
(163) Gardner, P. R.; Gradner, A. M.; Martin, L. A.; Salzman, A. L. *Proc. Natl. Acad. Sci. U.S.A.* **1998**, *95*, 10378.
(164) Kim, S. O.; Orii, Y.; Lloyd, D.; Hughes, M. N.; Poole, R. K. *FEBS Lett.* **1999**, *445*, 389.
(165) George, S. D.; Metz, M.; Szilagyi, R. K.; Wang, H.; Cramer, S. P.; Lu, Y.; Tolman, W. B.; Hedman, B.; Hodgson, K. O.; Solomon, E. I. *J. Am. Chem. Soc.* **2001**, *123*, 5757.
(166) Deinum, G.; Stone, J. R.; Babcock, G. T.; Marletta, M. A. *Biochemistry* **1996**, *35*, 1540.
(167) Kharitonov, V. G.; Sharma, V. S.; Pilz, R. B.; Magde, D.; Koesling, D. *Proc. Natl. Acad. Sci. U.S.A.* **1995**, *92*, 2568.
(168) Stone, J. R.; Marletta, M. A. *Biochemistry* **1996**, *35*, 1093.
(169) Watmough, N. J.; Butland, G.; Cheesman, M. R.; Moir, J. W.; Richardson, D. J.; Spiro, S. *Biochim. Biophys. Acta* **1999**, *1411*, 456.
(170) Butland, G.; Spiro, S.; Watmough, N. J.; Richardson, D. J. *J. Bacteriol.* **2001**, *183*, 189.
(171) deVries, S. Unpublished results.
(172) Brudvig, G. W.; Stevens, T. H.; Chan, S. I. *Biochemistry* **1980**, *19*, 5275.
(173) Brunori, M. *Trends Biochem. Sci.* **2001**, *26*, 21.
(174) Giuffre, A.; Stubauer, G.; Sarti, P.; Brunori, M.; Zumft, W. G.; Buse, G.; Soulimane, T. *Proc. Natl. Acad. Sci. U.S.A.* **1999**, *96*, 14718.
(175) Ralle, M.; Verkhovskaya, M. L.; Morgan, J. E.; Verkhovsky, M. I.; Wikstrom, M.; Blackburn, N. J. *Biochemistry* **1999**, *38*, 7185.
(176) Ferguson-Miller, S.; Babcock, G. T. *Chem. Rev.* **1996**, *96*, 2889.
(177) Buse, G.; Soulimane, T.; Dewor, M.; Meyer, H. E.; Bluggel, M. *Protein Sci.* **1999**, *8*, 985.
(178) Dove, J. E.; Schwartz, B.; Williams, N. K.; Klinman, J. P. *Biochemistry* **2000**, *39*, 3690.
(179) Ito, N.; Phillips, S. E.; Stevens, C.; Ogel, Z. B.; McPherson, M. J.; Keen, J. N.; Yadav, K. D.; Knowles, P. F. *Nature* **1991**, *350*, 87.
(180) MacMillan, F.; Kannt, A.; Behr, J.; Prisner, T.; Michel, H. *Biochemistry* **1999**, *38*, 9179.
(181) Proshlyakov, D. A.; Pressler, M. A.; DeMaso, C.; Leykam, J. F.; DeWitt, D. L.; Babcock, G. T. *Science* **2000**, *290*, 1588.
(182) Karlin, K. D. *Science* **1993**, *261*, 701.
(183) Karlin, S.; Zhu, Z.-Y.; Karlin, K. D. *Proc. Natl. Acad. Sci. U.S.A.* **1997**, *94*, 14225.
(184) Karlin, K. D.; Zhu, Z.-Y.; Karlin, S. *J. Biol. Inorg. Chem.* **1998**, *3*, 172.
(185) Tolman, W. B.; Spencer, D. J. E. *Curr. Opin. Chem. Biol.* **2001**, *5*, 188.
(186) Cotton, F. A.; Wilkinson, G. *Advanced Inorganic Chemistry*, 5th ed.; John Wiley & Sons: New York, 1988.
(187) Hitchman, M. A.; Rowbottom, G. L. *Coord. Chem. Rev.* **1982**, *42*, 55.
(188) Procter, I. M.; Stephens, F. S. *J. Chem. Soc. (A)* **1969**, 1248.
(189) Stephens, F. S. *J. Chem. Soc. A* **1969**, 2081.
(190) Ruggiero, C. E.; Carrier, S. M.; Tolman, W. B. *Angew. Chem., Int. Ed. Engl.* **1993**, *33*, 895.
(191) Jiang, F.; Conry, R. R.; Bubacco, L.; Tyeklár, Z.; Jacobson, R. R.; Karlin, K. D.; Peisach, J. *J. Am. Chem. Soc.* **1993**, *115*, 2093.
(192) Tolman, W. B. *Inorg. Chem.* **1991**, *30*, 4877.
(193) Komeda, N.; Nagao, H.; Adachi, G.; Suzuki, M.; Uehara, A.; Tanaka, K. *Chem. Lett.* **1993**, 1521.
(194) Komeda, N.; Nagao, H.; Kushi, Y.; Adachi, G.-y.; Suzuki, M.; Uehara, A.; Tanaka, K. *Bull. Chem. Soc. Jpn.* **1995**, *68*, 581.
(195) Isaacs, N. W.; Kennard, C. H. L. *J. Chem. Soc. A* **1969**, 386.
(196) Klandermann, K. A.; Hamilton, W. C.; Bernal, I. *Inorg. Chim. Acta* **1977**, *23*, 117.
(197) Cullen, D. L.; Lingafelter, E. C. *Inorg. Chem.* **1971**, *10*, 1264.
(198) Takagi, S.; Joesten, M. D.; Lenhert, P. G. *Acta Crystallogr.* **1975**, *B31*, 596.
(199) Takagi, S.; Joesten, M. D.; Lehnhert, P. G. *J. Am. Chem. Soc.* **1975**, *97*, 444.
(200) Klein, S.; Reinen, D. *J. Solid State Chem.* **1980**, *32*, 311.
(201) Mullen, D.; Heger, G.; Reinen, D. *Solid State Commun.* **1975**, *17*, 1249.
(202) Walsh, A.; Walsh, B.; Murphy, B.; Hathaway, B. J. *Acta Crystallogr.* **1981**, *B37*, 1512.
(203) Halfen, J. A.; Mahapatra, S.; Wilkinson, E. C.; Gengenbach, A. J.; Young, V. G., Jr.; Que, L., Jr.; Tolman, W. B. *J. Am. Chem. Soc.* **1996**, *118*, 763.
(204) Casella, L.; Carugo, O.; Gullotti, M.; Doldi, S.; Frassoni, M. *Inorg. Chem.* **1996**, *35*, 1101.

(205) Beretta, M.; Bouwman, E.; Casella, L.; Douziech, B.; Driessen, W. L.; Gutierrez-Soto, L.; Monzani, E.; Reedijk, J. *Inorg. Chim. Acta* **2000**, *310*, 41.
(206) Monzani, E.; Koolhaas, A. A.; Spandre, A.; Legieri, E.; Casella, L.; Gullotti, M.; Nardin, G.; Randaccio, L.; Fontani, M.; Zanello, P.; Reedijk, J. *J. Biol. Inorg. Chem.* **2000**, *5*, 251.
(207) Ambundo, E. A.; Deydier, M.-V.; Grall, A. J.; Aguera-Vega, N.; Dressel, L. T.; Cooper, T. H.; Heeg, M. J.; Ochrymowycz, L. A.; Rorabacher, D. B. *Inorg. Chem.* **1999**, *38*, 4233.
(208) Schatz, M.; Becker, M.; Thaler, F.; Hampel, F.; Schindler, S.; Jacobson, R. R.; Tyeklár, Z.; Murthy, N. N.; Ghosh, P.; Chen, Q.; Zubieta, J.; Karlin, K. D. *Inorg. Chem.* **2001**, *40*, 2312.
(209) Stibraney, R. T.; Potenza, J. A.; Schugar, H. J. *Inorg. Chim. Acta* **1996**, *243*, 33.
(210) Paul, P. P.; Karlin, K. D. *J. Am. Chem. Soc.* **1991**, *113*, 6331.
(211) Nagao, H.; Komeda, N.; Mukaida, M.; Suzuki, M.; Tanaka, K. *Inorg. Chem.* **1996**, *35*, 6809.
(212) Tran, D.; Ford, P. C. *Inorg. Chem.* **1996**, *35*, 2411.
(213) Tran, D.; Skelton, B. W.; White, A. H.; Laverman, L. E.; Ford, P. C. *Inorg. Chem.* **1998**, *37*, 2505.
(214) Paul, P. P.; Tyeklár, Z.; Farooq, A.; Karlin, K. D.; Liu, S.; Zubieta, J. *J. Am. Chem. Soc.* **1990**, *112*, 2430.
(215) Zubieta, J.; Karlin, K. D.; Hayes, J. C. In *Copper Coordination Chemistry: Biochemical and Inorganic Perspectives*; Karlin, K. D., Zubieta, J., Eds.; Adenine: Guilderland, NY, 1983; p 97.
(216) Karlin, K. D.; Hayes, J. C.; Juen, S.; Hutchinson, J. P.; Zubieta, J. *Inorg. Chem.* **1982**, *21*, 4106.
(217) Karlin, K. D.; Dahlstrom, P. L.; Hayes, J. C.; Simon, R. A.; Zubieta, J. *J. Cryst. Struct. Commun.* **1982**, *11*, 907.
(218) Kitajima, N. *Adv. Inorg. Chem.* **1992**, *39*, 1.
(219) Holm, R. H.; Kennepohl, P.; Solomon, E. I. *Chem. Rev.* **1996**, *96*, 2239.
(220) Messerschmidt, A. *Inorg. Chem.* **1993**, *32*, 121.
(221) Chapman, S. K. *Perspect. Bioinorg. Chem.* **1991**, *1*, 95.
(222) Holland, P. L.; Tolman, W. B. *J. Am. Chem. Soc.* **2000**, *122*, 6331.
(223) Cheng, L.; Richter-Addo, G. B. In *The Porphyrin Handbook*; Kadish, K. M., Smith, K. M., Guilard, R., Eds.; Academic Press: New York, 2000; p 33.
(224) Scheidt, W. R. *Chem. Rev.* **2002**, *102*, 1067−1090.
(225) Finnegan, M. G.; Lappin, A. G.; Scheidt, W. R. *Inorg. Chem.* **1990**, *29*, 181.
(226) Nasri, H.; Goodwin, J. A.; Scheidt, W. R. *Inorg. Chem.* **1990**, *29*, 185.
(227) Munro, O. Q.; Scheidt, W. R. *Inorg. Chem.* **1998**, *37*, 2308.
(228) Blumberg, W. E.; Peisach, J. *Adv. Chem. Ser.* **1971**, *100*, 271.
(229) Nasri, H.; Wang, Y.; Huynh, B. H.; Walker, F. A.; Scheidt, W. R. *Inorg. Chem.* **1991**, *30*, 1483.
(230) Nasri, H.; Haller, K. J.; Wang, Y.; Huynh, B. H.; Scheidt, W. R. *Inorg. Chem.* **1992**, *31*, 3459.
(231) Nasri, H.; Wang, Y.; Huynh, B. H.; Scheidt, W. R. *J. Am. Chem. Soc.* **1991**, *113*, 717.
(232) Nasri, H.; Ellison, M. K.; Chen, S.; Huynh, B. H.; Scheidt, W. R. *J. Am. Chem. Soc.* **1997**, *119*, 6274.
(233) Ellison, M. K.; Schulz, C. E.; Scheidt, W. R. *Inorg. Chem.* **1999**, *38*, 100.
(234) Nasri, H.; Ellison, M. K.; Krebs, C.; Huynh, B. H.; Scheidt, W. R. *J. Am. Chem. Soc.* **2000**, *122*, 10795.
(235) Castro, C. E.; O'Shea, S. K. *J. Org. Chem.* **1995**, *60*, 1922.
(236) Castro, C. E. *J. Am. Chem. Soc.* **1996**, *118*, 3984.
(237) O'Shea, S. K.; Wang, W.; Wade, R. S.; Castro, C. E. *J. Org. Chem.* **1996**, *61*, 6388.
(238) Frangione, M.; Port, J.; Baldiwala, M.; Judd, A.; Galley, J.; DeVega, M.; Linna, K.; Caron, L.; Anderson, E.; Goodwin, J. A. *Inorg. Chem.* **1997**, *36*, 1904.
(239) Spaulding, L. D.; Chang, C. C.; Yu, N.; Felton, R. H. *J. Am. Chem. Soc.* **1975**, *97*, 2517.
(240) Wayland, B. B.; Olson, L. W. *J. Am. Chem. Soc.* **1974**, *96*, 6037.
(241) Scheidt, W. R.; Ellison, M. K. *Acc. Chem. Res.* **1999**, *32*, 350.
(242) Scheidt, W. R.; Lee, Y. J.; Hatano, K. *J. Am. Chem. Soc.* **1984**, *106*, 3191.
(243) Ellison, M. K.; Scheidt, W. R. *J. Am. Chem. Soc.* **1999**, *121*, 5210.
(244) Ellison, M. K.; Schulz, C. E.; Scheidt, W. R. *Inorg. Chem.* **2000**, *39*, 5102.
(245) Cheng, L.; Powell, D. R.; Khan, M. A.; Richter-Addo, G. B. *J. Chem. Soc., Chem. Commun.* **2000**, 2301.
(246) Kadish, K. M. Manuscript in preparation.
(247) Olson, L. W.; Schaeper, D.; Lancon, D.; Kadish, K. M. *J. Am. Chem. Soc.* **1982**, *104*, 2042.
(248) Lancon, D.; Kadish, K. M. *J. Am. Chem. Soc.* **1983**, *105*, 5610.
(249) Mu, X. H.; Kadish, K. M. *Inorg. Chem.* **1988**, *27*, 4720.
(250) Barley, M. H.; Rhodes, M. R.; Meyer, T. J. *Inorg. Chem.* **1987**, *26*, 1746.
(251) Barley, M. H.; Takeuchi, K. J.; Meyer, T. J. *J. Am. Chem. Soc.* **1986**, *108*, 5876.
(252) Choi, I. K.; Ryan, M. D. *Inorg. Chim. Acta* **1988**, *153*, 25.
(253) Liu, Y.; Ryan, M. D. *J. Electroanal. Chem.* **1994**, *368*, 209.
(254) Choi, I.-K.; Lium, Y.; Feng, D.; Paeng, K.-J.; Ryan, M. D. *Inorg. Chem.* **1991**, *30*, 1832.

(255) Feng, D. W.; Ting, Y. S.; Ryan, M. D. *Inorg. Chem.* **1985**, *24*, 612.
(256) Fernandes, J. B.; Feng, D.; Chang, A.; Keyser, A.; Ryan, M. D. *Inorg. Chem.* **1986**, *25*, 2606.
(257) Feng, D.; Ryan, M. D. *Inorg. Chem.* **1987**, *26*, 2480.
(258) Choi, I. K.; Ryan, M. D. *New. J. Chem.* **1992**, *16*, 591.
(259) Liu, Y.; Ryan, M. D. *Inorg. Chim. Acta* **1994**, *225*, 57.
(260) Liu, Y.; DeSilva, C.; Ryan, M. D. *Inorg. Chim. Acta* **1997**, *258*, 247.
(261) Wei, Z.; Ryan, M. D. *Inorg. Chim. Acta* **2001**, *314*, 49.
(262) Wayland, B.; Olson, L. W. *J. Am. Chem. Soc.* **1974**, *96*, 6037.
(263) Fujita, E.; Fajer, J. *J. Am. Chem. Soc.* **1983**, *106*, 6743.
(264) Yoshimura, T. *Inorg. Chim. Acta* **1984**, *83*, 17.
(265) Settin, M. F.; Fanning, J. C. *Inorg. Chem.* **1988**, *27*, 1431.
(266) Hoshino, M.; Ozawa, K.; Seki, H.; Ford, P. C. *J. Am. Chem. Soc.* **1993**, *115*, 9568.
(267) Ozawa, S.; Sakamoto, E.; Ichikawa, T.; Watanabe, Y.; Morishima, I. *Inorg. Chem.* **1995**, *34*, 6362.
(268) Yi, G.-B.; Chen, L.; Khan, M. A.; Richter-Addo, G. B. *Inorg. Chem.* **1997**, *36*, 3876.
(269) Autret, M.; Will, S.; Caemelbecke, E. V.; Lex, J.; Gisselbrecht, J.-P.; Gross, M.; Vogel, E.; Kadish, K. M. *J. Am. Chem. Soc.* **1994**, *116*, 9141.
(270) Chevalier, A. A.; Gentil, L. A.; Amorebieta, V. T.; Gutierrez, M. M.; Olabe, J. A. *J. Am. Chem. Soc.* **2000**, *122*, 11238.
(271) Trogler, W. C. *Coord. Chem. Rev.* **1999**, *187*, 303.
(272) MacNeil, J. H.; Berseth, P. A.; Bruner, E. L.; Perkins, T. L.; Wadia, Y.; Westwood, G.; Trogler, W. C. *J. Am. Chem. Soc.* **1997**, *119*, 1668.
(273) Chisholm, M. H.; Cook, C. M.; Folting, K.; Streib, W. E. *Inorg. Chim. Acta* **1992**, *198−200*, 63.
(274) Carrier, S. M.; Ruggiero, C. E.; Tolman, W. B. *J. Am. Chem. Soc.* **1992**, *114*, 4408.
(275) Tolman, W. B.; Carrier, S. M.; Ruggiero, C. E.; Antholine, W. E.; Whittaker, J. W. In *Bioinorganic Chemistry of Copper*; Karlin, K. D., Tyeklár, Z., Eds.; Chapman and Hall: New York, 1993; p 406.
(276) Ruggiero, C. E.; Carrier, S. M.; Antholine, W. E.; Whittaker, J. W.; Cramer, C. J.; Tolman, W. B. *J. Am. Chem. Soc.* **1993**, *115*, 11285.
(277) Schneider, J. L.; Carrier, S. M.; Ruggiero, C. E.; Young, J. V. E.; Tolman, W. B. *J. Am. Chem. Soc.* **1998**, *120*, 11408.
(278) Ruggiero, C. E.; Carrier, S. M.; Tolman, W. B. *Angew. Chem., Int. Ed. Engl.* **1994**, *33*, 895.
(279) Berreau, L. M.; Halfen, J. A.; Young, V. G., Jr.; Tolman, W. B. *Inorg. Chim. Acta* **2000**, *297*, 115.
(280) Mahapatra, S.; Halfen, J. A.; Tolman, W. B. *J. Chem. Soc., Chem. Commun.* **1994**, 1625.
(281) Richter-Addo, G. B.; Legzdins, P. *Metal Nitrosyls*; Oxford University Press: New York, 1992.
(282) Laverman, L. E.; Ford, P. C. *J. Chem. Soc., Chem. Commun.* **1999**, 1843.
(283) Laverman, L. E.; Hoshino, M.; Ford, P. C. *J. Am. Chem. Soc.* **1997**, *119*, 12663.
(284) Ford, P. C.; Bourassa, J.; Miranda, K.; Lee, B.; Lorkovic, I.; Boggs, S.; Kudo, S.; Laverman, L. *Coord. Chem. Rev.* **1998**, *171*, 185.
(285) Lin, R.; Farmer, P. J. *J. Am. Chem. Soc.* **2001**, *123*, 1143.
(286) Lorkovic, I.; Ford, P. C. *Inorg. Chem.* **2000**, *39*, 632.
(287) Lorkovic, I.; Ford, P. C. *J. Am. Chem. Soc.* **2000**, *122*, 6516.
(288) Zhang, Y.; Palosky, M. A.; Brown, C. A.; Westre, T. E.; Hedman, B.; Hodgson, K. O.; Solomon, E. I. *J. Am. Chem. Soc.* **1992**, *114*, 9189.
(289) Brown, C. A.; Palosky, M. A.; Westre, T. E.; Zhang, Y.; Hedman, B.; Hodgson, K. O.; Solomon, E. I. *J. Am. Chem. Soc.* **1995**, *117*, 715.
(290) Schneppensieper, T.; Finkler, S.; Czap, A.; van Eldik, R.; Heus, M.; Nieuwenhuizen, P.; Wreesman, C.; Abma, W. *Eur. J. Inorg. Chem.* **2001**, 491.
(291) Franz, K. J.; Lippard, S. J. *J. Am. Chem. Soc.* **1999**, *121*, 10504.
(292) Franz, K. J.; Singh, N.; Lippard, S. J. *Angew. Chem., Int. Ed. Engl.* **2000**, *39*, 2120.
(293) Hammes, B. S.; Ramos-Moldonado, D.; Yap, G. P. A.; Liable-Sands, L.; Rheingold, A. L.; Young, V. G., Jr.; Borovik, A. S. *Inorg. Chem.* **1997**, *36*, 3210.
(294) Ray, M.; Golombek, A. P.; Hendrich, M. P.; Yap, G. P. A.; Rheingold, A. L.; Borovik, A. S. *Inorg. Chem.* **1999**, *38*, 3110.
(295) Chiou, Y.-M.; Que, L., Jr. *Inorg. Chem.* **1995**, *34*, 3270.
(296) Randall, C. R.; Zang, Y.; True, A. E.; Que, L., Jr.; Charnock, J. M.; Garner, C. D.; Fujishima, Y.; Schofield, C. J.; Baldwin, J. E. *Biochemistry* **1993**, *32*, 6664.
(297) Zang, Y.; Que, L., Jr. *Inorg. Chem.* **1995**, *34*, 1030.
(298) *The Complex Formation in the NO Reductase Mimetic System Iron(II)/L(+) Ascorbic Acid/NO*; Jabs, W., Kruger, G., Trautwein, A. X., Schunemann, V., Bill, E., Eds.; Wiley-VCH Verlag GmbH: Weinheim, Germany, 1997.
(299) Que, L., Jr.; Dong, Y. *Acc. Chem. Res.* **1996**, *29*, 190.
(300) Que, L., Jr. *J. Chem. Soc., Dalton Trans.* **1997**, 3922.

(301) Hsu, H.-F.; Yoo, S. J.; Münck, E.; Que, L., Jr. *J. Am. Chem. Soc.* **2000**, *122*, 3789.
(302) MacMurdo, V. L.; Zheng, H.; Que, L., Jr. *Inorg. Chem.* **2000**, *39*, 2254.
(303) Costas, M.; Chen, K.; Que, L., Jr. *Coord. Chem. Rev.* **2000**, *200–202*, 517.
(304) Kryatov, S. V.; Rybak-Akimova, E. V.; MacMurdo, V. L.; Que, L., Jr. *Inorg. Chem.* **2001**, *40*, 2220.
(305) Feig, A. L.; Becker, M.; Schindler, S.; van Eldik, R.; Lippard, S. J. *Inorg. Chem.* **1996**, *35*, 2590.
(306) Feig, A. L.; Masschelein, A.; Bakac, A.; Lippard, S. J. *J. Am. Chem. Soc.* **1997**, *119*, 334.
(307) Herold, S.; Lippard, S. J. *J. Am. Chem. Soc.* **1997**, *119*, 145.
(308) LeCloux, D. D.; Barrios, A. M.; Mizoguchi, T. J.; Lippard, S. J. *J. Am. Chem. Soc.* **1998**, *120*, 9001.
(309) LeCloux, D. D.; Barrios, A. M.; Lippard, S. J. *Bioorg. Med. Chem.* **1999**, *7*, 763.
(310) Feig, A. L.; Bautista, M. T.; Lippard, S. J. *Inorg. Chem.* **1996**, *35*, 6892.
(311) Coufal, D. E.; Tavares, P.; Pereira, A. S.; Hyunh, B. H.; Lippard, S. J. *Biochemistry* **1999**, *38*, 4504.
(312) Haskin, C. J.; Ravi, N.; Lynch, J. B.; Münck, E.; Que, L., Jr. *Biochemistry* **1995**, *34*, 11090.
(313) Feelisch, M.; Stamler, J. S. In *Methods in Nitric Oxide Research*; Feelisch, M., Stamler, J. S., Eds.; Wiley: New York, 1996; p 303.
(314) Moncanda, S.; Palmer, R. M. J.; Higgs, E. A. *Pharmacol. Rev.* **1991**, *43*, 109.
(315) Wink, D. A.; Mitchell, J. B. *Free Rad. Biol. Med.* **1998**, *25*, 434.
(316) Franz, K. J.; Singh, N.; Springler, B.; Lippard, S. J. *Inorg. Chem.* **2000**, *39*, 4081.
(317) Padden, K. M.; Krebs, J. F.; MacBeth, C. E.; Scarrow, R. C.; Borovik, A. S. *J. Am. Chem. Soc.* **2001**, *123*, 1072.
(318) Keefer, L. K.; Hrabie, J. A. *Chem. Rev.* **2002**, *102*, 1135–1154|
(319) Christodoulou, D.; George, C.; Keefer, L. K. *J. Chem. Soc., Chem. Commun.* **1993**, 937.
(320) Christodoulou, D.; Maragos, C. M.; George, C.; Morley, D.; Dunams, T. M.; Wink, D. A.; Keefer, L. K. In *Bioinorganic Chemistry of Copper*; Karlin, K. D., Tyeklár, Z., Eds.; Chapman & Hall: New York, 1993; p 427.
(321) Maragos, C. M.; Morley, D.; Wink, D. A.; Dunams, T. M.; Saavedra, J. E.; Hoffman, A.; Bove, A. A.; Isaac, L.; Hrabie, J. A.; Keefer, L. K. *J. Med. Chem.* **1991**, *34*, 3242.
(322) Wink, D. A.; Hanbauer, I.; Krishna, M. C.; DeGraff, W.; Gamson, J.; Mitchell, J. B. *Proc. Natl. Acad. Sci. U.S.A.* **1993**, *90*, 9813.
(323) Diodati, J. G.; Quyyumi, A. A.; Hussain, N.; Keefer, L. K. *Thromb. Haemostasis.* **1993**, *70*, 654.
(324) Maragos, C. M.; Wang, J. M.; Hrabie, J. A.; Oppenheim, J. J.; Keefer, L. K. *Cancer Res.* **1993**, *53*, 564.
(325) Christodoulou, D. D.; Wink, D. A., Jr.; Keefer, L. K. U.S. Patent 5 389 675, 1995.
(326) Christodoulou, D.; Wink, D.; George, C. F.; Saavedra, J. E.; Keefer, L. K. In *Nitrosoamine and Related N-Nitroso Compounds*; Loeppky, R. N., Michejada, C. J., Eds.; ACS Symposium Series 553; American Chemical Society: Washington, DC, 1994; p 307.
(327) Schneider, J. L.; Young, V. G., Jr.; Tolman, W. B. *Inorg. Chem.* **1996**, *35*, 5410.
(328) Schneider, J. L.; Halfen, J. A.; Young, V. G., Jr.; Tolman, W. B. *New. J. Chem.* **1998**, *22*, 459.
(329) Yi, G.-B.; Khan, M. A.; Richter-Addo, G. B. *Inorg. Chem.* **1995**, *34*, 5703.
(330) Piciulo, P. L.; Scheidt, W. R. *Inorg. Nucl. Chem. Lett.* **1975**, *11*, 309.
(331) Allen, J. W. A.; Ferguson, S. J.; Fülop, V. In *Handbook of Metalloproteins*; Messerschmidt, A., Huber, R., Poulos, T., Weighardt, K., Eds.; Wiley: New York, 2001; pp 424–439.
(332) Adman, E. T.; Murphy, M. E. P. In *Handbook of Metalloproteins*; Messerschmidt, A., Huber, R., Poulos, T., Weighardt, K., Eds.; Wiley: New York, 2001; pp 1381–1390.
(333) Burdette, S. C.; Lipard, S. J. *Coord. Chem. Rev.* **2001**, *216–217*, 333.